UNIVERSITÀ DEGLI STUDI DI PALERMO

Dottorato di Ricerca in Tecnologie e Scienze per la Salute dell'Uomo

Dipartimento di Scienze e Tecnologie Biologiche Chimiche e Farmaceutiche (STEBICEF)

XXXVII Ciclo

MODIFIED-RELEASE MICROPARTICLES PRODUCED BY SPRAY-DRYING FOR THE TREATMENT OF INFLAMMATORY BOWEL DISEASES

IL DOTTORE

Dott.ssa Francesca Terracina

IL COORDINATORE

Prof. Bruno Giuseppe Pignataro

IL TUTOR

Prof. Mariano Licciardi

IL CO TUTOR

Prof.ssa Maria Grazia Zizzo

ANNO CONSEGUIMENTO TITOLO 2024

Università degli Studi di Palermo

AREA RICERCA E TRASFERIMENTO TECNOLOGICO
SETTORE DOTTORATI E CONTRATTI PER LA RICERCA
U. O. DOTTORATI DI RICERCA

Tecnologie e Scienze per la Salute dell'Uomo
Dipartimento di Scienze e Tecnologie Biologiche Chimiche e Farmaceutiche (STEBICEF)
CHEM-08/A

MODIFIED-RELEASE MICROPARTICLES PRODUCED BY SPRAY-DRYING FOR THE TREATMENT OF INFLAMMATORY BOWEL DISEASES

IL DOTTORE

Dott.ssa Francesca Terracina

IL COORDINATORE

Prof. Bruno Giuseppe Pignataro

IL TUTOR

Prof. Mariano Licciardi

IL CO TUTOR

Prof.ssa Maria Grazia Zizzo

CICLO XXXVII

ANNO CONSEGUIMENTO TITOLO 2024

TABLE OF CONTENTS

1 INTRODUCTION

1.1 Inflammatory Bowel Diseases (IBD)

1.1.1 Clinical Status, Epidemiology, and Risk Factors

Inflammatory bowel diseases (IBD) are a group of inflammatory conditions in which the body's immune system attacks parts of the digestive system. The two most common inflammatory bowel diseases are Crohn's disease (CD) and ulcerative colitis (UC) [1]. IBD have a serious impact on patients' quality of life, social functioning, and psychological health. The confounding pathogenesis and complex clinical features of the natural course of relapsing-remitting IBD result in its inherent complexity and hinder accurate diagnosis and development of precision medicine [2].

Ulcerative colitis is a long-term, idiopathic inflammatory condition that primarily targets the colon, typically affecting adults aged 30-40 and leading to disability. It features recurrent and remitting mucosal inflammation, starting from the rectum and extending to other parts of the colon (Figure 1). Treatment aims to achieve and sustain both clinical and endoscopic remission. Aminosalicylates are the preferred treatment for mild to moderate cases, while topical and systemic steroids are used for flare-ups. Immunosuppressants and biological drugs are reserved for moderate to severe cases. Up to 15% of ulcerative colitis patients may need a colectomy. The yearly direct and indirect costs associated with ulcerative colitis are estimated to range between €12.5–29.1 billion in Europe and $8.1–14.9 billion in the USA [3].

Crohn's disease is a chronic inflammatory disorder of the gastrointestinal tract, characterized by recurring and remitting symptoms. It is a progressive condition leading to bowel damage and disability, potentially affecting any part of the gastrointestinal tract, most commonly the terminal ileum and colon (Figure 1). Inflammation is usually segmental, asymmetrical, and transmural. Most patients initially present with an inflammatory phenotype, but over time,

complications such as strictures, fistulas, or abscesses develop in about half of the patients, often necessitating surgery. Current therapeutic strategies focus on achieving deep and sustained remission to prevent complications and slow disease progression [4].

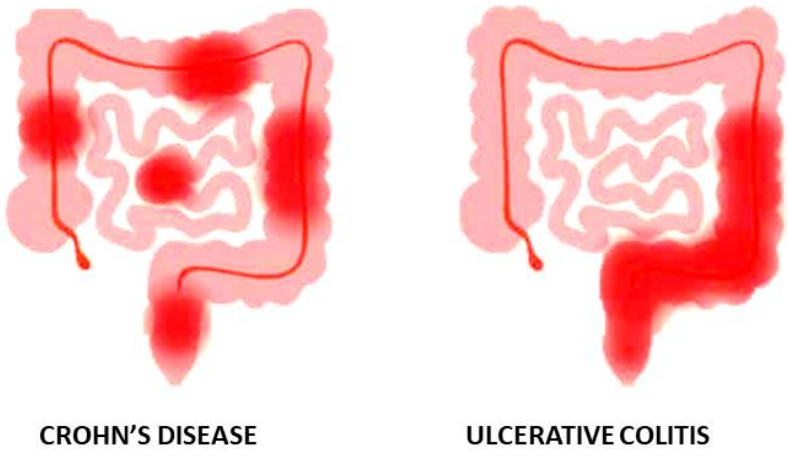

Figure 1 Illustration showing the differences in location and nature of inflammation between Crohn's disease (which can affect any part of the GI tract) and ulcerative colitis (limited to the colon and rectum).

Historically, IBD was most commonly observed in North America and Europe, with a notable increase in prevalence from north to south. Over the past 100 years, there has been a significant increase in IBD cases, particularly among children, and in the last 50 years, the disease has spread to developing countries. A key risk factor for developing IBD is having family members who are affected by the disease. The likelihood of both dizygotic twins having IBD is around 4%, whereas for monozygotic twins, the probability can be as high as 50%, with most of these twins being diagnosed within two years of each other. Despite this, most individuals with IBD do not have a family history of the disease. Over 200 genes have been identified that are associated with an increased risk of IBD. Still, these genetic associations are generally weak,

with odds ratios ranging from 1.2 to 2.0, indicating that environmental factors are also significant in the disease's development [5].

IBD is more prevalent in urban areas than in rural ones and is associated with higher standards of domestic hygiene during childhood. This observation supports the hygiene hypothesis, which suggests that reduced exposure to microbes in early life may negatively impact immune system development, thereby increasing the risk of autoimmune diseases like IBD. Furthermore, people who migrate from regions with low IBD prevalence to areas with high prevalence are more likely to develop the disease, suggesting that changes in environmental factors can influence IBD risk [6].

The prevalence of IBD, which includes Crohn's disease (CD) and ulcerative colitis (UC), has risen significantly over the past three decades. According to the Global Burden of Disease Study (GBD) (1990-2019), the number of IBD patients globally increased from 3.3 million in 1990 to 4.9 million in 2019. This rise, however, contrasts with a decrease in age-standardized prevalence, which adjusts for population age structures. Regionally, the incidence of IBD is stable or decreasing in high-burden areas like North America, but increasing in newly industrialized regions such as Asia, Africa, and parts of Latin America. In India, the number of IBD patients rose from 130,000 in 1990 to 270,000 in 2019 [7], [8].

From these studies, it is evident that while the burden of IBD remains significant in Western countries due to prolonged disability, the incidence is either stable or declining. Conversely, in newly industrialized regions, the incidence is on the rise, although the current disease burden in these areas remains low. The GBD study reported a rise in the total number of deaths due to IBD, but a decline in the age-standardized death rate, indicating advancements in healthcare and disease management. This shift towards more years lived with disability (YLD) and fewer

years of life lost (YLL) demonstrates improved care and a growing emphasis on enhancing the quality of life for patients [7].

The triggering cause of IBD is not singular but rather these are multifactorial diseases: genetic predisposition factors have been identified, intersecting with components related to the intestinal microbiome, the environment, and the lifestyle of patients. All of these act as a trigger for the activation of an inflammatory cascade that tends to become chronic. This interaction not only adds to the complexity of the disease's pathogenesis but also presents multiple opportunities for interventions to enhance patient outcomes (Figure 2) [9].

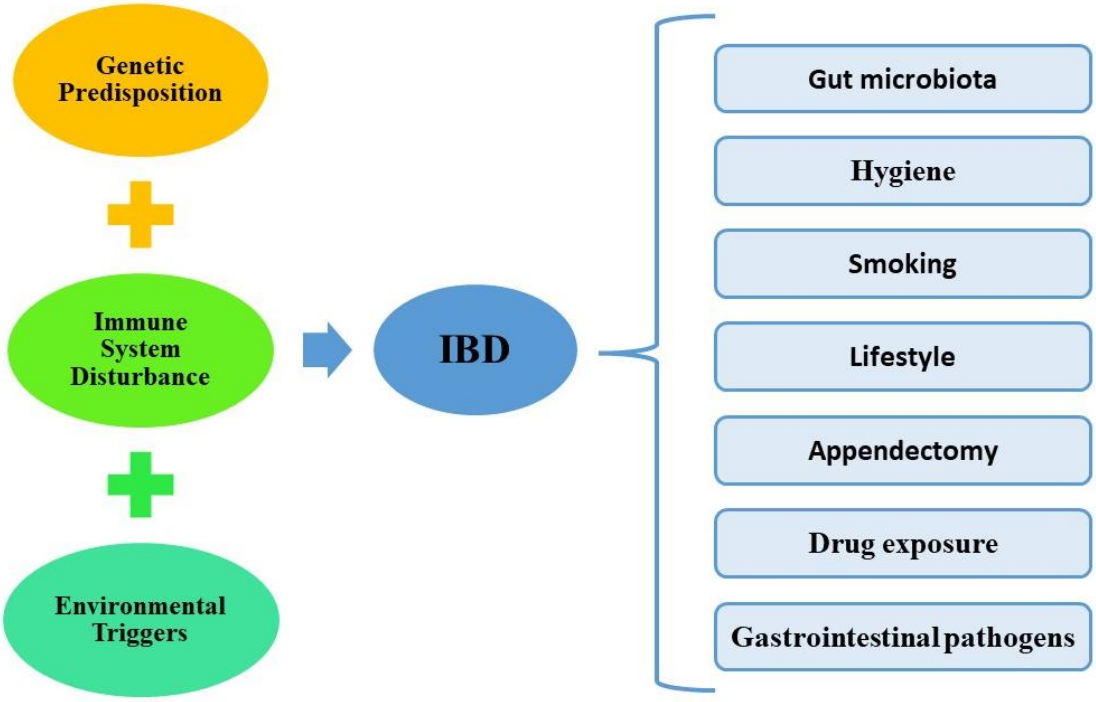

Figure 2 Summary of risk factors for Inflammatory Bowel Diseases (IBD): genetic predisposition, environmental influences (such as smoking, gut microbiota, and antibiotic use), and alterations in the immune system. These factors contribute to the development and progression of Crohn's disease and ulcerative colitis.

Genetic factors are widely recognized as major risk factors for the onset of IBD, though the impact of individual variants is quite modest. IBD are probably the most extensively studied

diseases of those with complex genetic architecture. Genome-wide association studies (GWAS) have been extremely successful in dissecting the genetic background and revealing pathogenetic pathways, which may lead to pathway-specific therapy. There are now over 200 loci identified as risk factors for CD and UC. The most significant genetic influences are associated with IL23R, NOD2, and HLA [10].

Moreover, these genetic variants can have different effects on disease predisposition; for instance, NOD2 and PTPN22 are risk factors for Crohn's disease (CD) but protective against ulcerative colitis (UC). Additionally, these variants generally have low or intermediate penetrance, highlighting the complex and polygenic nature of IBD. Therefore, even if a person carries the NOD2 variant, which has the highest genetic risk for CD with an odds ratio of 3 and an estimated average lifetime risk for IBD of 1%, their lifetime risk increases only to 3%. This means 97% of individuals with the risk variant will never develop the disease, while those without the variant may still develop either UC or CD [11].

Due to the polygenic nature of IBD, individual genetic risk factors are not particularly useful for screening and prediction. Thus, a polygenic risk score (PRS), which calculates the genetic burden by aggregating risk alleles, is considered more beneficial. The PRS, which may eventually include other risk factors, has become increasingly used in the study of complex diseases and has recently been applied to IBD. Generally, IBD patients tend to have a higher PRS, but there is significant overlap with the general population. A higher PRS has been observed in family clusters with IBD, potentially helping to prioritize preventive measures in unaffected relatives, such as avoiding smoking. However, a single randomized trial found that providing DNA-based risk assessments did not motivate behavior change in healthy relatives [12].

IBD is an autoimmune disease characterized by intestinal inflammation, which has attracted significant attention due to the interaction between the gut microbiota and the immune system. It has been observed that the gut microbiota can initiate events leading to IBD, with differences in microbial composition between healthy individuals and those with IBD [13]. Antibiotic use has been linked to the onset of IBD by altering the gut microbiota's composition and function. The interaction between the gut microbiota and the host is crucial for maintaining the immune system's functionality. Environmental changes, such as the overuse of antibiotics and dietary shifts, can enhance autoimmune and inflammatory disorders by disrupting the gut microbiota, leading to dysbiosis. Therefore, a critical relationship exists between IBD and the microbial communities in the human gut [14].

While IBD is commonly attributed to altered interactions between gut microbes and the intestinal immune system, the precise mechanism of gut microbiota dysfunction in IBD remains unclear. Although the exact pathogenesis of IBD is unknown, the inflamed gastrointestinal tract in IBD patients is consistently associated with an imbalance (dysbiosis) in the gut microbiota. Recent evidence suggests that gut dysbiosis disrupts immune tolerance, potentially inducing or worsening IBD. Studies involving human participants have confirmed that the gut microbiota composition in IBD patients differs from that in healthy individuals. Moreover, the gut microbiota varies between patients with ulcerative colitis (UC) and those with Crohn's disease (CD). Global analyses of the gut microbiota in IBD patients have revealed that dysbiosis includes specific increases or decreases in certain intestinal bacterial species [15].

Environmental risk factors contribute to the development of both types of IBD, however the precise process is yet unclear. Numerous environmental factors, including exposures in early childhood, lifestyle, hygiene practices, surgeries, drug exposure, and gastrointestinal pathogens, can raise the chance of developing inflammatory bowel diseases [16].

Many theories propose that events that occur during the "early life" period, which is defined as prenatal life to age five, increase the risk of IBD. According to a systematic study by Agrawal et al., there is a correlation between a higher risk of IBD and early life otitis media, passive tobacco smoke, and prenatal exposure to antibiotics within the first year of life [17].

Numerous lifestyle variables can impact the risk of developing the disease including physical activity, obesity, stress, sleep patterns, and smoking. These variables can greatly impact the course of the illness and the results of clinical care of the disease and the results of clinical care can be greatly impacted by these variables in individuals with established IBD. It has been demonstrated that recreational exercise lowers the likelihood of weariness and IBD flare-ups in patients. On the other hand, obesity raises the chance of relapse and is associated with elevated levels of pain, exhaustion, anxiety, and depression in addition to a higher risk of treatment failure. Regardless of the severity of the illness, sleep disruptions are prevalent in IBD patients and raise the risk of relapse and chronic fatigue. Stress, particularly the kind that is felt as opposed to significant life events, can cause IBD patients' symptoms to flare up, yet it is still unknown how stress directly affects inflammation. In patients with Crohn's disease, cigarette smoking is linked to unfavorable outcomes such as a higher chance of corticosteroid use, surgery, and disease progression [18].

Living on a farm, having more siblings, having a larger family, consuming unpasteurized milk, and being around pets, especially as young children, have all been associated with a lower chance of developing ulcerative colitis or Crohn's disease [19]. Studies have also looked into the potential effects of these early life variables on the development of immune responses and the gut microbiota. Breastfeeding has been linked to a lower risk of IBD, but this correlation is stronger in ulcerative colitis cases than in Crohn's disease [20]. Birthing style significantly impacts gut microbiota in infancy, and hygiene practices have been linked to an increased risk

of ulcerative colitis, contrary to the inverse association reported in Western countries, suggesting a significant impact on the development of IBD [21].

The incidence of ulcerative colitis was significantly lower in patients who had undergone an appendectomy for either perforated or non-perforated appendicitis, as well as for mesenteric lymphadenitis, compared to those who had the surgery for nonspecific abdominal pain. This suggests that the inflammation of the appendix, rather than simply the removal of the organ, may contribute to the observed protective effect [22]. In contrast, the link between appendectomy and Crohn's disease is less clear. The varying results across studies may be influenced by the fact that some individuals may have had surgery for abdominal pain due to undiagnosed Crohn's disease, which could create a misleading association suggesting an increased risk [9].

Several studies revealed that antibiotic exposure significantly increases the risk of Crohn's disease but not ulcerative colitis. Most antibiotics, except narrow-spectrum penicillins, were linked to an increased risk of IBD, with metronidazole and fluoroquinolones being most strongly associated. The timing of antibiotic exposure is crucial, especially during the first year of life when the gut microbiome and immune system are developing [23].

Experimental and translational studies suggest that specific pathogens may cause gut dysbiosis, exacerbate existing dysbiosis, induce immune responses, or damage the intestinal mucosa, potentially triggering IBD. For genetically susceptible individuals, these pathogens might alter immune responses, contributing to IBD onset or flares. A defective intestinal barrier is a significant feature of both IBD and infections, with increased permeability possibly preceding IBD diagnosis. Various mechanisms, including microbial sensing issues, mucin barrier defects, autophagy impairments, and tight junction permeability changes, contribute to this loss of barrier integrity [24].

In summary, IBD results from the interplay of genetics, the environment, and the gut microbiota, with no single factor solely responsible for the disease. The growing incidence and emergence of new populations highlight the environmental impact. Genetic and microbiome research reveals the significant role of immune-microbiota interactions. While many environmental links are known, further high-quality studies are needed. Comprehensive IBD management should address inflammation, mucosal healing, and environmental modifications to sustain remission and enhance patient outcomes.

1.1.2 Therapeutic Options for Crohn's Disease and Ulcerative Colitis

Conventional IBD treatment approaches have often taken a gradual approach, introducing more rigorous therapy only after more conservative measures have failed to reduce symptoms. Nonetheless, new research indicates that initiating more advanced disease-modifying treatments early in the course of the illness may affect how the disease progresses and even alter the path of IBD naturally. Inducing remission is the main objective of the first IBD treatment, with the following medications aimed at sustaining this remission. In the past, clinical remission was regarded as an adequate therapeutic objective. But with the latest developments in medicine, doctors can now target more exacting outcomes like histologic and endoscopic remission [25]. Each patient's treatment plan needs to be customized depending on their disease severity, desired course of treatment, and tolerance to different drugs. Current research has demonstrated the advantages of combination therapy, which is frequently administered to patients with more advanced illness and involves biologics and immunomodulators in particular. Patients undergoing sophisticated therapies need to be carefully managed, which includes counseling and taking into account the potential side effects as well as the drug's efficacy and consequences for surgical care [26].

Overall, the IBD treatment concept can be represented as a multi-step line. This treatment line has been used over the past couple of decades as newer medications for treating inflammatory bowel disease has emerged. Originally, the concept was that as the disease became more severe, we moved up the line to use "stronger" treatments (Figure 3).

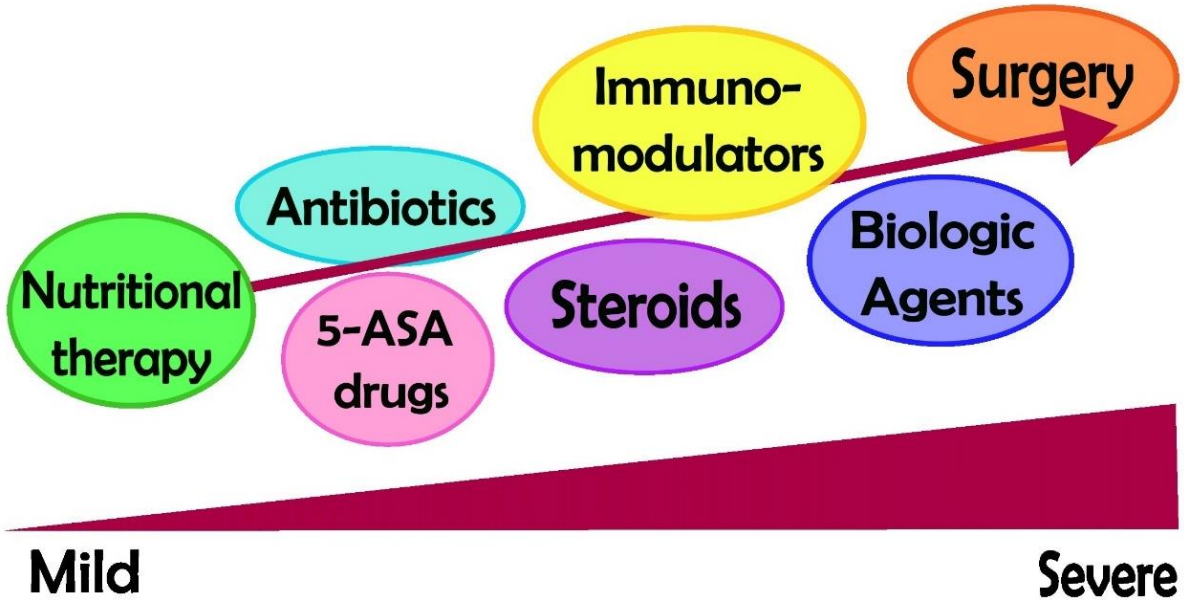

Figure 3 Medical treatment approach for Inflammatory bowel diseases (inspired by [27]).

Aminosalicylates used for IBD primarily consist of traditional sulfasalazine (SASP) and various forms of 5-aminosalicylic acid (5-ASA) drugs. They have been the conventional first-line therapy in the treatment of mild to moderate ulcerative colitis (UC); efficacy in Crohn's disease (CD) remains controversial. Sulfasalazine, oral mesalamine, rectal mesalamine, olsalazine, and balsalazide deliver 5-ASA to various parts of the gut. Sulfasalazine, which has been used for IBD treatment for 80 years, is composed of 5-ASA linked to sulphapyridine (SP) via a diazo bond. In this context, SASP acts as a prodrug, with SP serving as the carrier and 5-ASA being the active component. The mechanisms of action for 5-ASA involve disrupting arachidonic acid metabolism (which leads to the formation of prostaglandins and leukotrienes), neutralizing reactive oxygen species, and influencing white blood cell function and cytokine production

[28]. Another one proposed mechanism is the inhibition of cytokine synthesis by upregulating peroxisome proliferator activated receptor-γ and its target genes, which in turn suppresses the activation of Nuclear factor-kappa beta (NFkB) and toll-like receptors [29]. It is also thought to inhibit the biological functions of proinflammatory cytokines interleukin (IL)-1, tumor necrosis factor-α (TNF-α), IL-2, IL-8, and NFkB [30]. Recent studies have indicated that oral 5-ASA is more effective than a placebo in treating UC, with comparable clinical remission rates between once-daily dosing and traditional dosing schedules (two or three times daily). SASP is found to be equally effective as other 5-ASA drugs for UC, but it may be preferred in clinical practice due to its lower cost compared to other 5-ASA options. Furthermore, a case-control study has shown that maintenance therapy with 5-ASA can reduce the risk of colorectal cancer in UC patients by 75% [31]. Additionally, 5-ASA has been reported to help prevent CD relapse after surgery, and high-dose mesalamine has been identified as a viable option for inducing remission in mild-to-moderate CD patients who wish to avoid steroids [32].

Sulfasalazine commonly causes adverse reactions, leading 20-25% of patients to discontinue its use. Frequent side effects include headache, nausea, vomiting, and rash, while rare but serious reactions like hepatitis and pancreatitis may require immediate discontinuation. Sulfasalazine can also cause folic acid deficiency, reversible oligospermia, but is safe during pregnancy and breastfeeding. Mesalamine, olsalazine, and balsalazide are generally better tolerated, with fewer side effects, though they can occasionally worsen colitis or cause serious conditions like interstitial nephritis [26].

Given the significant role of intestinal bacteria in the development of IBD, modulating the gut microbiota has become a focus of research. This can be done through prebiotics, probiotics, fecal transplants, and antibiotics. Prebiotics are dietary substances that promote beneficial changes in gut microbiota, while probiotics are live organisms that provide health benefits when consumed in sufficient amounts. Antibiotics can influence IBD by reducing harmful bacteria in

the gut and altering the microbiota to favor beneficial strains [33]. Antibiotics may target specific bacteria believed to contribute to IBD, such as using ciprofloxacin, aminoglycosides, or rifaximin against virulent strains of *Escherichia coli* and other gram-negative bacteria, or metronidazole to target anaerobes like *Bacteroides fragilis*. Additionally, anti-tuberculosis drugs may be used in cases where *Mycobacterium avium paratuberculosis* (MAP) is suspected to play a role in Crohn's disease [34].

In CD, treatments with metronidazole, either alone or combined with ciprofloxacin, and rifaximin have shown modest benefits, particularly for active luminal disease affecting the colon. Metronidazole, ciprofloxacin, or their combination is often recommended for managing perianal fistulas and suppurative complications like abscesses. Antibiotics may also help in maintaining remission and preventing post-operative recurrence in CD patients [35]. For UC, while antibiotics haven't consistently shown benefits in treating non-severe colitis, broad-spectrum antibiotics might be useful in severe or fulminant cases. Antibiotics are particularly important in treating pouchitis. However, it's crucial to clearly define when antibiotics should be used in IBD to avoid unnecessary treatments that could lead to increased antibiotic resistance in the gut flora [36].

Corticosteroids (CSs) are effective for controlling severe intestinal inflammation in IBD by inhibiting multiple inflammatory pathways, including suppressing interleukin transcription, stabilizing the NF-κB complex, reducing arachidonic acid metabolism, and promoting lymphocyte apoptosis in the gut. However, long-term use of CSs should be avoided due to potential side effects. CSs have been used since the 1950s to manage UC flares and remain highly effective [37]. While the optimal dose and duration are not precisely defined, guidelines recommend starting with an oral dose of 40–60 mg of prednisolone daily, followed by a tapering regimen. In severe UC, high-dose intravenous CSs are used in hospitalized patients, with treatment typically limited to 7–10 days. Systemic CSs or budesonide (especially for ileocecal

CD) are often used in active CD. Budesonide at 9 mg daily has shown better efficacy compared to lower doses and is also more effective than mesalamine or sulfasalazine, with fewer typical CS-associated side effects. However, systemic CSs are necessary for patients with extensive CD. The ultimate goal in CD treatment is to achieve steroid-free remission, as CSs are not suitable for long-term maintenance in either UC or CD [27].

Immunomodulators are a key class of drugs used in IBD, particularly for maintaining remission and as steroid-sparing agents. Among these, azathioprine (AZA) is commonly used to maintain remission in patients with moderate to severe disease who are dependent on corticosteroids or who do not respond to 5-ASA. The recommended dose of azathioprine is generally 2–3 mg/kg/day, administered orally. However, it requires some time to show therapeutic effects, so it is not indicated for inducing remission. Nonetheless, up to 30% of patients may develop adverse effects such as hepatic toxicity, leukopenia, pancreatitis, fever, and an increased risk of infections and malignancies, particularly non-melanoma skin cancers [38]. 6-Mercaptopurine (6-MP), similar to azathioprine, is another immunomodulator used for maintaining remission, especially in patients who cannot tolerate azathioprine. The standard dose is 1.5 mg/kg/day. Its side effects are similar to those of azathioprine, including myelotoxicity, hepatotoxicity, and an increased risk of infections and cancers [39].

Methotrexate (MTX) is primarily used in the treatment of Crohn's disease, particularly in patients who do not respond to or cannot tolerate thiopurines. It is administered subcutaneously or intramuscularly at a dose of 15-25 mg once a week. Common side effects include nausea, fatigue, hepatic and pulmonary toxicity, as well as the risk of myelosuppression with higher doses [40].

Calcineurin inhibitors, such as cyclosporine and tacrolimus, are a class of immunosuppressive drugs used in particular cases where conventional therapies are not effective. These drugs work

by inhibiting the activity of calcineurin, a key enzyme in the activation of T-cells, which are involved in the immune response. By inhibiting calcineurin, these drugs reduce the production of pro-inflammatory cytokines, thereby diminishing the immune response that contributes to inflammation in IBD [41].

Cyclosporine is used in emergency situations, such as in cases of severe ulcerative colitis that do not respond to corticosteroids, to prevent the need for colectomy. It can be administered intravenously at a dose of 2-4 mg/kg/day or orally in less severe situations. However, cyclosporine is associated with significant side effects, including nephrotoxicity, hypertension, infections, and tremors, requiring close monitoring of blood levels [42]. Finally, tacrolimus is used in patients with refractory disease, particularly in severe ulcerative colitis or Crohn's fistulas. It is administered orally or topically (in fistulas) at initial doses of 0.1-0.2 mg/kg/day. The side effects of tacrolimus include nephrotoxicity, neurotoxicity, hypertension, and an increased risk of infections and diabetes mellitus, also necessitating careful monitoring of blood levels [43].

The use of biologic agents in the treatment of UC and CD has dramatically transformed patient care over the past two decades, due to their ability to modulate the immune system and target specific inflammatory pathways. These medications work by interfering with the immune system's signaling processes that lead to inflammation. By blocking specific proteins or pathways involved in the inflammatory response, biologics help to reduce the inflammatory cascade that exacerbates the symptoms of IBD. The introduction of biologics has marked a significant advancement in IBD treatment, particularly for patients who have not responded adequately to conventional therapies like corticosteroids or immunomodulators. Biologics can induce and maintain remission, improve quality of life, and reduce the need for surgical interventions. They have become a cornerstone of treatment for moderate to severe cases of

IBD and are particularly beneficial for patients with refractory disease or those who experience complications such as fistulas or strictures [44].

The rise of biologics began in the late 1990s with the approval of infliximab, a tumor necrosis factor-alpha (TNF-α) inhibitor. This marked a pivotal moment in the management of IBD, introducing a new era of treatment options. Since then, the development of biologics has expanded significantly, including additional TNF-α inhibitors such as adalimumab, certolizumab, and golimumab, as well as other classes like integrin antagonists, including vedolizumab, and cytokine inhibitors such as ustekinumab.For example, TNF-α inhibitors are employed to induce and maintain remission in both Crohn's disease (CD) and ulcerative colitis (UC). Integrin antagonists, on the other hand, are particularly effective for UC patients who have not responded to other therapies. Ustekinumab targets interleukin-12 and interleukin-23, and is utilized in both CD and UC [45].

However, despite their benefits, biologics come with limitations and potential risks. They are often expensive, which can be a significant barrier to access for some patients. Additionally, the use of biologics requires careful monitoring due to potential adverse effects. Common side effects include infusion reactions and an increased risk of infections, which necessitate ongoing surveillance. There is also a concern about long-term risks, such as an elevated risk of malignancies, including lymphomas and skin cancers. Moreover, the development of antibodies against the biologic can sometimes reduce its effectiveness, requiring adjustments in therapy [46].

While pharmacological therapies have revolutionized the management of inflammatory bowel disease (IBD) by targeting the underlying inflammatory processes and inducing remission, surgery remains a crucial component in the treatment paradigm for both ulcerative colitis (UC) and Crohn's disease (CD). Despite the advancements in medical treatments, some patients may

not achieve adequate control of their symptoms with drugs alone, or they may experience significant side effects or complications that necessitate surgical intervention [47].

Up to 30% of patients with ulcerative colitis and up to 70% of patients with Crohn's disease will require surgery at some point during their illness. Surgery for ulcerative colitis is considered curative, and with the advent of the ileal-pouch-anal anastomosis (IPAA) procedure, a permanent ileostomy is no longer required. On the other hand, surgery for Crohn's disease is typically only a temporary solution due to the high rate of disease recurrence [48].

1.1.3 New APIs as Enhancing Therapies in IBD: Quercetin, Phycocyanin, and Cholecalciferol

The management of IBD, encompassing both Crohn's disease and ulcerative colitis, has evolved significantly over the past few decades. Traditional therapeutic approaches, including corticosteroids, immunomodulators, and biologic agents, have transformed the landscape of IBD treatment, leading to improved clinical outcomes and quality of life for many patients. However, despite these advancements, significant challenges remain. The long-term use of conventional therapies often comes with a range of adverse effects, potential toxicity, and the looming threat of loss of efficacy due to the development of drug resistance or intolerance. These limitations underscore the urgent need for novel therapeutic strategies that can either enhance existing treatments or provide alternative options for patients. In this context, natural compounds have emerged as a promising area of interest, offering a potential complementary approach to IBD management. Derived from plants, herbs, and other natural sources, these compounds have been recognized for their anti-inflammatory, antioxidant, and immunomodulatory properties, which could be leveraged to modulate the complex pathophysiological processes underlying IBD.

The aim is to provide an in-depth examination of the role that natural compounds can play as complementary therapies in the treatment of IBD. We will explore the diverse mechanisms through which these compounds exert their effects, including their ability to modulate immune responses, protect against oxidative stress, and influence gut microbiota. The potential for natural compounds to be used in combination with existing therapies to enhance their efficacy, reduce side effects, or even as stand-alone treatments for certain patient populations, represents an exciting frontier in IBD management. As we continue to deepen our understanding of the complex interactions between natural compounds and the human body, we may unlock new pathways for treating chronic inflammatory diseases in a more personalized manner [49].

Inflammation is a complex and protective process that involves a coordinated response at the molecular, cellular, and vascular levels to address injuries caused by chemical, physical, or biological factors, with the ultimate goal of restoring tissue function. Inflammatory diseases are characterized by a persistent pro-inflammatory state, which leads to changes such as increased vascular permeability, enhanced blood flow, mobilization of white blood cells, and the production of various inflammatory mediators. Inflammatory bowel diseases (IBDs) are a subset of these conditions, defined by chronic and uncontrolled inflammation resulting from the dysregulation of both the adaptive and innate immune systems, primarily affecting the gastrointestinal tract [50]. Plant products are a source of new active pharmaceutical ingredients (APIs) with therapeutic potential and have been extensively studied for their anti-inflammatory potential in cellular and animal models as well as in humans. Among these, polyphenols, particularly flavonoids, are potent anti-inflammatory compounds that could represent an alternative in the management of IBD [51].

Quercetin, a prominent flavonoid in the flavonol group and a subclass of polyphenols, is widely recognized for its range of biological activities and significant dietary presence. Structurally, it is characterized by a backbone consisting of two aromatic rings linked by a three-carbon bridge

that forms a heterocyclic ring. Key structural elements include hydroxyl groups attached to the rings, which contribute to its strong antioxidant properties. This complex structure is integral to quercetin's biochemical properties, particularly its strong antioxidant activity, which enables it to neutralize free radicals and mitigate oxidative damage within the body (Figure 4).

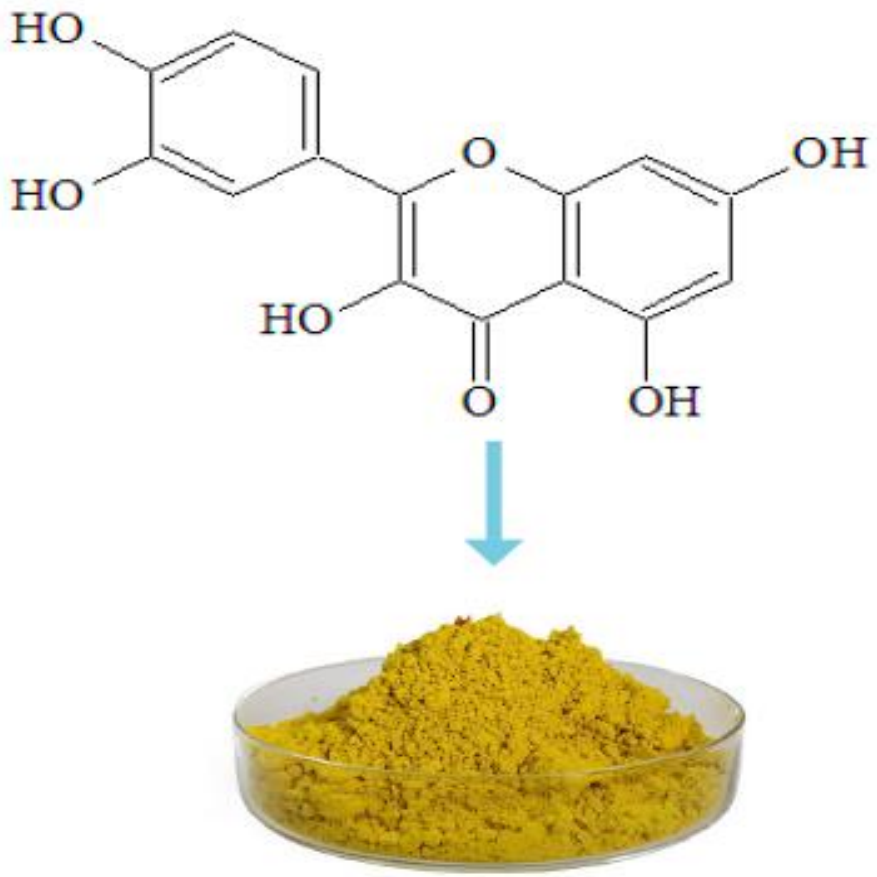

Figure 4 Quercetin is a flavonoid with the molecular formula $C_{15}H_{10}O_7$. Macroscopically, quercetin typically appears as a yellow to yellow-brown crystalline powder.

Quercetin is widely distributed in nature and can be found in a variety of plant-based foods. It is especially abundant in fruits and vegetables such as apples, onions, grapes, berries, and citrus fruits. Onions, particularly the red and yellow varieties, are among the richest sources of quercetin. Additionally, it is present in leafy greens, tea, capers, broccoli, and nuts. The

presence of quercetin in these foods not only contributes to their nutritional value but also enhances their health-promoting properties [52].

The biological activities of quercetin are diverse and have been the subject of extensive research. One of its most notable properties is its anti-inflammatory effect, which occurs through the inhibition of myeloperoxidase, an enzyme released by activated neutrophils and macrophages at inflammation sites. Additionally, it can impede neutrophil recruitment, reduce the production of pro-inflammatory cytokines like IL-1β, and enhance the production of anti-inflammatory cytokines such as IL-10. It is also effective in scavenging free radicals and chelating transition metal ions, as well as modulating endogenous antioxidants like reduced glutathione. These mechanisms, which make quercetin beneficial in various inflammation models, are also relevant for treating ulcerative colitis [53].

In the study by Khater et al., quercetin nanoparticles (QT-NPs) were assessed for their antioxidant and anti-inflammatory effects in a dextran sulfate sodium (DSS)-induced colitis model. The results showed that higher concentrations of QT-NPs restored the oxidant/antioxidant balance in the colon by normalizing levels of reactive oxygen species (ROS), hydrogen peroxide (H2O2), malondialdehyde (MDA), superoxide dismutase (SOD), catalase (CAT), glutathione peroxidase (GPX), and total antioxidant capacity (TAC). They also upregulated the expression of genes associated with tight junctions and mucin production, such as occludin, MUC-2, and JAM, and helped restore the healthy architecture of colonic tissues. These findings suggest that quercetin may offer a promising alternative to current IBD treatments by addressing oxidative stress and inflammation effectively [54].

Caruana et al. focused on enhancing quercetin's anticancer effectiveness by using a specialized microparticle formulation created through spray-drying with food-based materials like whey proteins. The microparticles significantly increased quercetin’s bioavailability, showing 26-

fold higher absorption in vivo compared to pure quercetin. Additionally, in vivo studies using colon cancer models demonstrated that the MPs had stronger anticancer effects, leading to a notable reduction in tumor growth. Overall, this food-based quercetin delivery system provided a natural and efficient approach to enhancing quercetin's anticancer potency, supporting its potential application as a therapeutic supplement in cancer treatment [55].

Among these new APIs, Phycocyanin (PC), a water-soluble blue-colored pigment-protein, has been highlighted by the World Health Organization (WHO) as a potential medicinal natural compound. Found primarily in cyanobacteria, like *Spirulina platensis*, and certain red algae, phycocyanin is an integral part of the photosynthetic machinery in these organisms [56]. Phycocyanin is composed of two types of subunits, alpha (α) and beta (β), which combine to form a heterodimer, whose subunits are proteins that each contain a covalently attached chromophore known as phycocyanobilin (PCB). Phycocyanobilin is responsible for the distinctive blue color of phycocyanin and plays a crucial role in its ability to absorb light, particularly in the orange and red regions of the spectrum (around 620 nm) [57]. PCB is attached to the protein through a thioether bond, which is formed between a cysteine residue on the protein and the chromophore. This bond is essential for the stability and function of the protein, as it helps anchor the chromophore in the correct position for effective light absorption. The basic αβ heterodimers can further assemble into higher-order structures, such as trimers or hexamers (Figure 5) [58].

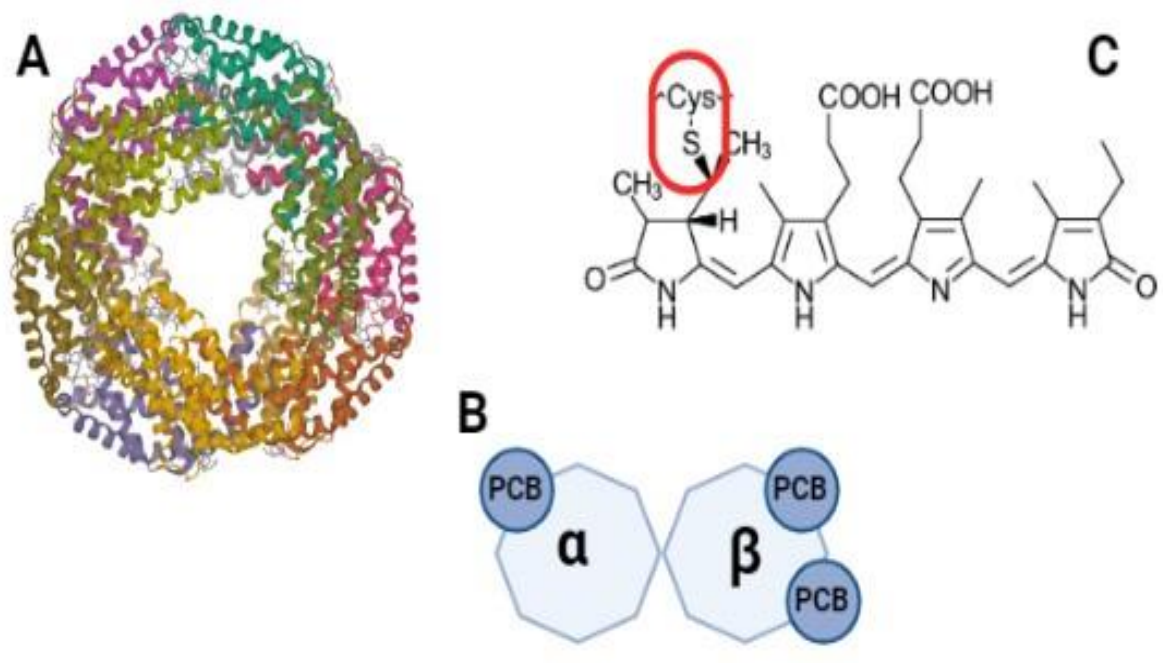

Figure 5 (**A**) The quaternary structure of phycocyanin, showcasing its oligomeric assembly, typically in a hexameric form, which enhances its stability and functionality in photosynthesis. (**B**) The α and β subunits of phycocyanin, each bound to PCB, which are responsible for light absorption. (**C**) The chemical structure of phycocyanobilin, the linear tetrapyrrole chromophore covalently attached to the protein through a thioether bond with a cysteine residue.

Beyond its role in nature, phycocyanin is attracting attention for its therapeutic potential. One of its most notable features is its strong anti-inflammatory and antioxidant properties, these qualities make phycocyanin a promising candidate for treating conditions where inflammation and oxidative stress are major issues, such as inflammatory bowel diseases. Research has shown that phycocyanin can inhibit enzymes involved in inflammation, reduce the recruitment of inflammatory cells, and neutralize harmful free radicals, offering protection against cellular damage [59].

In addition, PC has shown potential in cancer prevention and therapy. It can induce apoptosis, or programmed cell death, in cancer cells, inhibit tumor growth, and even prevent the formation of new blood vessels that supply tumors [60].

It also appears to have neuroprotective effects, which could be beneficial in treating neurodegenerative diseases by reducing oxidative stress in the brain, it may help protect neurons from damage, potentially slowing the progression of these debilitating conditions [61]. Moreover, phycocyanin has been found to modulate the immune system, enhancing the production of anti-inflammatory cytokines while reducing those that promote inflammation. This makes it a potential therapeutic agent for managing autoimmune diseases and chronic inflammatory conditions [62].

In addition to its therapeutic potential, phycocyanin is widely used in biotechnology. Its vibrant blue color makes it a popular natural food colorant, and its fluorescence is utilized in research as a marker in various imaging techniques. In summary, phycocyanin is a versatile and powerful natural compound with a wide range of potential applications in medicine, biotechnology, and nutrition. Its anti-inflammatory, antioxidant, and anticancer properties, coupled with its safety profile, make it a compelling subject for further research and development [57].

Guo and colleagues investigated the therapeutic effects of PC and PCB in a dextran sodium sulfate-induced colitis model in mice and Caco-2 cells. They found that both phycocyanin and phycocyanobilin demonstrated significant potential in protecting the intestinal epithelial barrier and exerting anti-inflammatory effects. They even outperformed mesalazine in improving colonic tight junction proteins, mucus composition, and reducing pro-inflammatory cytokines [63]. Similarly, research by Li et al. validated these findings by examining microalgae polysaccharides (MAPS), including those from *Spirulina platensis*, for their antioxidant and anti-inflammatory properties. Their study revealed that MAPS, like mesalazine, were effective in mitigating colitis symptoms in mice and improving intestinal epithelial barrier function compromised by dextran sodium sulfate [64].

Emerging research highlights the significant role that Vitamin D, particularly in its active form as cholecalciferol (Vitamin D3), may play in the pathogenesis and progression of inflammatory bowel disease (IBD). Vitamin D is not only crucial for maintaining bone health but also has profound effects on the immune system, which are especially relevant to IBD.

Vitamin D3 is metabolized in the liver to 25-hydroxyvitamin D [25(OH)D], and subsequently in the kidneys to its active form, 1,25-dihydroxyvitamin D3 [1,25(OH)2D3]. This active form exerts its biological effects by binding to the Vitamin D receptor (VDR), which is expressed in various tissues, including immune cells. The link between Vitamin D deficiency and IBD has gained considerable attention, as lower levels of 1,25(OH)2D3 have been associated with an increased risk of developing colitis. Studies using animal models have demonstrated that Vitamin D deficiency or genetic deletion of the VDR leads to a higher susceptibility to IBD, characterized by more severe inflammation and an impaired ability to resolve the disease [65].

In the innate immune system, Vitamin D enhances the expression of antimicrobial peptides, such as cathelicidins and defensins, which play a crucial role in maintaining gut barrier integrity and preventing pathogenic infections. This action is particularly important in the context of IBD, where a compromised intestinal barrier can exacerbate inflammation [66]. Moreover, Vitamin D promotes the differentiation of regulatory T cells (Tregs), which are essential for maintaining immune tolerance and preventing excessive inflammatory responses. Vitamin D also reduces the production of pro-inflammatory cytokines, such as IL-17 and IFN-γ, while increasing the levels of anti-inflammatory cytokines like IL-10. These effects contribute to a more balanced immune response, which is critical in the context of chronic inflammatory conditions like IBD [67]. In clinical settings, studies have shown that patients with IBD often have lower serum levels of Vitamin D, and supplementation with Vitamin D3 has been associated with improvements in disease symptoms and a reduced need for immunosuppressive medications. However, the optimal dosing and long-term effects of Vitamin D supplementation

in IBD patients are still under investigation, and more research is needed to fully understand its therapeutic potential [68].

Overall, Vitamin D appears to be a promising adjunctive therapy for IBD, with its ability to modulate both innate and adaptive immune responses and potentially ameliorate the chronic inflammation characteristic of the disease.

1.2 Oral Administration Route

Over the years, medical, pharmaceutical, and biological research advancements have greatly enhanced our understanding of diseases, their causes, and potential treatments. This progress has been driven by the integration of advanced technologies, leading to the development of biologically and chemically active molecules known as drugs or drug-like substances [69]. A critical aspect of the drug development process is selecting the appropriate route of administration based on the drug's chemical, physical, and biological properties. Drug administration routes are generally classified as enteral, parenteral, and topical, each with its specific uses depending on whether a localized or systemic effect is desired. These routes can be natural, where absorption occurs through skin or mucosal epithelia, or artificial, requiring medical devices for administration [70].

The oral route is the most common and preferred method due to its ease of use, cost-effectiveness, and safety. However, it also has limitations, such as delayed onset of action and variability in absorption due to factors like the hepatic first-pass effect, which can reduce the drug's effectiveness. The absorption of a drug taken orally involves its release from the formulation, dissolution in intestinal fluids, and passage through the gastrointestinal membrane into systemic circulation [71].

To improve the therapeutic efficacy of a pharmaceutical formulation and minimize the incidence of side effects, it is crucial to thoroughly examine its pharmacokinetic properties. These properties encompass four key stages: absorption, distribution, metabolism, and elimination. Specifically, the absorption phase for an orally administered drug involves the release of the active substance from its formulation, its dissolution within the intestinal fluid, and subsequent passage through the gastrointestinal membrane into the bloodstream [70].

For a solid dosage form to produce a therapeutic effect after ingestion, it must first break down into smaller particles. These smaller particles are responsible for releasing the active ingredient into a solution, making it available for absorption. While disintegration is a critical step in the absorption process, it is not sufficient by itself. Without the subsequent dissolution of the active ingredient, absorption would not occur, and the drug would not reach the bloodstream to exert its therapeutic effects.

The importance of the dissolution process and, consequently, the absorption phase of the released active ingredient is justified by numerous exogenous and endogenous factors that influence its course:

- Chemical-physical properties of the drug: size, solubility, pKa.
- Pharmaceutical forms
- Gastrointestinal tract characteristics: pH, gastric emptying time, intestinal blood flow, food intake, presence of mucus and bile [71].

Most drugs are weak organic acids or bases that exist in ionized and non-ionized forms in an aqueous environment. The proportion of the non-ionized form is determined by the environmental pH and the drug's pKa (acid dissociation constant). The non-ionized form is usually liposoluble and diffuses easily across cell membranes. When a weak acid is administered orally, most of the drug in the stomach is in the non-ionized form, favoring passive diffusion through the gastric mucosa [72].

The pharmaceutical form plays a crucial role in determining how effectively the API is absorbed. Solutions offer a distinct advantage in this regard, as the drug is already dissolved at the molecular level, making it readily available for absorption. This immediate availability

allows the active ingredient to easily diffuse across the gastro-enteric membrane and enter the systemic circulation, where it can begin to exert its therapeutic effects.

On the other hand, suspensions are more complex systems. They are heterogeneous mixtures in which solid, insoluble particles are dispersed within a liquid medium. These particles are not in molecular form and thus require additional steps before the drug can be absorbed. Some suspensions are prepared and ready to use, offering a certain convenience and stability. However, others are formulated as solid mixtures of powders or granules. These need to be reconstituted with a suitable liquid just before administration, which helps to overcome potential stability issues that could compromise the efficacy of the drug [73].

The choice between using a solution or a suspension depends on various factors, including the drug's chemical nature, stability, and therapeutic action's intended speed. Solutions provide faster absorption and onset of action, making them ideal for situations where rapid therapeutic effects are needed. Suspensions, however, offer flexibility in cases where a drug might be unstable in solution form or when a controlled release of the active ingredient is desired.

1.2.1 Overview of Gastrointestinal Tract Characteristics

The gastrointestinal system is a complex organ responsible for the effective digestion and absorption of nutrients. It possesses specialized and region-specific anatomical, histological, and functional diversities, which are regulated by a sophisticated interplay of neural, hormonal, and paracrine elements. The gastrointestinal tract comprises various organs, including the liver, pancreas, and gallbladder. It extends to a total length of about twelve meters and can be divided into an upper and a lower portion. The upper digestive tract includes the mouth, pharynx, esophagus, stomach, and the initial portion of the small intestine, known as the duodenum. The lower portion consists of the remaining small intestine segments (jejunum and ileum) as well

as the large intestine, which includes the cecum, ascending colon, transverse colon, descending colon, sigmoid colon, and rectum [74] (Figure 6).

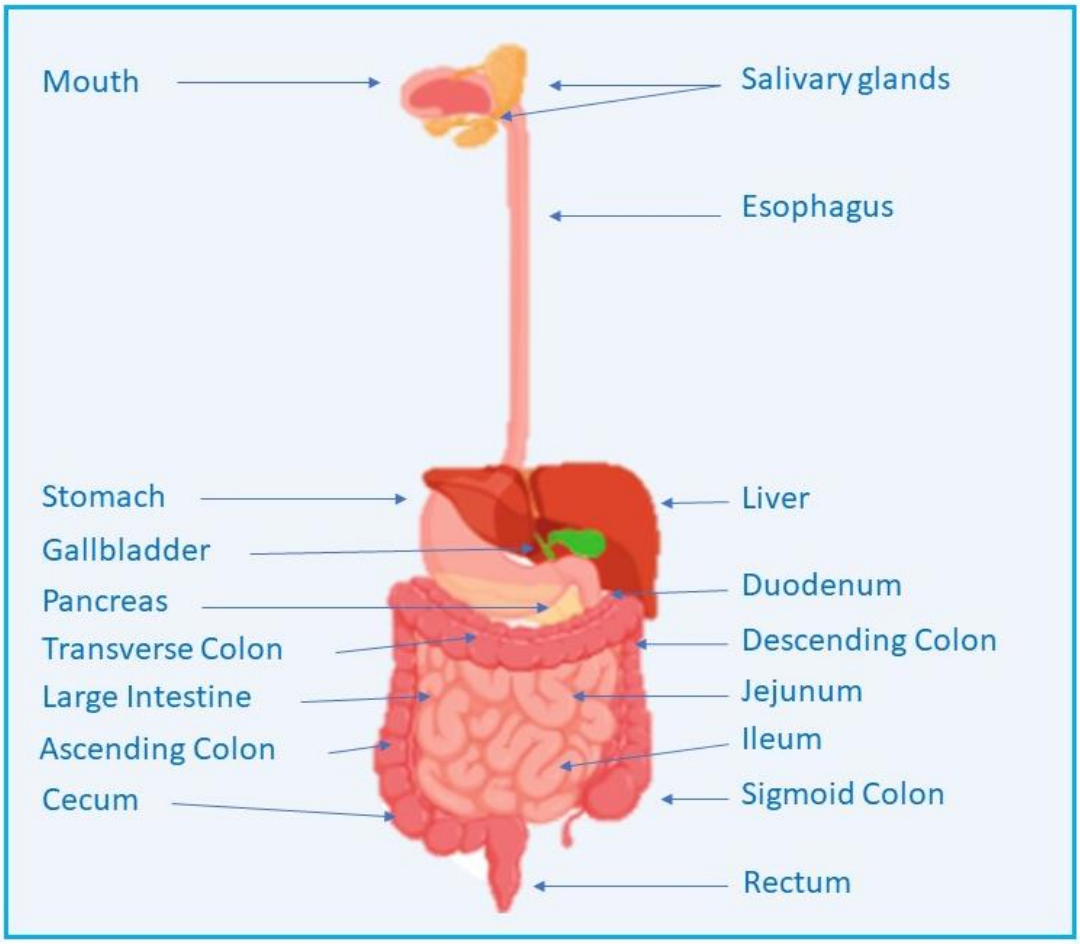

Figure 6 Anatomical description of the different sections of the gastrointestinal tract.

Apart from the oral cavity, the different segments of the gastrointestinal tract share significant structural similarities in their walls, which are composed of four distinct layers with varying functions:

- Mucosal Layer: The innermost layer, facing the lumen, consists of a single layer of epithelial cells, a subepithelial connective tissue layer, and a thin muscle layer. It

features structural modifications such as folds, villi, and crypts, which enhance the surface area for nutrient absorption.

- Submucosal Layer: Located beneath the mucosa, this layer is made up of connective tissue containing blood vessels, lymphatics, and Meissner's plexus, a network of intrinsic nerve fibers and scattered neurons.
- Muscularis Externa: This layer is divided into two parts: the inner circular fibers, which constrict the lumen, and the outer longitudinal fibers, which shorten the intestinal segment.
- Serosal Layer: The outermost layer is a connective membrane covered by mesothelial cells, which connects to the peritoneal membrane that envelops the intestinal cavity. This layer forms the mesentery, securing the intestinal loops in place. However, in areas like the oral cavity, pharynx, esophagus, and rectum, it is replaced by a network of collagen fibers that firmly anchor these sections to adjacent structures.

There are four main functions of the digestive system: ingestion, digestion, absorption, and defecation. The gastrointestinal tract serves as a gateway for the intake of solid and liquid nutrients into the body. Food and beverages are transformed by the digestive tract into more absorbable forms and delivered to the primary absorption sites at a regulated rate. The absorption of ingested substances occurs through the movement of organic substrates from the digestive epithelium into the interstitial fluid of the digestive tract. Materials that are not digested by the time they reach the lower end of the small intestine may undergo fermentation by the bacteria residing in that part of the tract; otherwise, they are excreted in feces. In addition to its digestive and absorptive functions, the gastrointestinal tract also plays a key role in homeostasis. It has been estimated that approximately nine liters of fluid enter the gastrointestinal tract daily, of which only about two liters are ingested orally [75].

By examining the physiological characteristics of the various segments of the gastrointestinal tract, one can better understand how the absorption process of substances, particularly drugs, is influenced by numerous intrinsic factors when oral administration is chosen as the delivery route for pharmaceutical forms (Table 1).

Section	pH	Length (cm)	Average Diameter (cm)	Average Mucus Thickness (µm)	Mucus Turnover (h)
Stomach	1-5	20	5-10	245 ± 200	24-48
Duodenum	~7	17-56	4	15,5	24-48
Jejunum	≥7	280-1000	2-2,5	15,5	24-48
Ileum	≥7	280-1000	3	15,5	24-48
Colon	7-8	80-313	4-4,8	135 ± 25	24-48

Table 1 Physiological characteristics of different segments of the gastrointestinal tract, including pH, length, average diameter, average mucus thickness, and mucus turnover time.

The pH, length, average diameter of the targeted tract, average mucus thickness, and mucus turnover time are key factors to consider when designing an oral pharmaceutical form. These elements help optimize the drug's release profile, site of action, and therapeutic efficacy.

The first biological barrier to the absorption of any orally administered drug is the highly acidic environment of the stomach (pH 1-5), which denatures most molecules, significantly reducing their effectiveness. In addition to stomach acidity, gastric enzymes like pepsin, as well as pancreatic enzymes such as lipases, trypsin, amylase, and peptidases, further decrease the stability of biomolecules. These enzymes, particularly concentrated in the duodenum, can

compromise the gastric stability of administered drugs. The flow of gastric fluids also reduces the contact time between drug molecules and the epithelial layer, hindering absorption [76].

The entire gastrointestinal tract is coated with mucus, a sticky, elastic, and viscous layer that traps foreign substances, especially hydrophobic molecules, preventing them from reaching the underlying epithelial layer. This mucus layer is primarily composed of water and mucin glycoproteins, along with globular proteins, salts, lipids, DNA, cells, and cellular debris. Mucins are large macromolecules made up of monomers connected by disulfide bridges, and these macromolecules are further crosslinked to form the mucus layer. The mucus layer is generally composed of two overlapping layers: a loosely adherent outer layer and a tightly adherent inner layer. It has been suggested that the thicker outer mucus layer acts as a barrier against the passage of released drugs to the submucosal tissue. On the other hand, the thinner inner mucus layer is thought to enhance the absorption efficiency of drugs, highlighting the dual role of mucus in drug absorption and desorption during oral administration [77].

Thus, mucus acts as a selective filter for drugs and other molecules, limiting their therapeutic efficacy while playing a key role in the immune system. There is a balance between the secretion, degradation, and clearance of mucin in each gastrointestinal segment, which protects the epithelium and controls the absorption rate of molecules. This balance also determines the final thickness of the regional mucus layer [78].

The size and diameter of the gastrointestinal lumen can further damage drug molecules. Osmotic stresses along the gastrointestinal tract, gastrointestinal muscle peristalsis, and shear forces due to the flow rate of gastric fluids are additional factors that reduce drug efficiency through mechanical degradation within the lumen [79].

There are also other factors that influence the absorption of an orally administered pharmaceutical form, which are specific to its final site of action within the gastrointestinal tract. These factors include:

- Local blood flow
- Microflora
- Gastric motility
- Presence of food
- Bile salts

The digestive system is supplied by vessels originating from the celiac trunk and the two mesenteric arteries. The characteristic feature of splanchnic arteries is the constant presence of anastomoses between collateral branches, forming arcades, from which smaller branches originate, which in turn create even smaller arcades. This results in a dense capillary network that ensures a constant and abundant blood flow to all tissues of the gastrointestinal tract, facilitating the absorption of administered drugs. The venous blood drains into the portal vein, establishing an enterohepatic connection. The intestinal microflora can metabolize a variety of chemicals, reducing their absorption in the intestine. The toxicological consequences of this metabolism can be significant depending on the chemical being metabolized. Reactions such as hydrolysis of glucosides, glucuronides, amides, esters, dehydroxylation, deamidation, decarboxylation, dealkylation, deamination, reduction of double bonds, nitro and diazo groups, acetylation, and esterification occur in the presence of intestinal microflora [79].

In an empty stomach, gastric motility is regulated by the migrating myoelectric complex (MMC), which follows a three-phase cyclic pattern. The first phase is a quiescent period where no gastric fluid movement occurs, lasting about 45-60 minutes. The second phase consists of 30-45 minutes of irregular activity, followed by the third phase: an intense contraction period

lasting 2 to 10 minutes, during which the entire stomach contents are emptied into the small intestine. When one cycle is ending in the distal ileum, the next cycle begins in the stomach. Food intake disrupts the appearance of MMCs, and motility becomes more regular. Depending on the caloric load and specific nutrient content of the meal, this period of mild to moderate contractions can last for several hours. The presence of food not only changes the motility pattern of the stomach but is also likely to increase the viscosity of gastric fluid. Consequently, shear forces on solid dosage forms may increase, potentially resulting in higher dissolution/release rates. The gastric residence time of a solid dosage form depends on its size, and whether the formulation is taken with a meal. In a fasted state, small solids (<2 mm) can empty from the stomach during all MMC phases, with average gastric half-lives typically less than an hour. In the presence of food, gastric residence time increases and becomes more variable, potentially exceeding two hours, depending on meal composition. The effect of food on the residence time of larger solids is even more pronounced.

Food intake also affects drug absorption by altering splanchnic blood flow. Protein-rich foods in the lumen increase blood flow, while carbohydrate-rich foods inhibit it. For instance, in situations of reduced blood flow, lipophilic drugs—whose absorption rate is strongly blood flow-dependent—are absorbed less efficiently. Conversely, slowly absorbed substances, such as more hydrophilic ones, benefit from a slower flow, and their absorption increases [80].

The importance of bile fluid in the absorption of fat-soluble vitamins, steroids, and dietary lipids has long been recognized. Bile salts aid in intestinal absorption of lipophilic compounds by increasing their dissolution rate and solubility. They are also crucial for the lymphatic absorption of lipids and lipophilic drugs [81].

1.2.2 Influences on Oral Bioavailability

Bioavailability is a term used to indicate the fraction of the administered drug dose that reaches its site of action or the biological fluid to which the drug has access from its site of action. A drug's bioavailability is a crucial pharmacokinetic parameter because it determines how much of the active ingredient becomes available in the bloodstream to exert its therapeutic effects.

The most reliable measure of a drug's bioavailability is the Area Under the Curve (AUC) of the plasma drug concentration over time. The AUC provides a quantitative measure of drug exposure, reflecting the total amount of unchanged drug that enters systemic circulation. A higher AUC indicates greater bioavailability, meaning more of the drug is absorbed and available for therapeutic action (Figure 7).

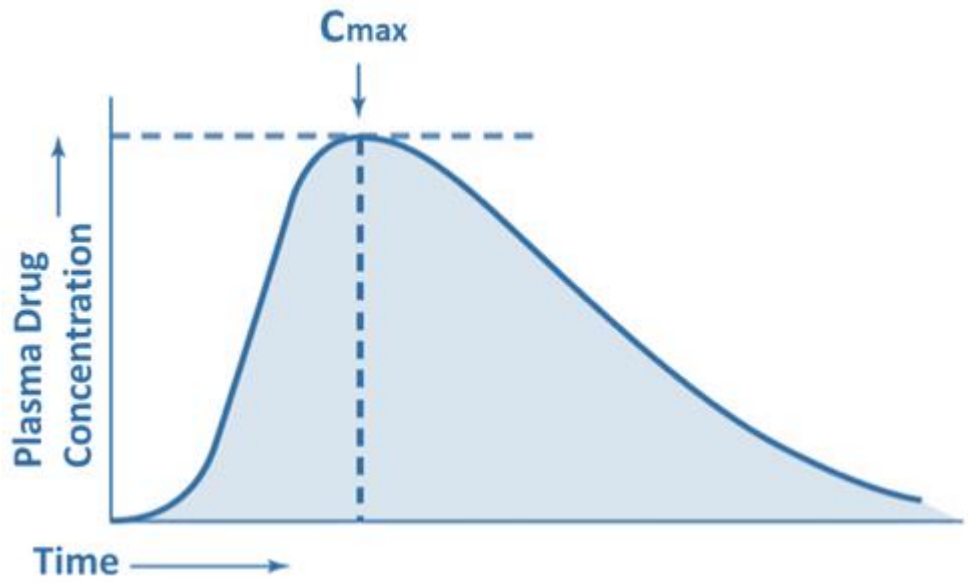

Figure 7 Representative plasma drug concentration over time after oral administration of a single drug dose.

In simple terms, the AUC is used to calculate the drug's exposure in the body after administration, and it is proportional to the amount of the drug that effectively reaches the bloodstream in its active form. The shape and extent of the AUC can help compare the

bioavailability of different formulations of the same drug, such as oral tablets versus intravenous administration. For drugs with poor bioavailability, modifications in formulation or delivery routes may be needed to enhance their therapeutic potential [82].

A drug administered orally must first be absorbed in the gastrointestinal tract, but this process can be hindered by factors such as the characteristics of the drug formulation, the drug's physicochemical properties, intestinal metabolism, and transport mechanisms back into the intestinal lumen. After absorption, the drug passes through the liver, where metabolism and biliary excretion can occur before the drug enters the systemic circulation. As a result, a portion of the administered and absorbed drug dose will be inactivated before reaching the bloodstream and being distributed to its sites of action. The hepatic first-pass effect explains why the peak plasma concentration of orally administered drugs is lower, and the concentration-time curve typically has a bell-shaped pattern. This is in stark contrast to intravenously administered drugs, where the drug is introduced directly into the systemic circulation, resulting in an immediate peak in concentration at time zero, followed by a decline due to metabolism and elimination processes. This reduction in bioavailability is influenced by the anatomical site where absorption occurs. Additionally, other anatomical, physiological, and pathological factors can impact bioavailability, which is why selecting the appropriate route of administration requires a thorough understanding of these parameters [83].

The factors affecting a drug's bioavailability are linked to its chemical and physical characteristics, including the water solubility of the active ingredient and its permeability across the gastrointestinal membrane. Based on these two parameters, the Biopharmaceutics Classification System (BCS) was developed, an experimental model designed to predict the in vivo pharmacokinetic performance of pharmaceutical products [84].

The BCS classifies drugs into four categories (Figure 8):

Figure 8 The Biopharmaceutics Classification System (BCS).

- Class 1: Highly soluble and highly permeable.
- Class 2: Poorly soluble but highly permeable.
- Class 3: Highly soluble but poorly permeable.
- Class 4: Poorly soluble and poorly permeable.

A drug is considered highly soluble if the highest marketed dose is soluble in 250 ml of an aqueous medium across the entire gastrointestinal pH range (1.2–7.4) at 37°C. Highly permeable means that the absorption rate (including hepatic first-pass metabolism) exceeds 90% of the administered dose. The BCS approach and the associated FDA guidance have set a new course that will undoubtedly continue to evolve, providing a solid scientific and mechanistic basis for establishing performance standards for pharmaceutical products, applicable worldwide [85].

1.3 Gastro-Resistant Micro Delivery Systems

1.3.1 Amorphous Solid Dispersions (ASDs)

Drugs with low solubility pose a significant challenge in pharmaceutical formulation development, so improving solubility is therefore regarded as a key driver for greater bioavailability. Various pre-formulation strategies are used to overcome this issue (Table 2) [86], [87], [88], [89], [90], [91], [92].

APPROACH	TECHNIQUE
PHYSICAL	Micronization or nanoparticles
	Inclusion complexes of drugs using cyclodextrins
	Self-emulsifying emulsion and microemulsion systems
	Conversion of the crystalline drug into a stabilized amorphous form (solid dispersion, solid solution)
CHEMICAL	Salt forms of poorly soluble acidic or basic drug
	Conversion to inactive but soluble pro-drugs with functional groups such as esters for metabolic conversion to parent drug
	Conversion to co-crystals with a conformer

Table 2 Techniques to improve solubility and bioavailability of poorly water-soluble drugs.

The transformation of drugs into an amorphous solid dispersion (ASD) form is one of these strategies that has drawn a lot of interest in recent decades. An ASD is defined as a dispersion of the API in an amorphous polymer matrix at the molecular level [93].

A solid dispersion is a straightforward two-component system in which the polymer serves as the solvent and the drug is used as the solute. These two-component systems can create a variety of configurations based on their composition and sample preparation. The drug is molecularly distributed throughout the polymer matrix (Figure 9A) and ought to create a homogeneous, thermodynamically stable solution when the drug loading is less than the drug's equilibrium solubility in the polymer. For solid dispersion, this is the ideal structure. Nevertheless, this condition only manifests at extremely low drug loading or elevated temperatures. The drug has a tendency to precipitate as the mixture turns into a supersaturated solution at lower temperatures. This may cause crystalline drug particles to disperse in a polymer matrix, where the concentration of the drug is equal to its equilibrium solubility at that temperature (Figure 9B). Amorphous drug aggregates may be distributed in a polymer matrix containing drug at its amorphous solubility at that temperature, forming an intermediate meta-stable structure. This is because drug crystallization is a slower process with a higher energy barrier than amorphous phase separation (Figure 9C) [94].

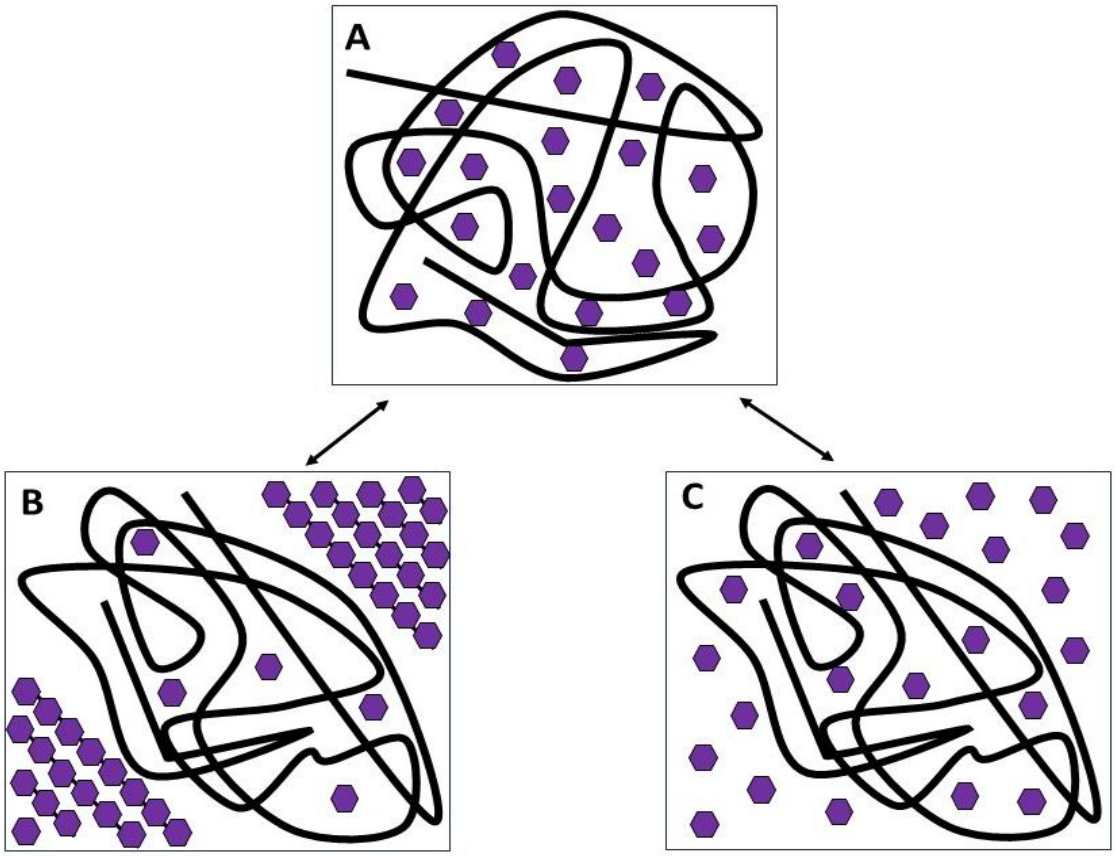

Figure 9 Three different structures of a drug/polymer solid dispersion where hexagonal symbols represent drug molecules and curvy lines represent polymer chains. (A) Homogeneous molecular dispersion of drug within the polymer matrix, representing the ideal solid dispersion with a stable, uniform distribution; (B) a crystalline dispersion, where the drug precipitates out of the polymer matrix in crystalline form due to oversaturation, (C) a drug–polymer system containing amorphous drug-rich domains dispersed in the polymer matrix (inspired by [94]).

Several polymers are used in solid dispersion manufacturing, such as:

- PHEA is a polymer with a protein-like structure, high water solubility, non-toxicity, and biocompatibility. It is used for drug delivery systems with controlled, targeted release [95].

- Cellulose acetate phthalate (CAP) is a tablet-coating material used in producing enteric films, resisting gastric fluid pH but dissolves in intestinal environments. It is commonly used for controlled drug release in dosage forms and as a coating agent [96].
- Maltodextrin is a starch-derived polysaccharide with glucose bonds, used as a coating agent and highly soluble in water. Its hygroscopic properties make it suitable for tablet compression and drug formulation strategies like spray-drying and freeze-drying, improving solubility and dissolution rates of drugs [97].
- Polyvinylpyrrolidone (PVP) is a water-soluble polymer widely used in pharmaceuticals, particularly for improving the solubility of poorly soluble drugs. PVP can form hydrogen bonds with drugs, enhancing their miscibility and dissolution rate. Available in different molecular weights, PVP is compatible with various drug delivery systems and is often used in processes like spray drying and hot melt extrusion [97].

ASDs are effective for improving drug solubility but face stability challenges, primarily due to crystallization and amorphous-amorphous phase separation (AAPS). Crystallization occurs because the amorphous form of a drug has higher free energy than its crystalline form, driving the transition. AAPS involves the formation of drug-rich and polymer-rich phases, which accelerates crystallization due to reduced polymer inhibition. Increasing polymer concentration does not always improve stability when AAPS occurs [98]. Moisture exposure can also trigger AAPS in ASDs. Crystallization involves nucleation, where small crystalline nuclei form, followed by crystal growth. Polymers in ASDs can protect against crystallization by altering the thermodynamics and kinetics of the system, primarily through drug-polymer intermolecular interactions, which reduce the free energy difference between amorphous and crystalline states. The polymer's glass transition temperature (Tg) is crucial, as a higher Tg increases the kinetic barrier to crystallization. A viscous polymer matrix reduces drug mobility, further delaying

crystallization. To achieve stability, a miscible drug-polymer system with drug loading below the polymer's saturation solubility is essential [99].

Overall, selecting polymers with appropriate Tg, miscibility, and hydrophilic properties can enhance ASD stability and drug dissolution. These polymers also help maintain the amorphous state and improve wettability, thereby supporting the effective delivery of poorly soluble drugs.

Amorphous solid dispersions can be produced using various methods, but the core principle remains the same: breaking the crystalline drug's lattice structure and converting it into a liquid or amorphous state. Afterward, rapid cooling or drying shifts the system out of equilibrium, trapping the drug in its amorphous form. Solvent-based methods like spray drying, electrospraying, and rotary evaporation involve dissolving both the drug and polymer in a solvent, which is then evaporated. These methods are suitable for temperature-sensitive drugs. In melting or fusion methods, the drug and polymer mixture is heated and then rapidly solidified. Although traditional ASD production methods are well-established, ongoing research continues to refine these techniques and explore novel approaches to enhance their efficiency and drug stability [100].

Among the different production techniques, spray drying is one of the widely used processes for manufacturing ASDs because it provides flexibility in the selection of solvents, range of temperatures, kind of liquid dispersions injectable, and pump speeds. The changing of these parameters can modify the final product properties improving particle size homogeneity, wettability, moisture content, and solubility, through the reduction of the particle size. Finally, the combination of the technological advantage offered by the spray-drying combined with the formulation benefits provided by the selection of suitable compounds within amorphous solid dispersion would lead to the manufacturing of a complete and functional drug delivery system [101].

1.3.2 Generally Recognize as Safe (GRAS) Excipients

Excipients are the components that, together with active ingredients, constitute dosage forms. Excipients can serve many functions, such as acting as protective agents or, in some cases, being used to improve the bioavailability of drugs. As an essential component of medicines, excipients must be evaluated for their safety and stability. Various interactions involving excipients, such as those between the drug and excipient, between different excipients, and between the packaging and excipient, can potentially make these technological elements harmful. Therefore, to be included in a formulation, the excipient must be highly stable, safe, effective, and, most importantly, meet the expected performance criteria [102].

This has led to the need for safer excipients, shifting the focus toward the use of natural-origin excipients and their derivatives, which can be employed as binders, diluents, colorants, preservatives, film-formers, etc., and are abundant in plants, animals, and minerals. Despite several challenges associated with natural-derived chemical substances, including their structural complexity and the slow, costly processes involved in their isolation and purification, these natural excipients are inert, biocompatible, and biodegradable with minimal toxic effects, while also being economically advantageous [103].

Among the various advantages these excipients offer, one of the most notable is their ability to protect active ingredients, particularly when they are sensitive to degradation. This is especially important for active ingredients administered orally, as they must overcome several physiological barriers (such as variable pH, pre-systemic metabolism, etc.) that can limit or even completely nullify their therapeutic effectiveness. The development of pH-sensitive formulations is a particularly significant strategy to protect both the gastric mucosa and the active molecule, as well as to control the release of the active ingredient in the targeted portion

of the gastrointestinal tract. This also serves as an attractive alternative to coating, offering greater safety and requiring fewer production steps.

Proteins, for example, are natural polymers that are biodegradable, biocompatible and possess functional properties relevant for use as encapsulating materials for pharmaceuticals. Animal-derived proteins have been studied for several years and have demonstrated that they have good solubility across a wide pH range, as well as flexibility, making them suitable for encapsulating active ingredients, even in pharmaceutical applications. On the other hand, considering the growing number of vegetarians and people avoiding lactose in their diets, plant proteins present a further alternative, although their potential for pharmaceutical applications has yet to be fully explored, unlike their well-established use in the food industry [104].

Whey proteins (WPs) are milk-derived proteins with different functional, biological, and nutritional properties. The main components of whey proteins are globular proteins including β-lactoglobulin, α-lactalbumin, and bovine serum albumin (Figure 10).

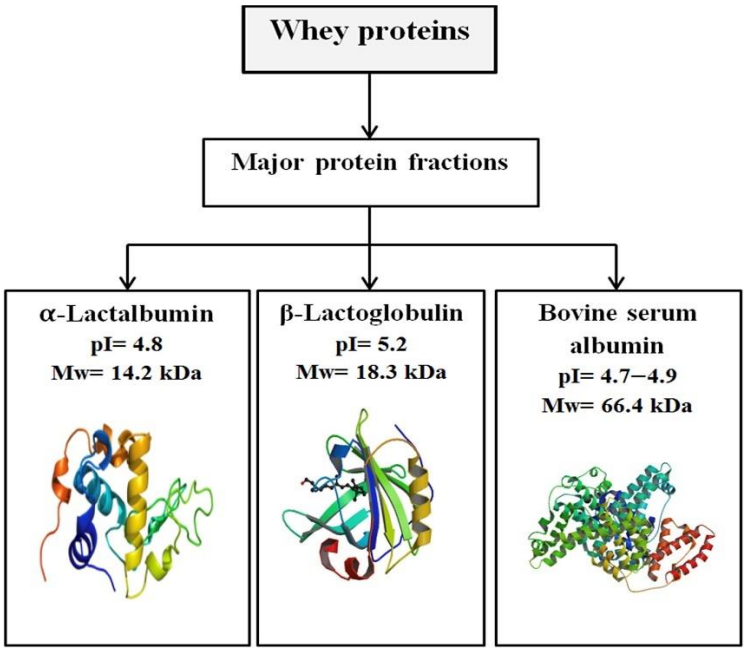

Figure 10 Main components of whey proteins; their structure, isoelectric points (pI), and molecular weights (Mw) [105].

A great number of studies have reported the usage of whey protein products, including whey protein isolate, whey protein concentrate, or specific components (especially β-lactoglobulin and bovine serum albumin) for the preparation of protein-based formulations to encase and deliver bioactive molecules [105]. The European Food Safety Authority defines whey proteins as a novel food ingredient, which is completely safe for consumption. The United States Food and Drug Administration (US-FDA) has also determined that native whey proteins in food are Generally Recognized as Safe (GRAS) [106].

WPs have been used as an excipient/carrier in the development of a variety of formulations, such as nanoemulsions, nanoparticles, nanosuspensions, and hydrogels. WPs played a variety of roles in these drug delivery systems, including improving the solubility of small molecules that were poorly soluble in water, regulating drug release, and producing an emulsifying effect. Based on the binding properties of small molecules to components in WPs, whey proteins have also been investigated as a co-former in ASD formulations [107].

Soy proteins, a key component of soy bean seeds, consist of glycinin and β-conglycinin globulin (Figure 11).

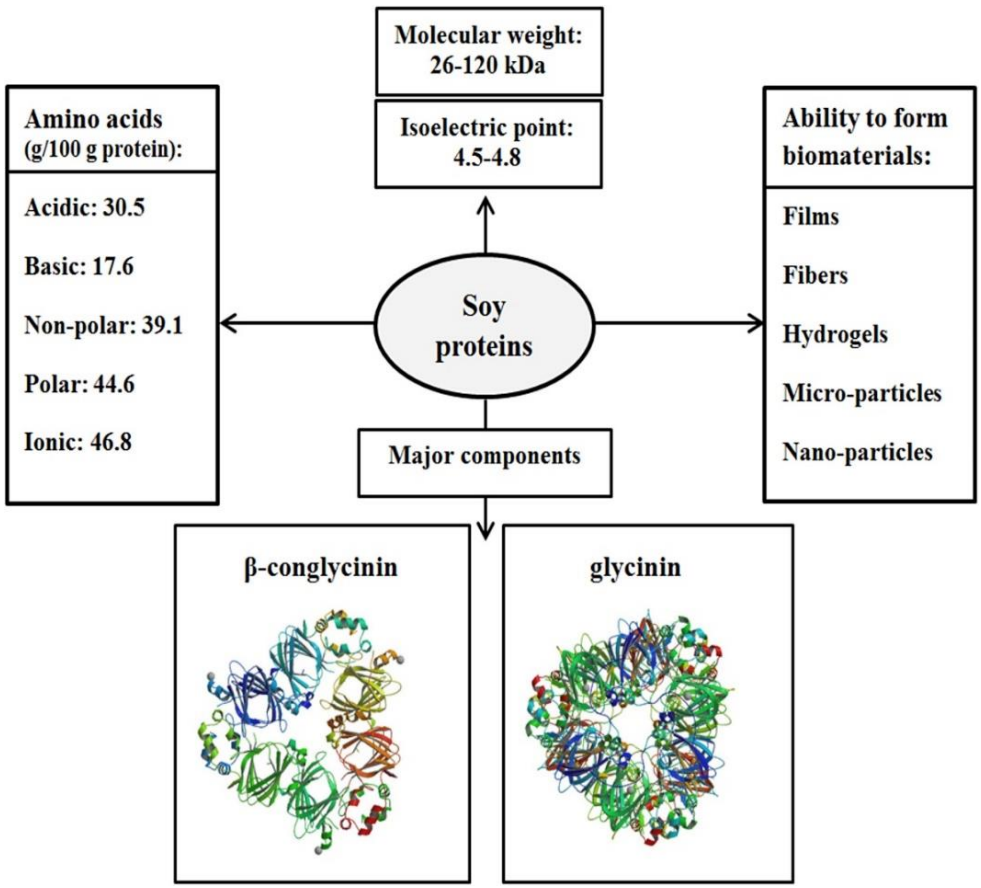

Figure 11 Some important properties of soy proteins including their molecular weight, isoelectric point, amino acids content, major components, and ability to form different biomaterials [105].

These proteins are purified into soy protein isolate and concentrate for industrial and research purposes. Soy proteins are increasingly being explored in the field of drug delivery, particularly in the development of amorphous solid dispersions (ASDs), due to their favorable properties such as biocompatibility, biodegradability, and ability to interact with various drugs. These plant-based proteins are composed of both hydrophilic and hydrophobic amino acid residues, enabling them to bind and stabilize a wide range of pharmaceutical compounds. Moreover, they exhibit excellent film-forming capabilities, which are beneficial for creating protective coatings around active pharmaceutical ingredients (APIs), aiding in their controlled release. Their pH-responsive solubility also allows for targeted release in specific areas of the gastrointestinal

tract, making them particularly useful in oral drug delivery systems. Despite these advantages, soy proteins are still under-researched in pharmaceutical applications compared to their widespread use in the food industry, presenting an opportunity for further exploration and optimization in drug delivery technologies [108].

1.3.3 Spray-drying Technique

Spray Drying is a method of drying a liquid stream by converting it into solid particles through exposure to a stream of hot gas in a single step. The feed material can be in the form of a solution, suspension, or emulsion. The resulting dried product can vary in form, including powders, granules, or agglomerates, depending on the characteristics of the atomized liquid, the design of the dryer, and the desired final properties [109].

The technique of spray drying was initially developed in 1860 to make the transportation of food and other materials more efficient by reducing their weight. Despite the technological challenges associated with industrial-scale spray drying, this method has become crucial in industries such as pharmaceuticals, food processing, and dairy production [110].

The advantages and limitations associated with this drying technique are numerous, some of which are outlined in Table 3.

Advantages	Limitations
Rapid drying process	High energy consumption
Control over powder size and final moisture content	Limited flexibility of the equipment during operation
Uniform powder quality	Low thermal efficiency
Single-step process	Low density of the final product
Usable for heat-sensitive substances	High investment cost

Design flexibility	
Various configuration options	
Lower transportation costs for the final product	

Table 3 Summary of the advantages and disadvantages of the Spray-Drying technique.

Structure and components of a Spray Dryer (Figure 12):

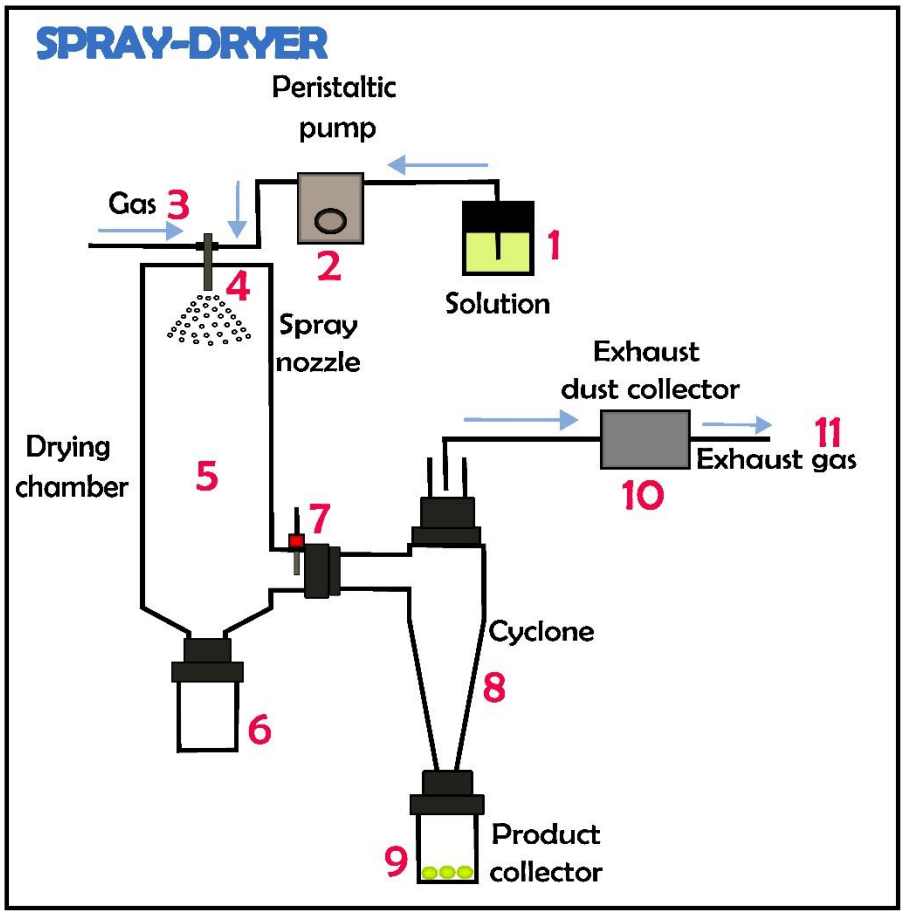

Figure 12 Schematic representation of the various components of a Spray Dryer.

1. Fluid Container: The vessel holding the fluid to be processed.
2. Peristaltic Pump: This pump draws the fluid from the reservoir and feeds it into the drying chamber at a constant flow rate set by the operator.
3. High-Pressure and Temperature Drying Gas Inlet: The entry point for the gas used to dry the fluid.

4. Atomization Nozzle: The device that sprays the fluid and incoming air.
5. Drying Chamber: The area where the drying process occurs.
6. Liquid Collector: Captures any liquid that does not get dried within the chamber.
7. Exit Temperature Sensor: Measures the temperature of the air leaving the drying chamber.
8. Cyclone: Separates the produced particles matter based on particle size.
9. Final Powder Collector: Gathers the finished powder product.
10. Oversized Powder Collection System: Collects powder particles that do not fall within the set size range.
11. Exhaust Gas Removal System: Disposes of the spent gas.

The Spray-Drying process involves four main stages: atomization of the liquid, interaction of the liquid with the drying gas, evaporation of the liquid, and separation of the dried particles from the gas. The fluid is extracted from the vessel and delivered to the nozzle via a pumping system, with peristaltic pumps being the most commonly used. Due to the use of pumps, there are limits on the fluid's viscosity since its physical properties must allow for a consistent and repeatable feed. Fluids that are too viscous can cause clogs in the intake pipes and nozzle. The solvent in the fluid is usually water, but in cases where a solid dispersion is prepared, hydroalcoholic mixtures or other organic solvents may be used [111].

Atomization converts the liquid into fine droplets by applying force and thus supplying energy to the system. The high surface-to-volume ratio promotes rapid and efficient drying of the droplets. Various atomization devices are available, depending on the type of energy applied.

The most common types of atomizers for Spray Dryers are:

- Rotating: Rotary atomizers operate by transferring centrifugal energy to the fluid through a spinning disk. The fluid supplied to the center of the disk is spread out

towards the perimeter, creating a broad cloud of droplets. Most disk atomizers have grooves, and the shape of these grooves depends on the desired properties of the dry particles. For producing powders with high density, curved grooves are recommended, whereas a combination of straight grooves with non-grooved regions is useful for generating free-flowing powders. However, disk atomizers tend to produce more deposits on the walls of the drying chamber, which makes them less suitable for expensive pharmaceutical formulations [112].

- Pressure nozzles: In pressure nozzles, the fluid flows under pressure through a tapered conduit. As the fluid exits the nozzle, it loses some of its pressure, which increases the velocity of the exiting particles and results in atomization. Unfortunately, this type of nozzle can be problematic and often shows rapid wear. Additionally, it is not suitable for drying high-viscosity fluids. The only adjustable parameter of the nozzle is the feed rate, which affects the pressure of the fluid being atomized. Pressure nozzles can produce particles within a narrow size range, most commonly in the form of hollow spheres with diameters ranging from 50 to 400 nm [113].
- Multi-phase: Pneumatic nozzles, also known as multi-phase nozzles, operate on the principle of atomizing the feed liquid within a flow of compressed transport gas. Atomization occurs due to the generation of high friction forces that break the liquid into fine droplets. This process depends on the properties of the feed (surface tension, density, and viscosity) and the properties of the transport gas (velocity and density) [114]. There are designs that allow for the feeding of two independent atomization gases. If such a system can atomize only one type of feed, it is referred to as a three-fluid construction. If it enables the atomization of two independent feeds, it is known as a four-fluid construction. Two-phase nozzles enable the production of various pharmaceutical products, including self-emulsifying drug delivery systems,

micro/nanoparticles, solid dispersions, modified-release particles, and powders with good stability [112].

This type of nozzle, like pressure nozzles, can become clogged; however, in this case, cleaning the obstructed nozzle is much simpler and does not affect the process conditions. To address this, a needle operated by bursts of compressed air is placed inside the nozzle (e.g., Buchi B-290 Atomizer, Figure 13). The compressed air driving the needle is supplied independently of the gas feed to the atomizer. Nonetheless, this solution is not perfect. The introduction of the needle reduces the area through which the feed can flow, which often leads to initial drying of the product, particularly with high-viscosity feeds [115].

Figure 13 Pneumatic or multi-phase nozzle (Mini Spray-Dryer Buchi B-290).

After atomization, the spray comes into contact with the gas. The gas used in this drying process can simply be pre-filtered and treated with pressurized air. For unstable substances, inert gases

such as nitrogen or argon are preferred. The way the spray and airflow interact and the motion they create in the drying chamber, due to the friction exerted by the airflow on the spray, significantly affects the properties of the resulting particles.

The evaporation of water or other solvents from a spray involves both mass and heat transfer. The atomization of the feed liquid provides a large surface area, allowing heat to be transferred from the air to the droplets through convection and converted into latent heat of evaporation. Additionally, the liquid exits the atomizer at a speed different from that of the incoming air, which also allows for momentum transfer between the droplets and the air. Initially, the evaporation rate and surface temperature of the droplets in the spray are nearly constant, with most of the water being removed during this phase. Once a certain moisture content is reached, the droplet becomes a particle with a solid, dried shell, and the drying process changes: the drying rate decreases, and the surface temperature of the particles increases. As the particle dries, its temperature approaches that of the surrounding gas [116].

After drying, particles may settle at the bottom of the chamber and be collected in specific devices, or they may exit the chamber with the outgoing air. In the latter case, separation is achieved using cyclones, which separate solid particles from the air using the centrifugal force generated by rapidly rotating the air. The particles are directed toward the walls of the device and separated from the air core formed around the device's axis. The cyclone is typically followed by a scrubber, a wet separator that purifies the outgoing air of any remaining suspended dust particles. Other separation devices, such as those based on electrostatic fields, are rarely used, primarily due to their high cost [117].

When the product is adequately separated from the airflow, it must be collected. In pharmaceutical applications, collection must consider the specific morphology of the particles, low flowability, or high hygroscopicity of the product, and often must be done aseptically. In a

laboratory or experimental scale system, the product is often collected in a sealed container and retrieved when the process is complete.

The primary operating factors that control the Spray-Dryer process are:

- Temperature at the inlet and outlet of the central chamber.
- Feed rate.
- Viscosity of the feed.
- Type of atomizer used.
- Solvent of the feed.
- Yield of the process.

Because of the rapid rate at which the solvent evaporates, high intake temperatures have an impact on the process of particle formation. This process may result in a pressure gradient both inside and outside the droplet, which could have an impact on the powder's final morphology. The particle may collapse completely or have a porous surface as a result of the solvent's internal vapor pressure. Higher temperatures can speed up the drying process, but heat-sensitive materials might be harmed [118].

The powder's final moisture content is determined by the air temperature at the output [119]. The mass of preparation transported per unit of time within the drying chamber is generally referred to as the feed rate. It has been shown that increased feed rates lead to decreased yield and greater final particle moisture content. Due to technological constraints, very high feed rates may cause a closed-loop circuit configuration's capacitors to overflow [115].

The final particle size increases as the feed's viscosity increases due to a drop in temperature or an increase in the amount of solids in a suspension. Reduced viscosity means that less force or energy is needed to produce a targeted spray pattern that improves drying [120].

Selecting the right type of atomizer depends on a number of factors:

1. Air-spray contact phase layout.
2. The final powder's dimensional distribution.
3. The atomizer's maximum capacity.
4. The atomizer's adaptability.
5. Fluid characteristics.

The equivalent configuration allows for the use of both rotary atomizers and two-phase nozzles, while the countercurrent arrangement is primarily used with two-phase nozzles, as the airflow tends to favor the impact of the spray with the walls, necessitating an increase in the already large diameter of the chamber [112].

The maximum discharge capacity and the particle size distribution are influenced by the type of atomizer that is utilized. The biphasic nozzles have a limited disposable flow rate and are better suited for the creation of raw products. Higher capacity and finer particle applications are also possible with rotary atomizers. Because they may modify the rotational speed to vary the feed rate while keeping the size distribution constant, rotary atomizers are often more flexible than two-phase nozzles. Lastly, an examination of the fluid's physicochemical characteristics is also required before atomization. If a different kind of atomizer is to be used, the viscosity of the very viscous liquids must be reduced by heating them beforehand. Otherwise, bifasic nozzles are necessary [121].

The drying process is impacted by the solvent selected during the feed fluid preparation stage. It is beneficial to utilize solvents with low boiling points because they evaporate easily and produce high-quality dried particles. In these circumstances, however, a closed-loop system with a condenser that recovers the evaporated solvent and keeps it from escaping into the

surrounding air should be employed, albeit at a considerable process cost increase. The following are some of the factors that make water a better solvent than organic ones [117].

The yield of the process is strongly influenced by two main factors: the loss due to suboptimal process factors and the formulation of the material. It is therefore necessary to select an appropriate Spray-Dryer with optimal design features, such as a large drying chamber for rotary atomizers or a high-efficiency collection cyclone [115].

2 AIM AND OBJECTIVES

The prevalence of inflammatory bowel disease (IBD), including Crohn's disease (CD) and ulcerative colitis (UC), has increased significantly over the past three decades. The triggering cause of IBD is not singular but rather multifactorial, with genetic predisposition factors intersecting with components related to the intestinal microbiome, environment, and patient lifestyle. This interaction not only adds to the complexity of the disease's pathogenesis but also presents multiple opportunities for interventions to enhance patient outcomes. Traditional therapeutic approaches, such as corticosteroids, immunomodulators, and biological agents, have transformed the landscape of IBD treatment, leading to improved clinical outcomes and quality of life for many patients. However, significant challenges remain, such as adverse effects, potential toxicity, and the threat of drug resistance or intolerance. These limitations underscore the urgent need for novel therapeutic strategies that can improve existing treatments or provide alternative options for patients.

Natural compounds have emerged as a promising area of interest, offering a potential complementary approach to IBD management. Derived from plants, herbs, and other natural sources, these compounds have been recognized for their anti-inflammatory, antioxidant, and immunomodulatory properties, which could be leveraged to modulate the complex pathophysiological processes underlying IBD.

Quercetin, a flavonoid, has been the subject of extensive research for its anti-inflammatory effect through the inhibition of myeloperoxidase, an enzyme released by activated neutrophils and macrophages at inflammation sites.

Phycocyanin (PC), a water-soluble blue-colored pigment protein, has been highlighted by the World Health Organization (WHO) as a potential medicinal natural compound. Research has shown that phycocyanin can inhibit enzymes involved in inflammation, reduce the recruitment

of inflammatory cells, and neutralize harmful free radicals, offering protection against cellular damage.

Vitamin D, particularly in its active form as cholecalciferol (Vitamin D3), may play a significant role in the pathogenesis and progression of IBD. Vitamin D is crucial for maintaining bone health and has profound effects on the immune system, which are especially relevant to IBD. In the innate immune system, Vitamin D enhances the expression of antimicrobial peptides, such as cathelicidins and defensins, which play a crucial role in maintaining gut barrier integrity and preventing pathogenic infections.

Quercetin and vitamin D are active molecules with low water solubility that pose a significant challenge in pharmaceutical formulation development, so improving their solubility is considered a key driver for greater bioavailability. On the other hand, phycocyanin is a water-soluble molecule but not very stable in the gastric environment due to its protein composition.

Various pre-formulation strategies, such as the transformation of drugs into an amorphous solid dispersion (ASD) form, have drawn interest in recent decades. An ASD is defined as a dispersion of the API in an amorphous polymer matrix at the molecular level. Overall, selecting polymers with appropriate Tg, miscibility, and hydrophilic properties can enhance ASD stability and drug dissolution. These polymers also help maintain the amorphous state and improve wettability, thereby supporting the effective delivery of poorly soluble drugs.

The above properties may also be shown by proteins, that are natural polymers, biodegradable, biocompatible, and possess functional properties relevant for use as pharmaceutical encapsulating materials. In particular, whey proteins have been studied for several years and have demonstrated good solubility across a wide pH range, as well as flexibility, making them suitable for encapsulating active ingredients, even in pharmaceutical applications; nevertheless, are recognized as Generally Recognized as Safe (GRAS). On the other hand, considering the

growing number of vegetarians and people avoiding lactose in their diets, plant proteins such as soy proteins present a further alternative, although their potential for pharmaceutical applications has yet to be fully explored, unlike their well-established use in the food industry.

Among the different production techniques, spray drying is one of the widely used processes for manufacturing ASDs because it provides flexibility in the selection of solvents, range of temperatures, kind of liquid dispersions injectable, and pump speeds. Changing these parameters can modify the final product properties improving particle size homogeneity, wettability, moisture content, and solubility, through the reduction of the particle size. Finally, the combination of the technological advantage offered by the spray-drying combined with the formulation benefits provided by the selection of suitable compounds within amorphous solid dispersion would lead to the manufacturing of a complete and functional drug delivery system.

Therefore, this work aimed to formulate, produce, and characterize modified-release microparticles produced using the spray drying technique, containing natural active ingredients such as quercetin (Q) and cholecalciferol (D), or phycocyanin (PC), based on soy and whey proteins as gastroresistant agents, to obtain an enteric release profile.

Several batches of microparticles containing the above-selected active ingredients were produced using the spray drying technique. Specifically, three different batches for each active ingredient were produced, one based on whey proteins and the active ingredient (MPs W-Q, W-D, and W-PC), another based on a 1-to-1 mix of whey proteins and soy proteins (MPs SW-Q, SW-D, and SW-PC), and finally a final batch containing whey proteins and milk used as the dispersing phase (MPs M-Q and M-D). Only for phycocyanin the third batch corresponds to a batch of microparticles based on soy proteins (MPs S-PC). This is justified by the difference in the chemical nature of this active ingredient compared to the other two.

All nine batches of microparticles were subjected to an accurate chemical-physical characterization study based on various instrumental investigations.

UV spectroscopic analysis was used to determine the efficiency of the microencapsulation process and also calculate the drug loading % (actual quantity of microencapsulated active ingredient).

Scanning electron microscopy (SEM) was used to study the morphology of the microparticles and their average diameter size.

FTIR analysis was used to evaluate degradation phenomena and verify that the APIs and excipients have been incorporated into the microparticles by comparing the spectra of the individual pure substances and the final product.

Thermogravimetric analysis (TGA) was used to determine the thermal stability of the produced systems by measuring the mass variation that occurs when the species is heated, subjecting the sample to a controlled thermal cycle.

The microparticles were also subjected to a solid state characterization carried out by X-ray Powder Diffraction (XRPD) analysis used to reveal the amorphous or crystalline nature of the APIs and excipients and to confirm whether an amorphous product was obtained from spray drying and by differential scanning calorimetry (DSC) analysis. The latter is a common technique for thermal investigation, that offers information about the thermal behavior of materials and is especially helpful for describing the physical state of pharmaceutical formulations. When it comes to ASDs, DSC is essential for figuring out whether the excipients and APIs are present in an amorphous state, which is critical for improving their solubility and bioavailability.

Furthermore, the batches of microparticles formulated with quercetin and phycocyanin were subjected to DPPH (2,2′-diphenyl-1-picrylhydrazyl radical) free radical scavenging assay to confirm the already known radical scavenger activity of these molecules even though the production process using the spray-drying technique requires the use of stringent operating parameters (such as high operating temperatures).

To demonstrate the ability of the microparticle systems produced to release the incorporated active molecules according to a specific profile, dissolution studies were conducted in systems appropriately designed to simulate the passage of the formulation through the gastrointestinal tract. The ex-vivo permeation studies on porcine intestinal mucosa aimed to assess whether the active molecules formulated in microparticles demonstrated increased permeation compared to pure APIs, thereby allowing for a potential prediction of improved bioavailability in vivo.

Based on the results obtained from the dissolution study and the permeation study through animal mucosa, five different batches (MPs SW-Q, MPs M-Q, MPs SW-D, MPs M-D, and MPs S-PC) were selected and then subjected to an in vivo model of 2,4-dinitrofluorobenzene sulfonic acid (DNBS)-induced colitis in rats. In particular, cholecalciferol and quercetin were tested in co-administration while the activity of phycocyanin was evaluated alone. The type of treatment we tested included a pre-treatment period and a subsequent treatment period.

Finally an in vivo bioavailability evaluation was also carried out on cholecalciferol and phycocyanin and the corresponding selected batches of these two active ingredients.

3 RESULTS AND DISCUSSION

3.1 Design and Preparation of Gastro-Resistant Microparticles using the Buchi B-290 Mini Spray-Dryer

The microparticles were produced starting from a suitably prepared dispersion (feed), containing both the active ingredient and the excipients, and were subsequently subjected to the drying process in the spray dryer (Figure 14).

Figure 14 Image of the Mini Spray-Dryer Buchi B-290.

The dispersed system was obtained by dispersing a mixture of specific excipients in water or milk, carefully selected to ensure both the gastroresistance of the final formulation and efficient

incorporation of the API within the microparticles. To improve the final characteristics of the microparticles produced each time, in terms of yield, encapsulation efficiency, and stability, special attention was given to the following aspects:

> Optimization of the operating parameters of the spray dryer;

> Composition and preparation method of the pharmaceutical formulation.

The process parameters of a spray dryer are interrelated, with the most relevant being: inlet and outlet temperature, the performance of the aspirator and peristaltic pump, nozzle cleanliness, and inlet airflow. These parameters can be adjusted by the operator as needed, using a display with control elements (Figure 15).

① LED display current value inlet air temperature
② LED display current value outlet air temperature
③ LED display set value inlet air temperature
④ LED display aspirator output in % of max. aspirator rate
⑤ LED display pump output in % of max. pump rate
⑥ LED display for nozzle cleaning
⑦ Feed switch valve button
⑧ Nozzle cleaner interval adjustment
⑨ Manual operation pneumatic nozzle cleaner
⑩ Regulating push-button pump
⑪ Main switch pump
⑫ Regulating push-button aspirator
⑬ Main switch aspirator
⑭ Regulating push-button heating
⑮ Main switch heating

Figure 15 Description of the control elements display of the Mini Spray-Dryer Buchi B-290.

During the optimization process, it was observed that maintaining a temperature gradient between the inlet temperature in the chamber (130°C) and the outlet temperature from the chamber (75°C) is essential to ensure a lower residual moisture content in the final product. An inlet temperature higher than 130°C would increase the outlet temperature as well, with the

consequent transfer of a greater amount of heat to the sample to be dried. For heat-sensitive active ingredients, this could lead to degradation and inactivation of the substances to be encapsulated. Several trials were conducted by varying the feed dispersion withdrawal rate: a sample withdrawal rate of about 4.5 ml/min (15%) ensures a final yield of around 50%, while higher withdrawal rates drastically decrease the yield and do not guarantee good atomization of the withdrawn product. For this spray drying process, a two-phase nozzle was used, which was found to be suitable for drying dispersed systems like those used in this study, allowing simultaneous entry of the feed and drying gas into the central chamber.

The operating parameters of the Buchi B-290 mini Spray-Dryer that were used for the production of the final microparticles were:

- Inlet temperature: 130°C
- Outlet temperature: 70-73°C
- Aspirations: 100%
- Feed pump: 15%
- Atomizer nozzle: 0.7mm
- Used gas: Compressed Air

The study on the formulation of the pharmaceutical form was based on the search for suitable excipients to guarantee a modified release profile of the drug of the gastro-resistant type, efficient incorporation of the active ingredients inside the microparticles, and the stability of the system. The fundamental premise was to find and test excipients of natural origin that had properties such as conferring technological advantages to the final microparticles. The choice, in particular, fell on whey proteins and soy protein. Together, whey and soy proteins are ideal excipients for encapsulating different APIs. Their complementary properties—whey for its solubility and bioavailability, and soy for its stability and resistance to acidic conditions—make

them an effective duo in ensuring that the final product remains stable, functional, and bioavailable.

Whey proteins and soy protein are used to create amorphous solid dispersions that can enhance the solubilization of lipophilic active ingredients. These proteins act as carriers, helping to stabilize the active compounds in an amorphous state, which is typically more soluble than their crystalline form. By dispersing lipophilic substances in a protein matrix, the surface area exposed to solvents is increased, facilitating better dissolution and absorption in the body.

This approach is particularly useful for improving the bioavailability of poorly water-soluble drugs, allowing them to be more effectively absorbed in the gastrointestinal tract [122], [123].

Milk has also been used as an excipient, particularly as a dispersed phase, to improve the solubilization and bioavailability of lipophilic active ingredients such as quercetin and cholecalciferol. Milk is a naturally occurring emulsion, rich in fats, proteins (casein and whey), and phospholipids, making it an excellent medium for enhancing the dispersion of lipophilic compounds. The fat content in milk provides a natural carrier for these compounds, improving their solubility and protecting them from degradation during formulation and digestion. Overall, milk serves as a functional excipient for these lipophilic compounds by enhancing their dispersion, protecting them from premature degradation, and improving their solubility, ultimately leading to increased bioavailability. This makes milk-based systems highly effective in pharmaceutical and nutraceutical formulations designed to deliver lipophilic active ingredients more efficiently [124].

The approach was to apply a preparation method as consistent as possible for each batch, making it reproducible and minimizing variations in the production process itself. The operational parameters of the spray dryer were also kept constant for every batch. The standardization of the process was further facilitated by the fact that the behavior of the

excipients during production was similar due to their comparable physicochemical properties. This allowed the exclusion of any differences between individual batches being attributed to the influence of the formulation process during subsequent characterization phases.

All batches were prepared by solubilizing the active pharmaceutical ingredients in ethanol (max 10 % v/v), while the proteins were added to the total solvent volume (distilled water or whole milk) under constant agitation. The two preparations were then mixed and processed using an ultra-turrax homogenizer to create ultra-fine dispersions, which were subsequently subjected to spray drying (Figure 16).

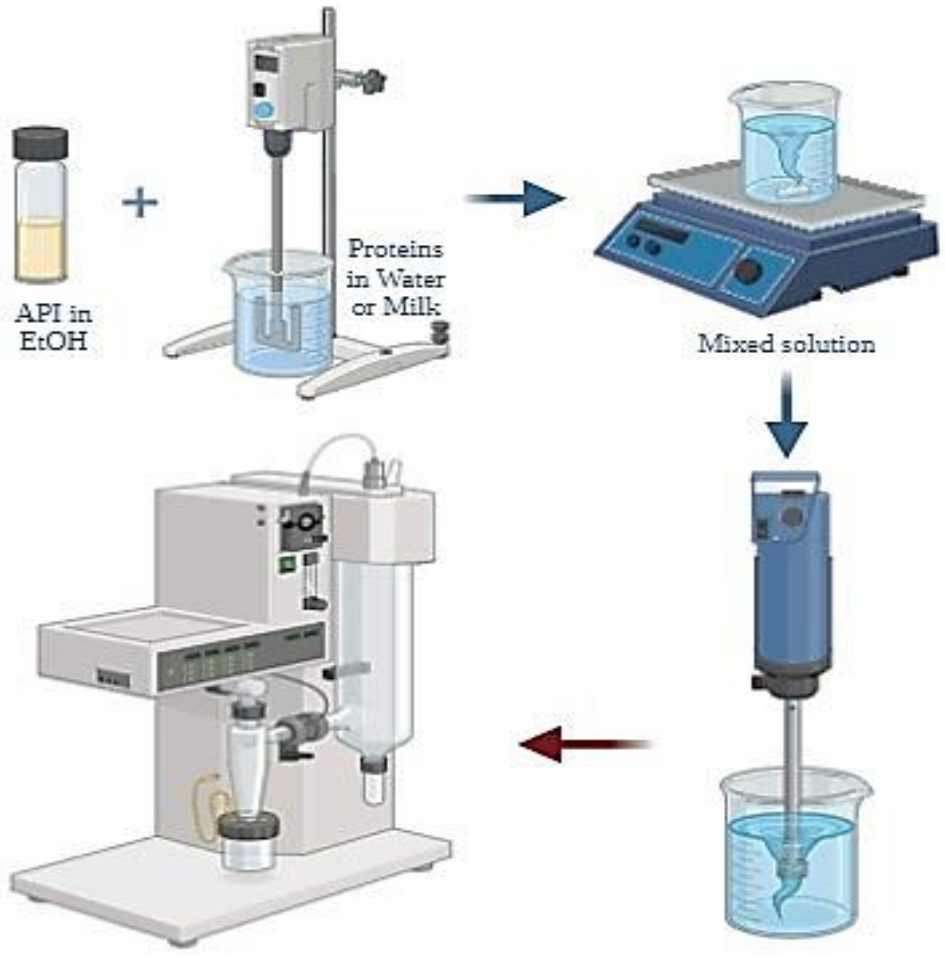

Figure 16 Summary of the formulation process steps.

This method minimized batch-to-batch variability, promoting a more consistent and reliable production process. Such consistency is essential for maintaining the quality and performance of all formulations.

In this work, three different batches were produced for the three selected active ingredients: quercetin, cholecalciferol, and phycocyanin.

To prepare Quercetin MPs (batches W-Q, SW-Q, and M-Q), the excipients (whey proteins and soy proteins) were dispersed in distilled water (W-Q and SW-Q) or milk (M-Q) under continuous stirring at 25 °C for 30 min. A specific amount of quercetin, previously solubilized in ethanol, was added and the dispersion was stirred for another 30 min. Then, 5 minutes of ultraturrax were applied to the final suspension (Table 4).

Batches with Quercetin	**Formulations' composition**
MPs WQ	2.5 g WPs; 0.65 g Quercetin; 10 ml Ethanol; 50 ml Water
MPs SW-Q	2.5 g WPs; 2.5 g SPs; 0.5 g Quercetin; 10 ml Ethanol; 100 ml Water
MPs M-Q	5,5 g di WPs; 2 g Quercetin; 10 ml Ethanol; 100 ml Milk

Table 4 Composition of the MPs formulations produced with quercetin.

To prepare Cholecalciferol MPs (batches W-D, SW-D, and M-D), the excipients (whey proteins and soy proteins) were dispersed in distilled water (W-D and SW-D) or milk (M-D) under continuous stirring at 25 °C for 30 min. A specific amount of cholecalciferol, previously solubilized in ethanol, was added and the dispersion was stirred for another 30 min. Then, 5 minutes of ultraturrax were applied to the final suspension (Table 5).

Batches with Cholecalciferol	Formulations' composition
MPs WD	2.5 g WPs; 0.1 g Cholecalciferol; 5 ml Ethanol; 50 ml Water
MPs SW-D	2.5 g WPs; 2.5 g SPs; 0.1 g Cholecalciferol; 5 ml Ethanol; 100 ml Water
MPs M-D	5.5 g WPs; 0.4 g Cholecalciferol; 5 ml Ethanol; 100 ml Milk

Table 5 Composition of the MPs formulations produced with cholecalciferol.

To prepare Phycocyanin MPs (batches W-PC, SW-PC, and S-PC), the excipients (whey proteins and soy proteins) were dispersed only in distilled water under continuous stirring at 25 °C for 30 min. A specific amount of phycocyanin was added and the dispersion was stirred for another 30 min. Then, 5 minutes of ultraturrax were applied to the final suspension (Table 6).

Batches with Phycocyanin	Formulations' composition
MPs W-PC	2.5 g WPs; 0.8 g Phycocyanin; 50 ml Water
MPs SW-PC	2.5 g WPs; 2.5 g SPs; 0.8 g Phycocyanin; 100 ml Water
MPs S-PC	2.5 g SPs; 0.8 g Phycocyanin; 50 ml Water

Table 6 Composition of the MPs formulations produced with phycocyanin.

3.2 Characterization Study of the Produced Microparticle Systems

In Figure 17, the macroscopic aspect of a batch of microparticles for each API among all those produced can be observed.

Figure 17 Macroscopic aspect of the produced microparticles containing quercetin (yellow), cholecalciferol (white), and phycocyanin (blu).

After the microparticle production, the characterization study of the produced microparticles began with the calculation of the percentage yield of the process (% Y), as:

$$\%Y = \frac{\text{Mass of excipients and active ingredient in the formulation}}{\text{mass of microparticles obtained}} \times 100$$

The drug loading (DL%) was calculated according to the formula below, and the amount of active molecules encapsulated in each micro-delivery system was assessed spectrophotometrically.

$$\%\ DL = \frac{\text{Mass of active ingredient in microparticles}}{\text{mass of microparticles}} \times 100$$

The encapsulation efficiency (%EE) was determined by accounting for the encapsulated active ingredients within their respective MPs systems and the amount introduced in the feed of the spray dryer.

$$\%\ EE = \frac{\text{Mass of active ingredient in microparticles}}{\text{mass of active in the feed}} \times 100$$

The percentage yield, drug loading, and encapsulation efficiency values for all the batches produced, are presented in Table 7:

Batches	Yield % ± SD	DL % ± SD	EE% ± SD
MPs WQ	73 % ± 0.4	8 % ± 1	76 % ± 1
MPs SW-Q	47 % ± 0.3	10 % ± 0.3	99% ± 1
MPs MQ	60 % ± 0.5	7 % ± 2	70% ± 2
MPs WD	71 % ± 0.3	1 % ± 2	56 % ± 2
MPs SW-D	42 % ± 0.1	3 % ± 1	99% ± 1
MPs MD	65 % ± 0.4	1.2 % ± 3	53 % ± 3
MPs W-PC	52% ± 0.3	17 % ± 2	71 % ± 2
MPs SW-PC	30 % ± 0.2	23 % ± 3	95 % ± 5
MPs S-PC	20 % ± 0.1	17 % ± 3	71 % ± 3

Table 7 Obtained values of yield, drug loading, and encapsulation efficiency of the batches of the produced microparticles.

The whey proteins batches labeled WQ, MQ, WD, MD, and W-PC all performed exceptionally well in terms of production yield. These batches' yield values were significantly higher than the spray-drying instrument's average, which is typically around 50%. This is due to the high efficiency of whey proteins in speeding up the spray-drying process and guaranteeing more efficient production of the final microparticles. The optimal physicochemical characteristics of whey proteins, such as their solubility, emulsifying potential, and film-forming qualities, are responsible for the higher yield. These qualities also probably helped with the better atomization and drying of the feed dispersion, reducing material loss and optimizing the recovery of the powder [125].

As opposed to the whey protein batches, the batches made with soy proteins showed a different performance profile, with production yields that were continuously less than 50%. This suggests that the end product was recovered less effectively. While soy proteins have similar emulsifying and film-forming qualities to whey proteins, they differ in structure and solubility. As a result, it's possible that during the spray-drying process, soy proteins will form aggregates or larger particles that are more likely to stick to the drying chamber walls or get lost in the drying gas stream. This can result in more material loss, which would ultimately reduce the production yield as a whole.

Moreover, these protein-based batches exhibit very promising encapsulation efficiency values. This indicates that during the drying process, a significant amount of the active ingredients, including phycocyanin, cholecalciferol, and quercetin, were effectively integrated into the final microparticles. Encapsulation efficiency is a critical spray drying data that measures how well the formulation traps and shields the APIs in the outcome. The high encapsulation efficiencies observed in these batches suggest that whey and soy proteins were highly effective in creating stable microparticles that kept the majority of the active substances in the finished product and shielded the APIs from degradation.

SEM analysis (Scanning Electron Microscopy) was used to observe the microparticles' surface characteristics and their average size.

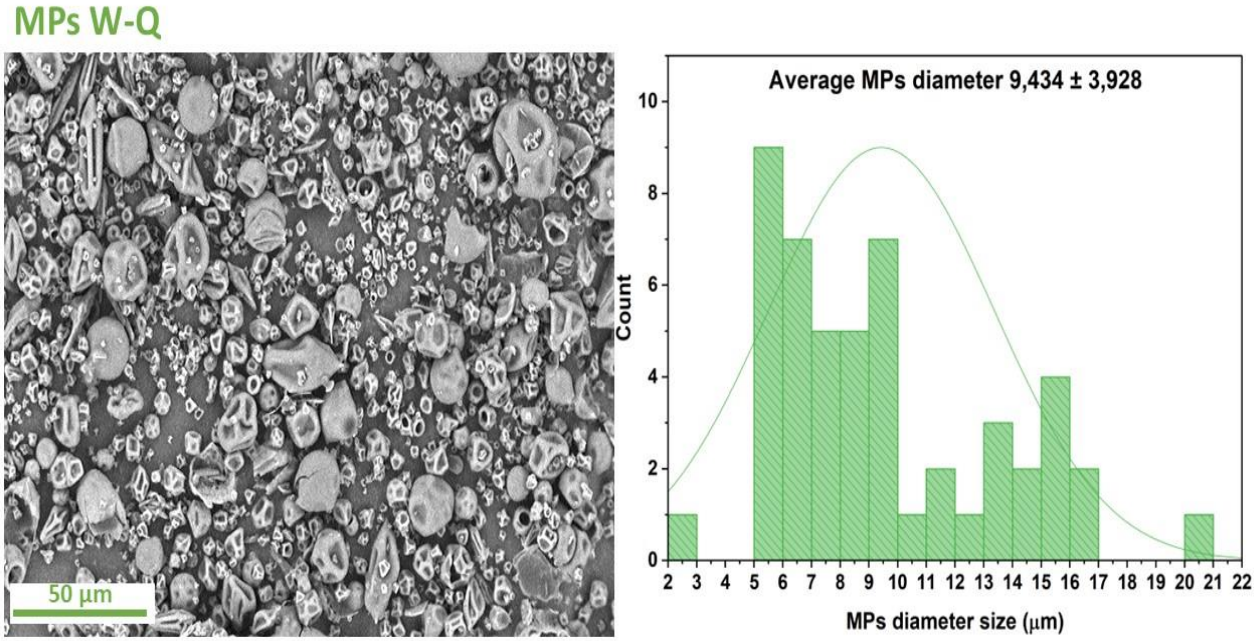

Figure 18 SEM image of the MPs W-Q and diameter distribution of the microparticles.

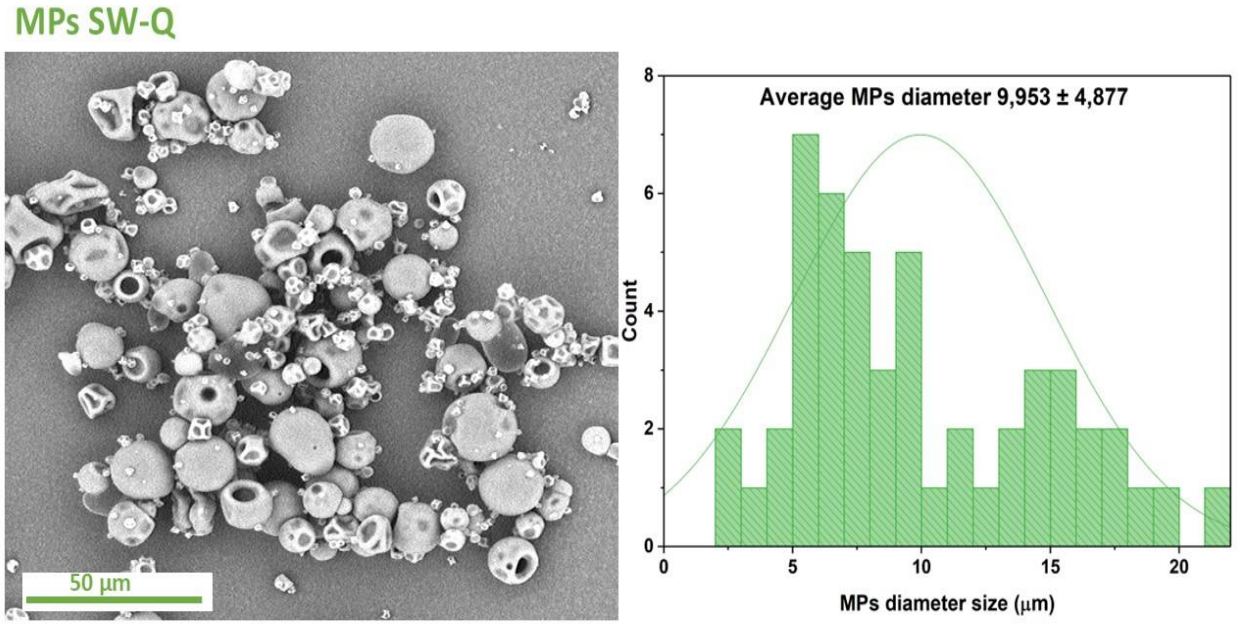

Figure 19 SEM image of the MPs SW-Q and diameter distribution of the microparticles.

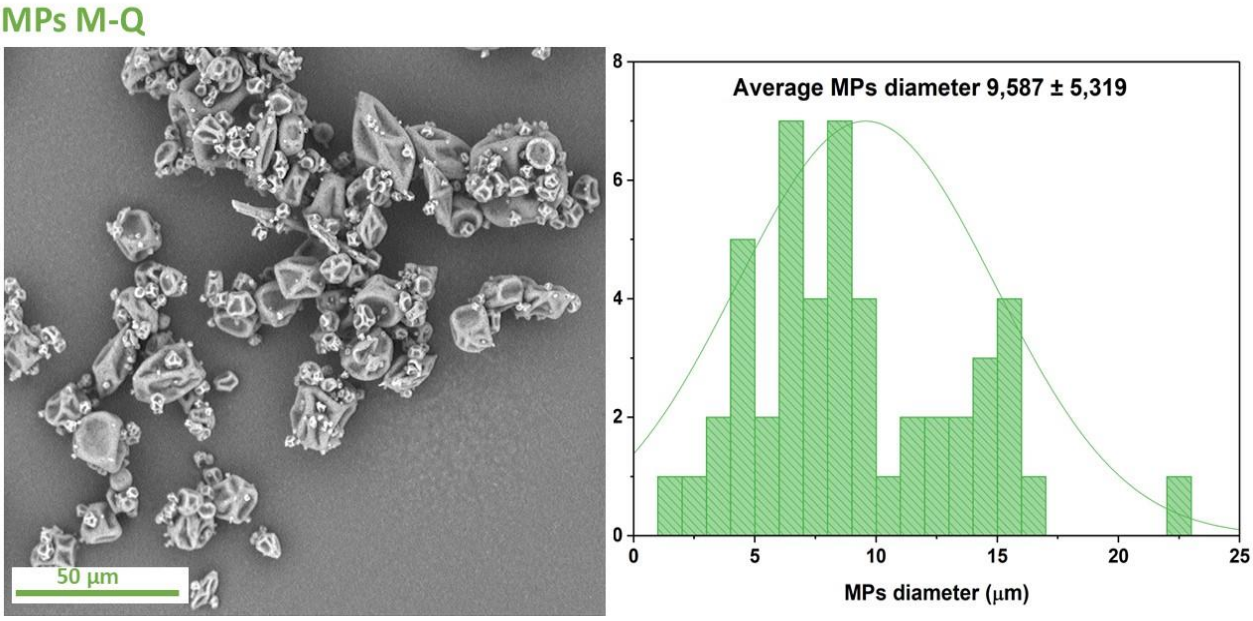

Figure 20 SEM image of the MPs M-Q and diameter distribution of the microparticles.

SEM images of quercetin microparticles (Figure 18-19-20) revealed a quite uniform morphology in all batches. The mean microparticles size distribution was 9 to 10 µm. Some of the microparticles appeared to have collapsed, likely from the high temperatures during spray drying. This is a common phenomenon in spray drying, this collapse occurs due to the possible heat deformation of particle structures. In particular, the rapid evaporation of the solvent and drying can create internal stress in particles leading to partial or complete breakdown. Even with these deformations, the general spherical structure of the particles remained, ensuring proper particle size and morphology for potential applications.

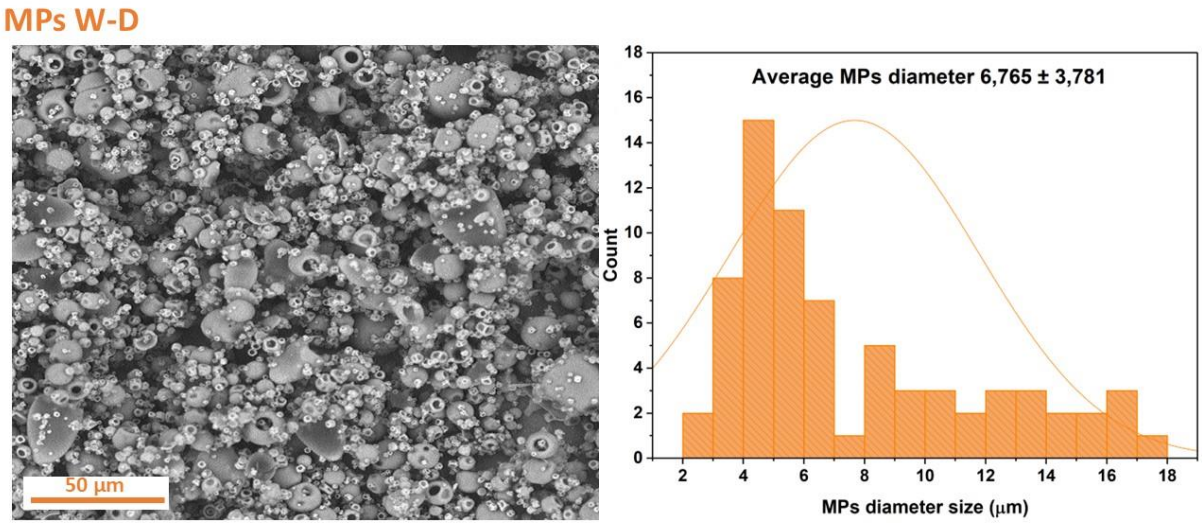

Figure 21 SEM image of the MPs W-D and diameter distribution of the microparticles.

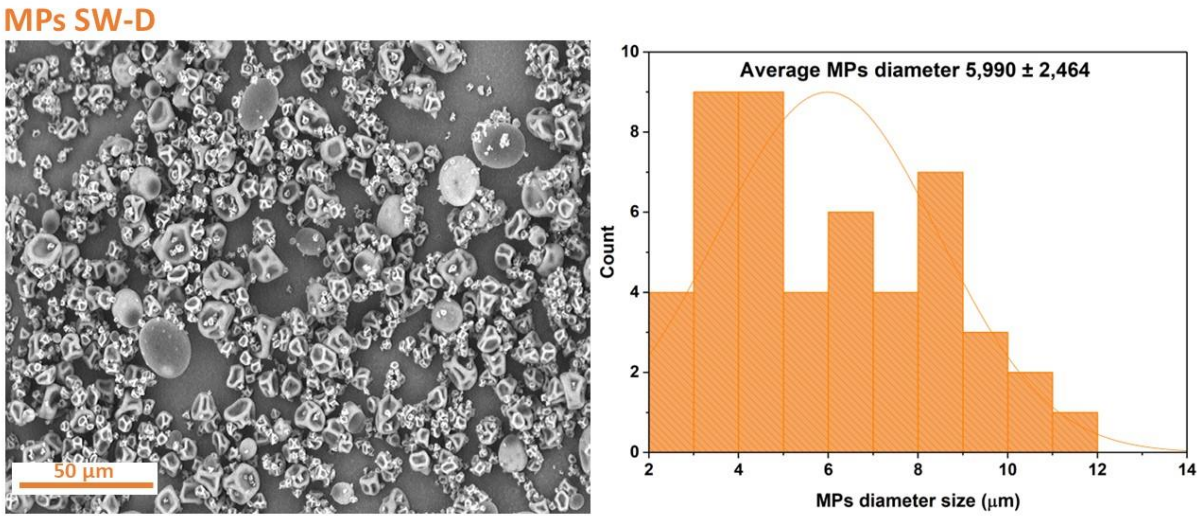

Figure 22 SEM image of the MPs SW-D and diameter distribution of the microparticles.

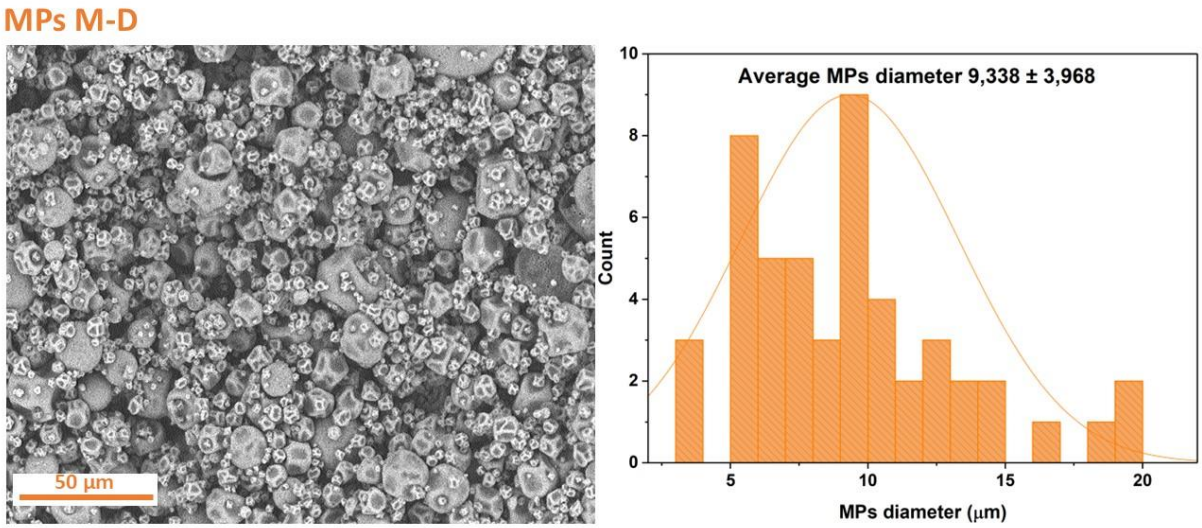

Figure 23 SEM image of the MPs M-D and diameter distribution of the microparticles.

In the case of cholecalciferol's microparticles (Figure 21-22-23), the mean microparticles size distribution was 6 to 9 µm. Also in this case, we can see how some of the microparticles appear to have a collapsed structure, while others present a regular spherical structure showing a certain diversity in the morphological uniformity.

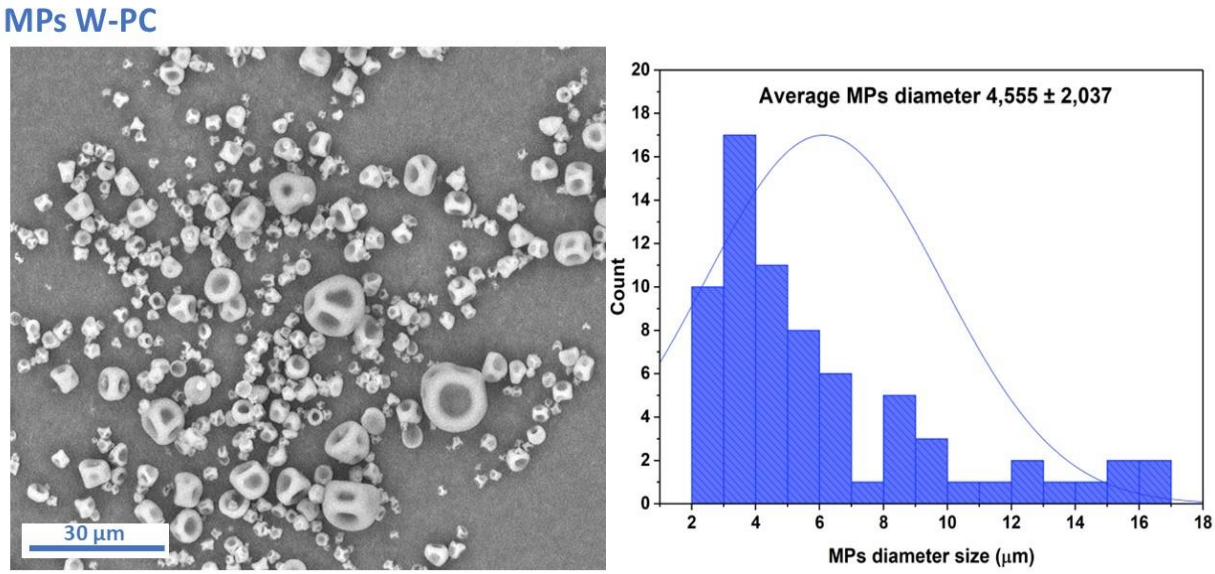

Figure 24 SEM image of the MPs W-PC and diameter distribution of the microparticles.

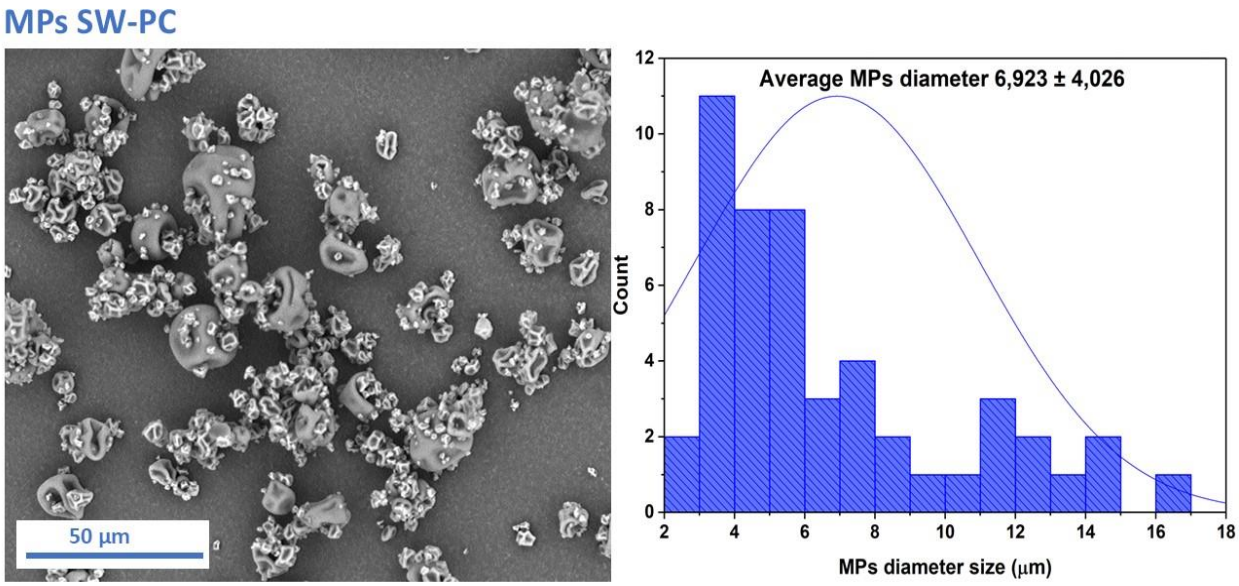

Figure 25 SEM image of the MPs SW-PC and diameter distribution of the microparticles.

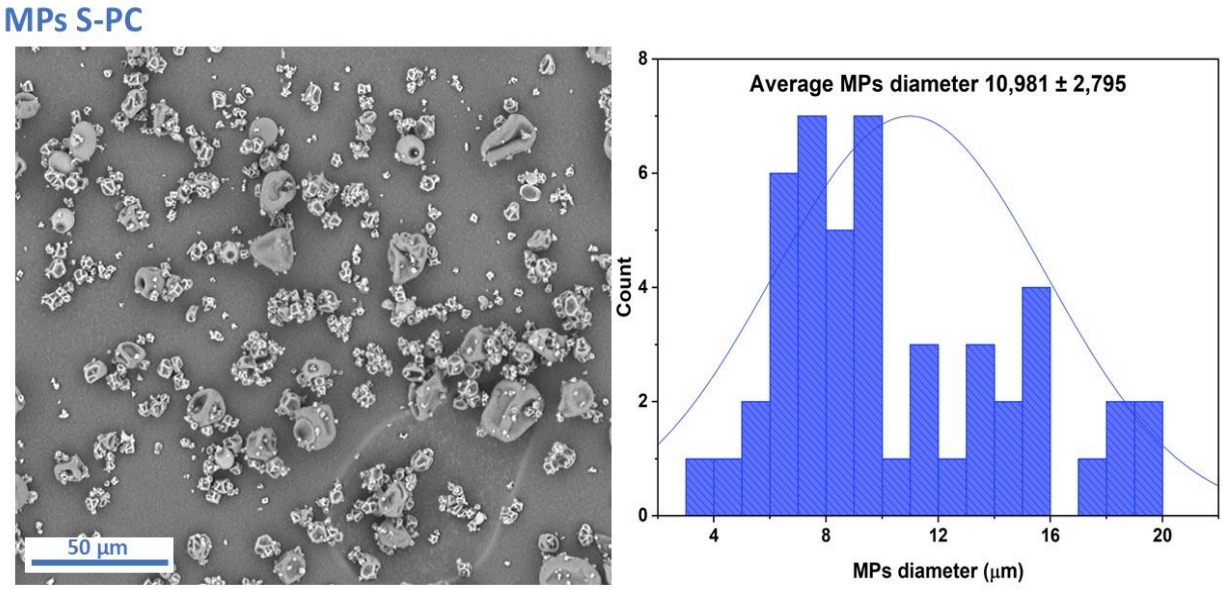

Figure 26 SEM image of the MPs S-PC and diameter distribution of the microparticles.

The mean PC's microparticles diameter distribution was 5 to 10 µm, with a more regular spherical uniform morphology compared to the other batches of the produced microparticles (Figure 24-25-26).

FTIR analysis was used to evaluate the actual incorporation of APIs into the microparticles, as well as the absence of any degradation to the components of the formulation. The IR spectrum is presented as a graph in which the following are reported: on the abscissa axis the frequency of the absorbed IR radiation expressed in wavenumbers and on the ordinate axis the percentage of transmittance (T %) is reported, that is the percentage of incident radiation that passes through the sample without being absorbed. FTIR analysis allows, through the attribution of the peaks to certain functional groups of the molecules, to trace the analyzed compound. To carry out the analysis, the powders of active ingredients, excipients, and formulations were mixed with potassium bromide (KBr) and compressed with a press. After compression, a thin compact of powder with a translucent appearance is obtained which will be placed inside a suitable support to be inserted into the instrument.

Table 8 summarizes the peak assignment of each pure API and the respective peaks found in each formulation. The identified peaks found relevant correspondence in the literature, and no particular signs of active ingredient degradation were detected (Table 8).

Quercetin cm^{-1} [126]	**MPs W-Q cm^{-1}**	**MPs SW-Q cm^{-1}**	**MPs M-Q cm^{-1}**
1661,82	1649,72	1655,24	1657,81
Stretching C=O			
1560,72	1536,78	1523,89	1530,41
Stretching C=C			
1260	1263,02	1263,02	1256,8
Bending C-O-C			

Cholecalciferol cm^{-1} [127]	**MPs W-D cm^{-1}**	**MPs SW-D cm^{-1}**	**MPs M-D cm^{-1}**
3309,73	3292,6	3299,1	3298,4
Stretching O-H			
2933,68	2963,6	2959,9	2960,3
Stretching -CH_2			
1645,91	1649,23	1655,24	1648,6
Stretching C=C			
Phycocyanin cm^{-1} [128]	**MPs W-PC cm^{-1}**	**MPs SW-PC cm^{-1}**	**MPs S-PC cm^{-1}**
2929,59	2931,43	2934,42	2930,2
Stretching O-H			
1655	1652,79	1649,72	1649,72
Stretching C=O ammide I			
1545	1543,4	1544.8	1545
Stretching C=O ammide II			

Table 8 FTIR peak assignment for each active molecule and the respective peaks found in each MPs formulation.

To verify the incorporation of each active ingredient into the microparticles, the spectra of the individual excipients, the API present in the formulations, and the microparticles obtained from each production batch were analyzed and compared (Figures 27 to 35).

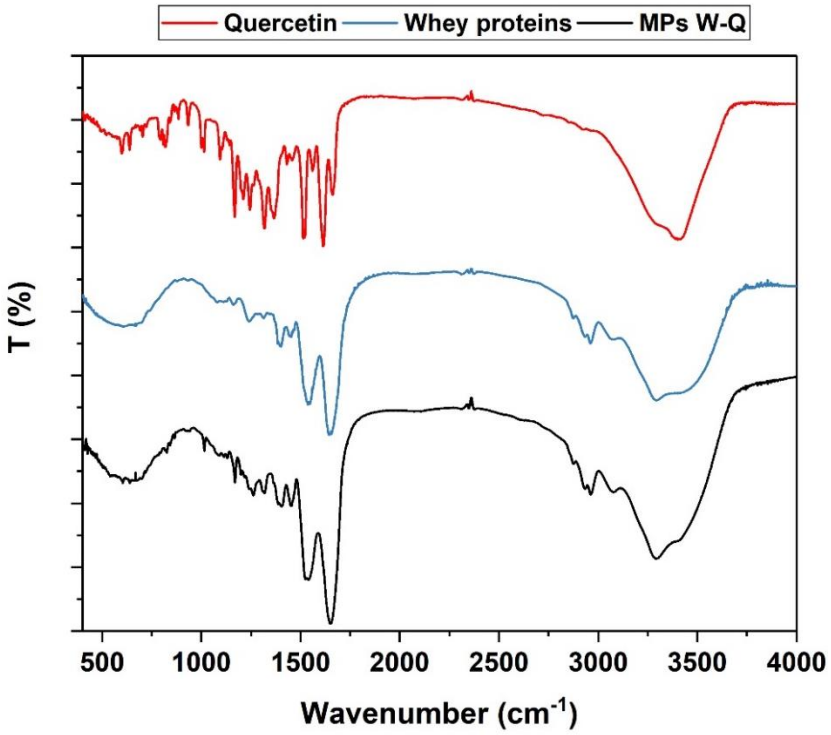

Figure 27 Comparison of FTIR spectra of quercetin, whey proteins, and MPs W-Q.

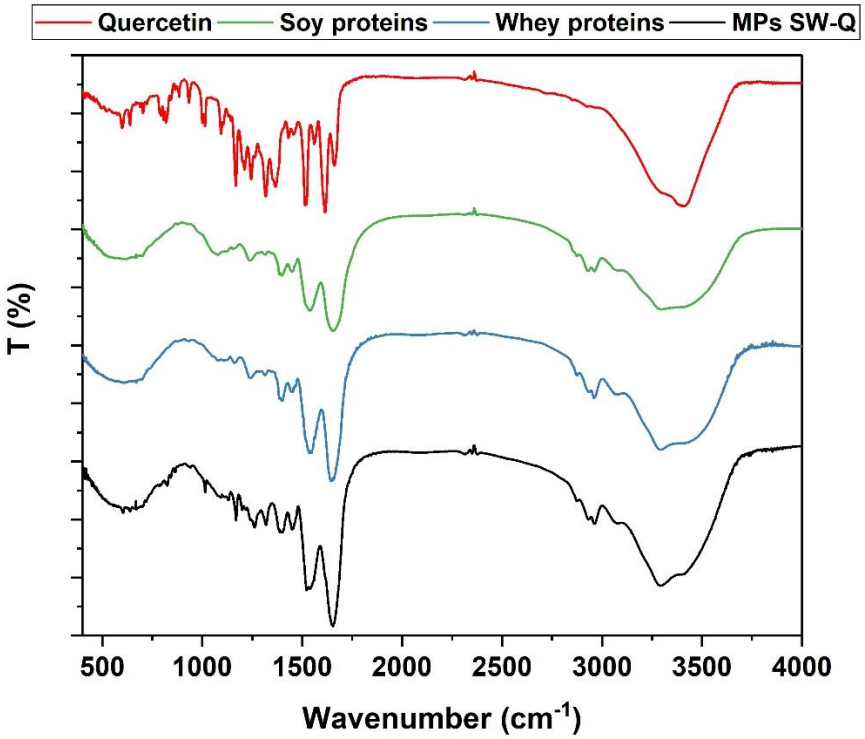

Figure 28 Comparison of FTIR spectra of quercetin, soy proteins, whey proteins, and MPs SW-Q.

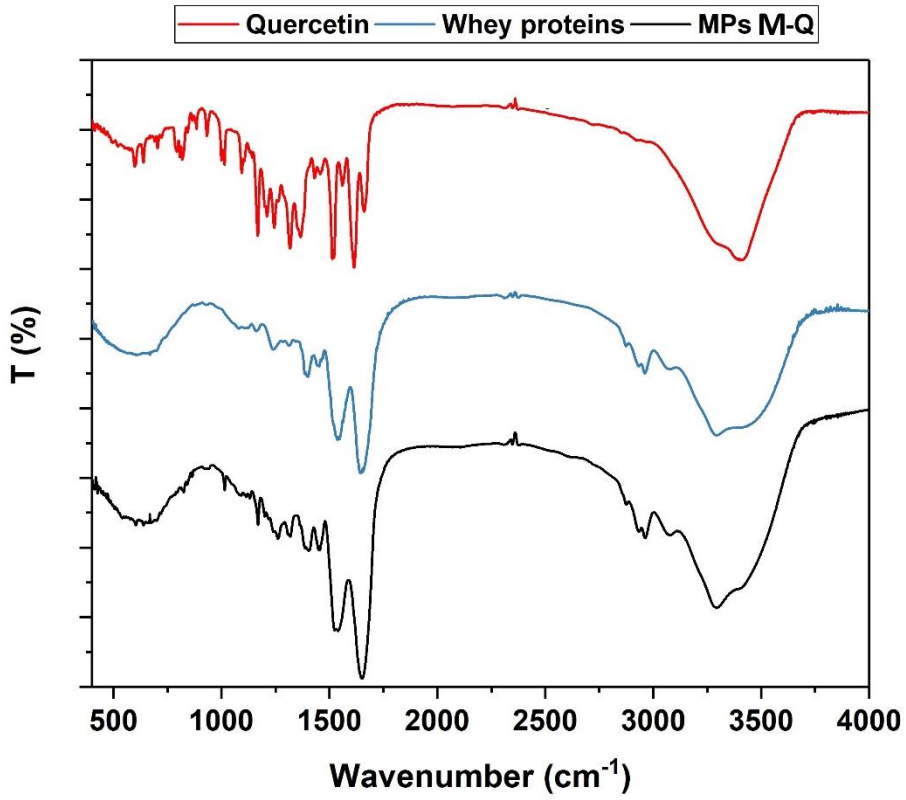

Figure 29 Comparison of FTIR spectra of quercetin, whey proteins, and MPs M-Q.

The effective incorporation of quercetin in the respective formulations is highlighted by the maintenance of the characteristic peaks present in the FTIR spectrum of the pure substances, albeit with slight variations in wavenumber and signal intensity probably due to the drug-excipient interaction and to the lower concentration of active ingredient in the formulation compared to the analysis relating to the pure substance. In particular, in the plots of the batches of MPs WQ (Figure 27), MPs SW-Q (Figure 28), and MPs M-Q (Figure 29) the peak at 1264 cm^{-1} relating to the stretching of the C–O–C bond, as well as the peaks at 1661 and 1560 cm^{-1} relating to the stretching C=O and C=C respectively, they are proof of the effective incorporation of the active ingredient within the microparticles produced.

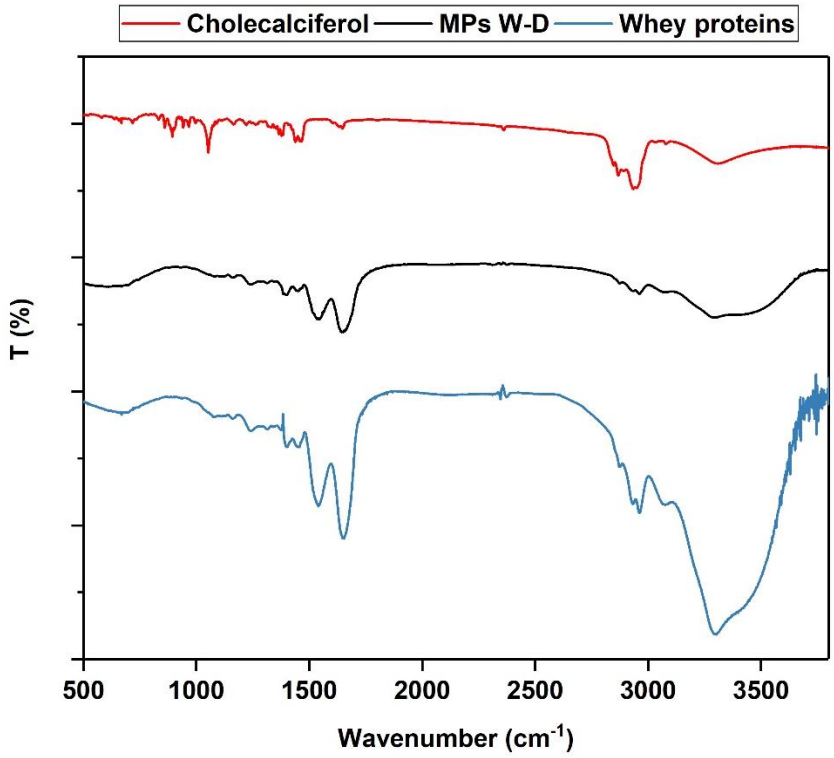

Figure 30 Comparison of FTIR spectra of cholecalciferol, whey proteins, and MPs W-D.

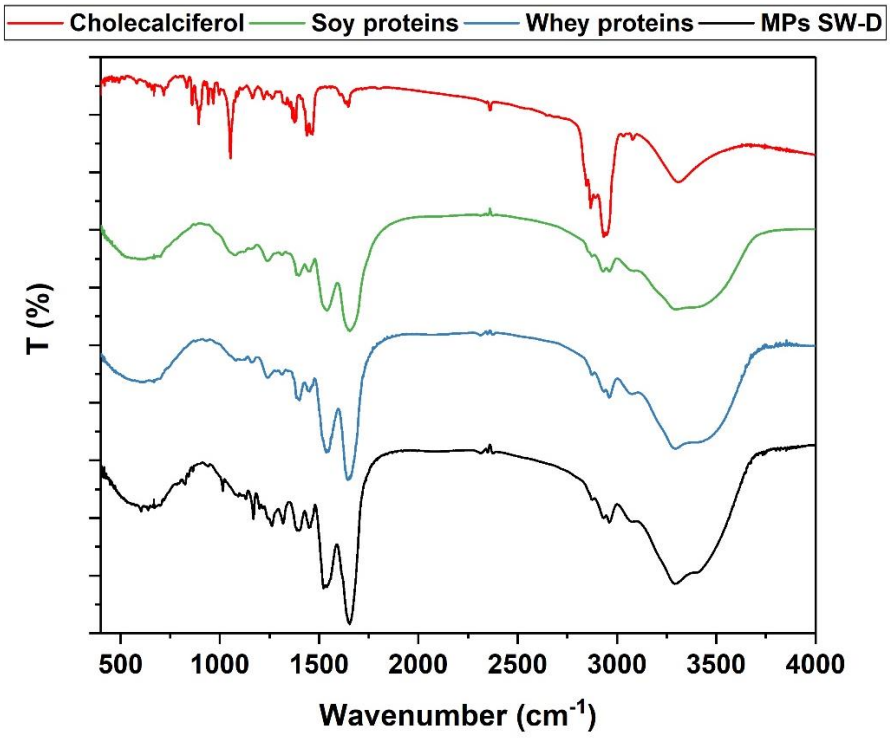

Figure 31 Comparison of FTIR spectra of cholecalciferol, soy proteins, whey proteins, and MPs SW-D.

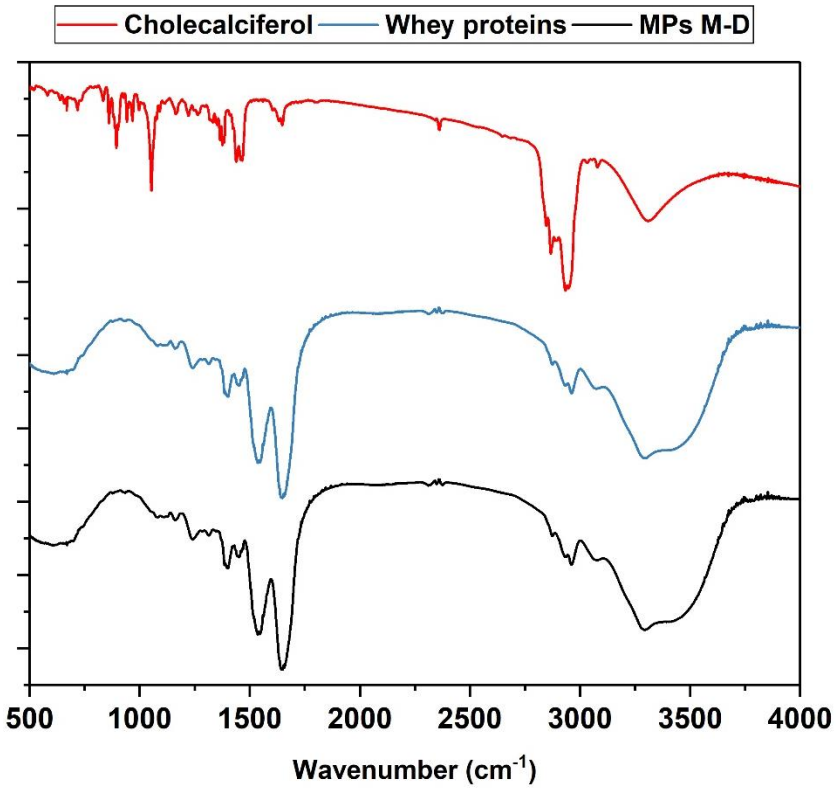

Figure 32 Comparison of FTIR spectra of cholecalciferol, whey proteins, and MPs M-D.

Even in MPs formulations containing cholecalciferol (Figures 30-31-32), it is possible to note the maintenance of the characteristic peaks, especially the absorption bands relating to the stretching of the -OH groups and the C-H bonds, present in the region between 2900 and 3400 cm-1.

The effectiveness of PC incorporation into the microparticles and the lack of formulation component degradation were assessed using the FT-IR technique (Figures 33-34-35). Characteristic peaks of PC can be identified at 3424 (stretching $-NH_2$), 2930 (stretching -OH), 1655 (stretching C=O amide I), and 1548 (stretching C=O amide II) cm^{-1}.

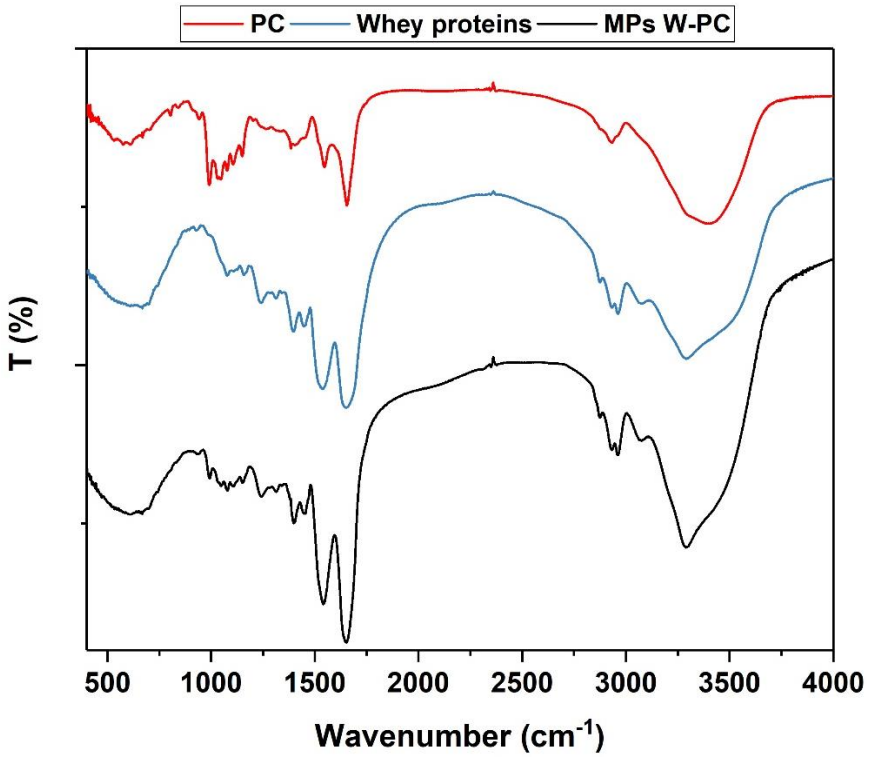

Figure 33 Comparison of FTIR spectra of phycocyanin, whey proteins, and MPs W-PC.

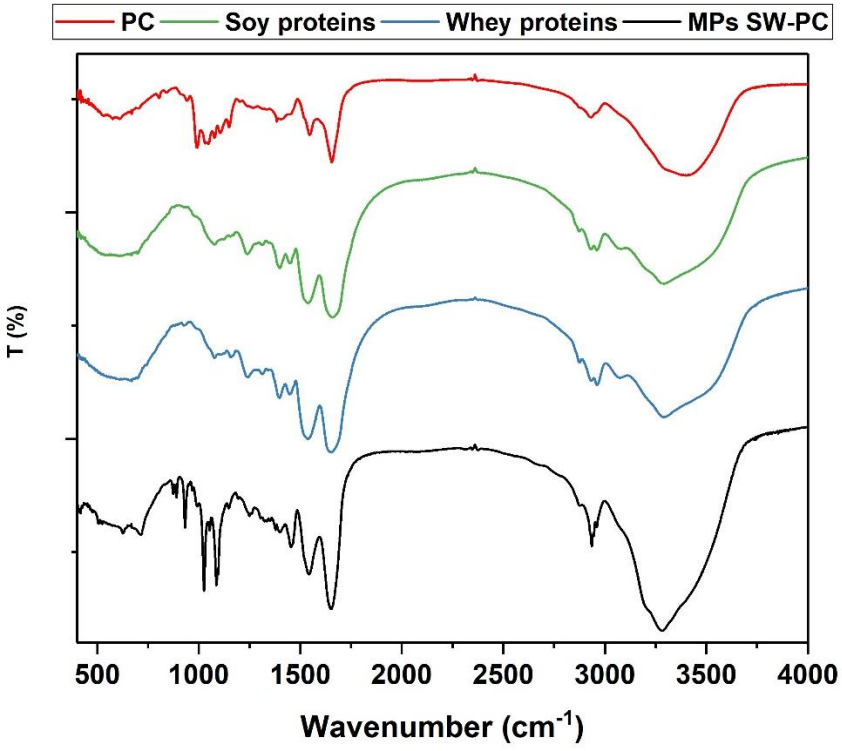

Figure 34 Comparison of FTIR spectra of phycocyanin, soy proteins, whey proteins, and MPs SW-PC.

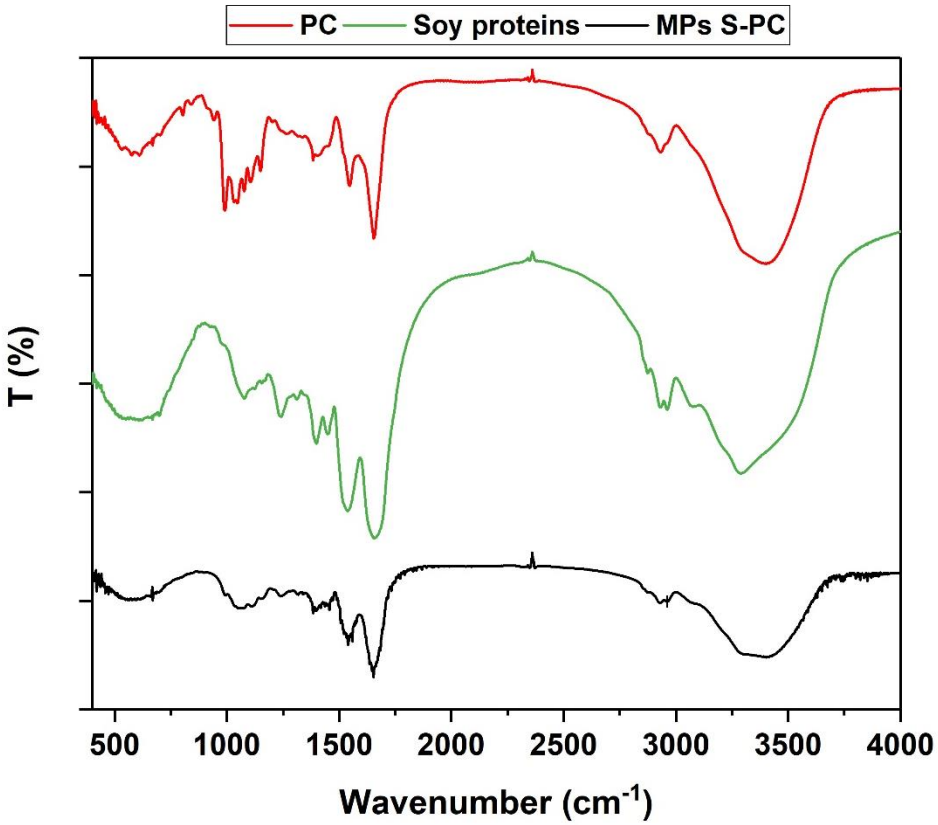

Figure 35 Comparison of FTIR spectra of phycocyanin, soy proteins, and MPs S-PC.

The absorption wavelengths of whey proteins and soy proteins are very similar to each other. This is probably because the chemical nature of both excipients is comparable since they are both protein substances. The most evident peaks are:

- related to the stretching of the C-N bonds and the N-H bending of the amide group II at 1535 cm^{-1} for whey proteins and 1530 cm^{-1} for soy proteins;
- related to the stretching of the C=O bond belonging to the amide group I present at 1648 and 1640 cm^{-1} respectively;
- related to the stretching of the CH of methyl groups in the band between 2980 and 2850 cm^{-1};
- related to the bands present at wavelengths between 3600 and 3000 cm^{-1} attributable to free OH and NH groups;

- soy proteins also present a characteristic peak at around 1230 cm^{-1} due to C-N stretching and N-H bending relating to the amide groups III [129], [130], [131].

Thermogravimetric analysis (TGA) was used to determine the thermal stability of the produced systems by measuring the mass variation that occurs when the species is heated, subjecting the sample to a controlled thermal cycle. In this work, the use of this analysis technique was to evaluate the hygroscopicity of microparticle powders, focusing on the weight loss of the sample in a temperature range between 25 and 120°C, corresponding to the complete evaporation of the water contained in the sample. The results obtained are shown in Table 9:

BATCH	Δm (mg) ± SD	Δm (%) ± SD
MPs W-Q	**0,463 ± 0,012**	**5,031% ± 0,012**
MPs SW-Q	**0,330 ± 0,015**	**6,114% ± 0,015**
MPs M-Q	**0,151 ± 0,018**	**2,525% ± 0,018**
MPs W-D	**0,234 ± 0,010**	**4,433% ± 0,010**
MPs SW-D	**0,463 ± 0,021**	**5,016% ± 0,021**
MPs M-D	**0,196 ± 0,013**	**2,378% ± 0,013**
MPs W-PC	**0,378 ± 0,017**	**4,141% ± 0,017**
MPs SW-PC	**0,421 ± 0,009**	**5,789% ± 0,009**
MPs S-PC	**0,415 ± 0,010**	**4,463% ± 0,010**

Table 9 Variations in the mass (Δm) expressed in mg and percentage of the samples of MPs subjected to thermogravimetric analysis.

The results show that the microparticles, despite having been stored in plastic containers inside refrigerators (at a temperature of about 4°C) for about 6 months, present hygroscopic characteristics: this is probably due to the intrinsic tendency of whey and soy proteins to absorb humidity from the air [132], [133]. The batches containing both types of proteins (SW-Q, SW-D, SW-PC batches) showed the highest percentage quantity of water compared to the other formulations. These results therefore suggest the need to store the microparticles in controlled conditions of temperature and inert atmosphere.

3.3 Solid-state Characterization of Microparticle Systems

Amorphous Solid Dispersions (ASDs) are pharmaceutical formulations used to improve the solubility and bioavailability of poorly water-soluble drugs compared to drug delivery systems containing the drug in a crystalline form. In an ASD, the drug is dispersed in an amorphous (non-crystalline) matrix of a polymer or co-former, which prevents the drug from reverting to its less soluble crystalline form. This amorphous state allows for a greater rate of dissolution and often improved oral absorption of the drug. ASDs are particularly useful for drugs that, in their crystalline form, exhibit low solubility and therefore limited absorption into the body. Thus, research efforts are directed toward finding excipients that stabilize the drug in its amorphous form such as proteins [134], [135].

In this study, quercetin and cholecalciferol represent our lipophilic APIs characterized by low solubility and low absorption, while phycocyanin is a hydrophilic substance.

The aim of this work was therefore to create an amorphous matrix in which to disperse the active pharmaceutical ingredients, both lipophilic and hydrophilic. For this purpose, natural proteins such as soy and whey proteins were selected to form an amorphous matrix that enhances the solubility of lipophilic active ingredients in the dispersion. This improvement is further supported by the use of the spray drying production process.

X-ray Powder Diffraction (XRPD) analysis was used to reveal the amorphous or crystalline nature of the APIs and excipients and to confirm whether an amorphous product was obtained from spray drying. Both soy protein and whey protein are in an amorphous state as is phycocyanin, all three being protein substances.

As we can see from figures 36, 37, and 38, quercetin, as a raw material, is in a partially crystalline state. It is possible to note how most of the active ingredient is in crystalline form but a portion is also in amorphous form probably due to the extraction processes of the

substance itself. In Figure 36 there is a comparison graph of quercetin, whey proteins, the physical mixture of MPs W-Q microparticles, and the microparticles produced. In particular, it is important to note the difference in the analysis conducted on the physical mixture and on the microparticles produced. It is precisely from this data that we can deduce how the spray drying process and the presence of co-formulants are fundamental in determining the passage of quercetin from an almost crystalline state to an almost amorphous state. The same reasoning also applies to the other two batches of microparticles produced with quercetin present in figures 37 and 38. These results turn out to be an important achievement in the development of these amorphous solid dispersions that could guarantee the final product an increase in solubility and therefore in permeation and bioavailability of this extremely lipophilic and poorly soluble active ingredient.

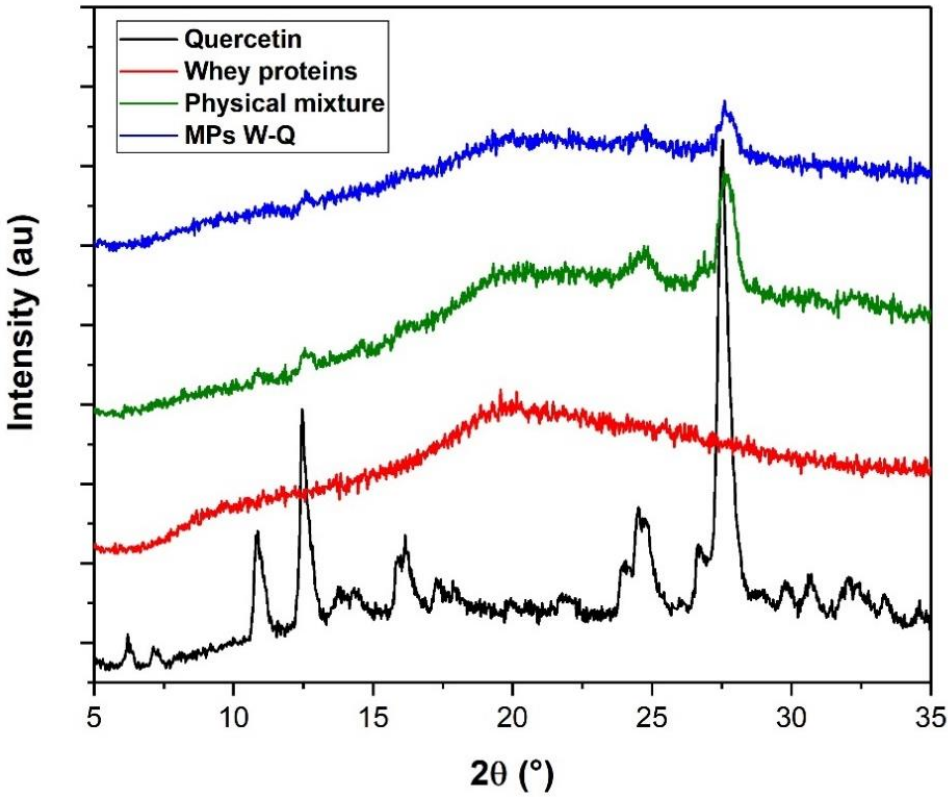

Figure 36 Comparison of XRPD spectra of quercetin, whey proteins, physical mixture, and MPs W-Q.

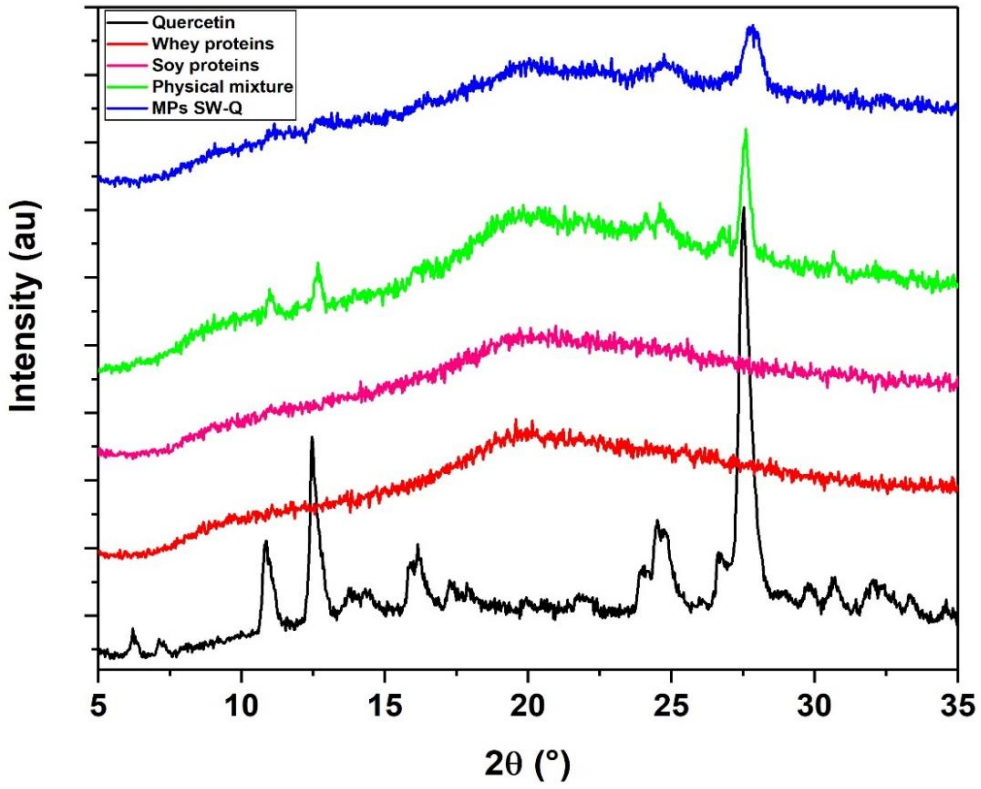

Figure 37 Comparison of XRPD spectra of quercetin, whey proteins, soy proteins, physical mixture, and MPs SW-Q.

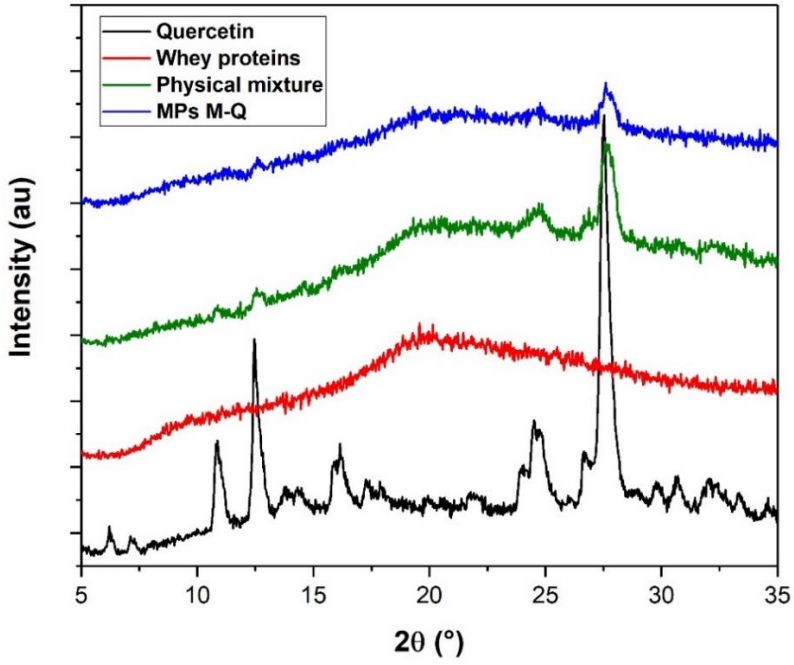

Figure 38 Comparison of XRPD spectra of quercetin, whey proteins, physical mixture, and MPs M-Q.

At the same time, even in the case of cholecalciferol, the drug in its elementary state is in an absolutely crystalline form. It is precisely the spray drying process together with the use of these amorphous co-formulants such as whey proteins and soy proteins, together with the milk used as a dispersing phase in the MPs M-D formulation, which promote and allow the transformation of the active ingredient from a crystalline form to an amorphous form, with all the advantages mentioned above that result from this (Figures 39-40-41).

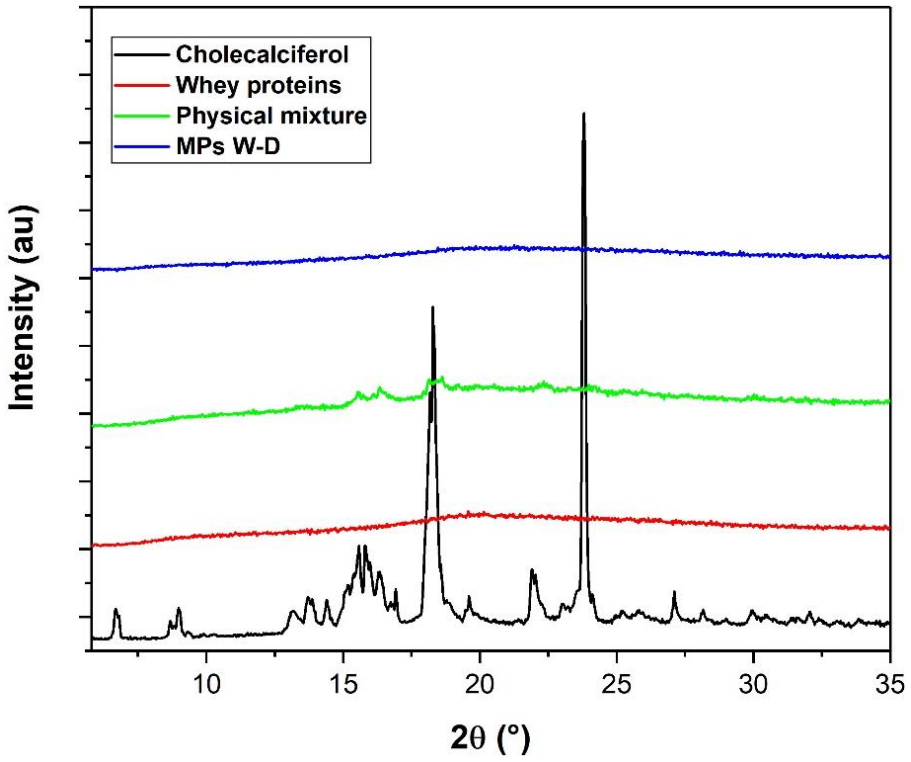

Figure 39 Comparison of XRPD spectra of cholecalciferol, whey proteins, physical mixture, and MPs W-D.

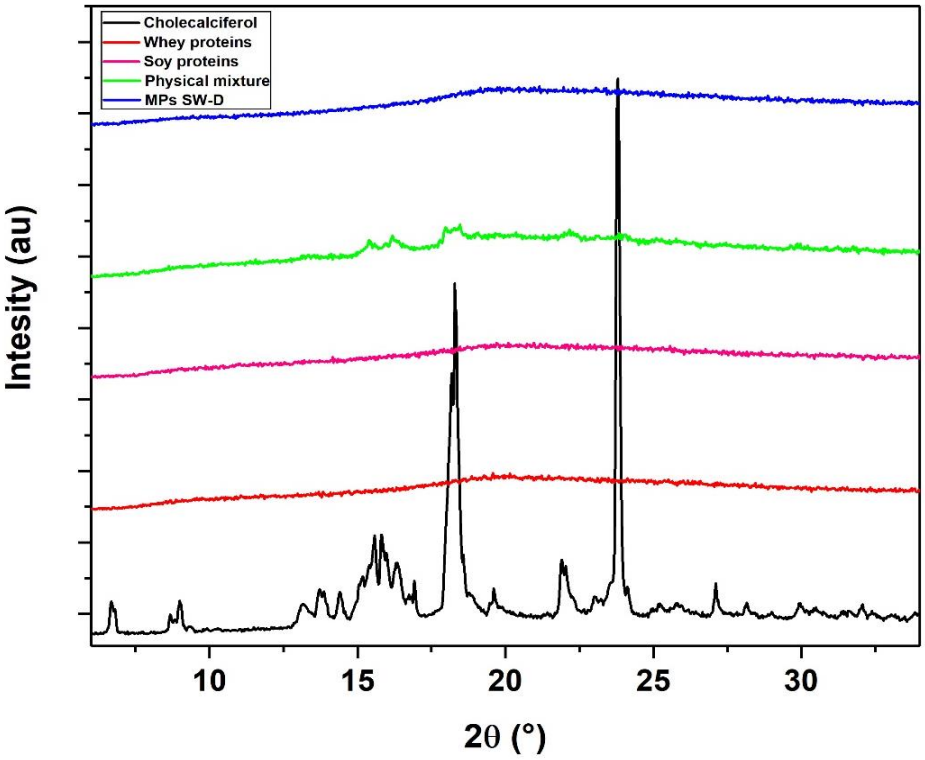

Figure 40 Comparison of XRPD spectra of cholecalciferol, whey proteins, soy proteins, physical mixture, and MPs SW-D.

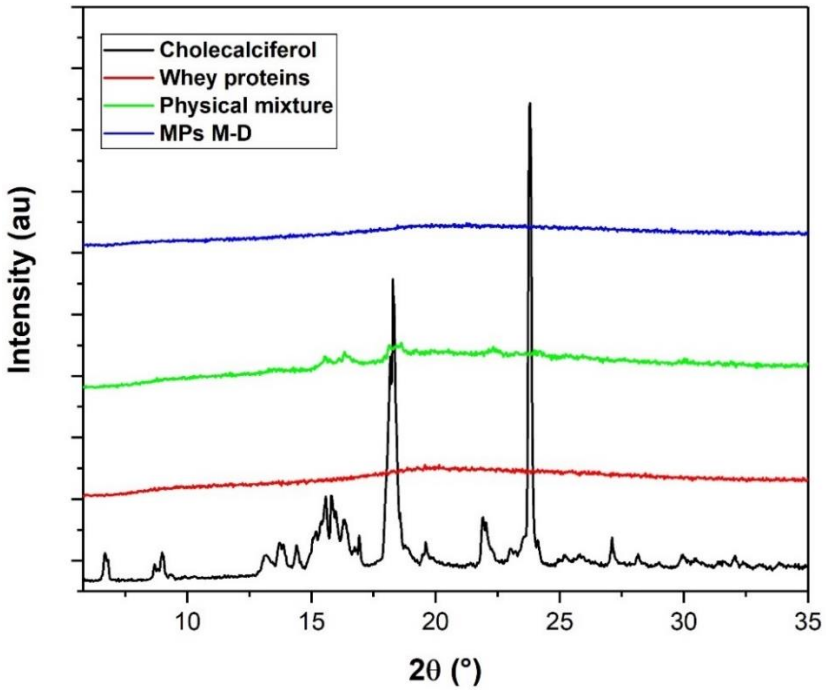

Figure 41 Comparison of XRPD spectra of cholecalciferol, whey proteins, physical mixture, and MPs M-D.

On the contrary, in the case of the batches of microparticles containing phycocyanin, since the latter is a protein of natural origin, it is also in an amorphous state, therefore the entire formulation contains both excipients and active ingredients of an amorphous nature as confirmed by the XRPD spectra present in the figures 42-43-44.

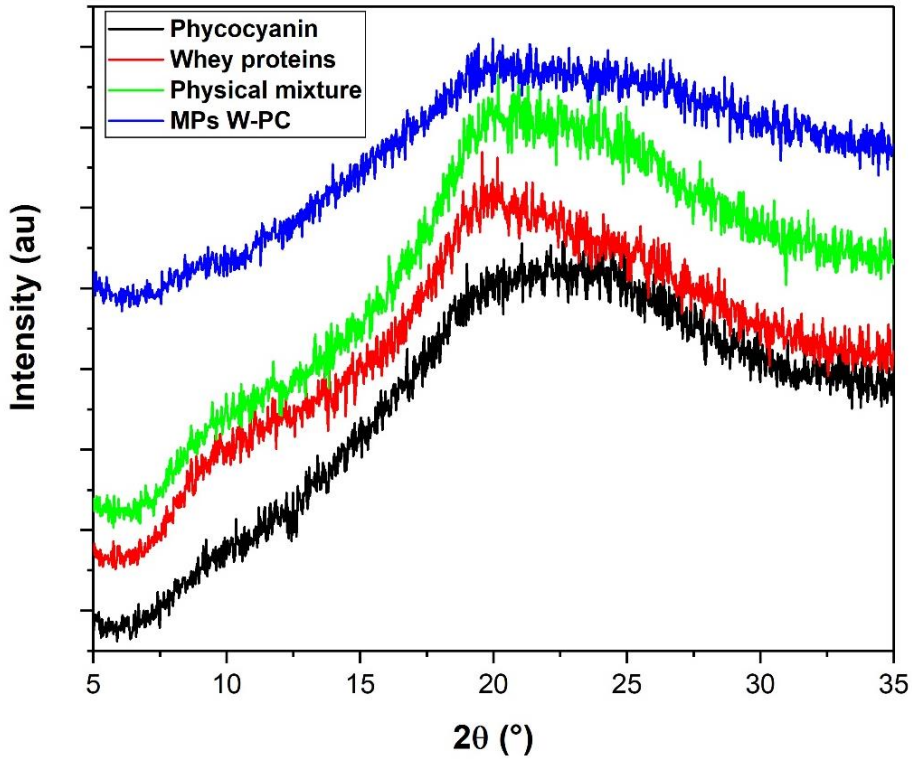

Figure 42 Comparison of XRPD spectra of phycocyanin, whey proteins, physical mixture, and MPs W-PC.

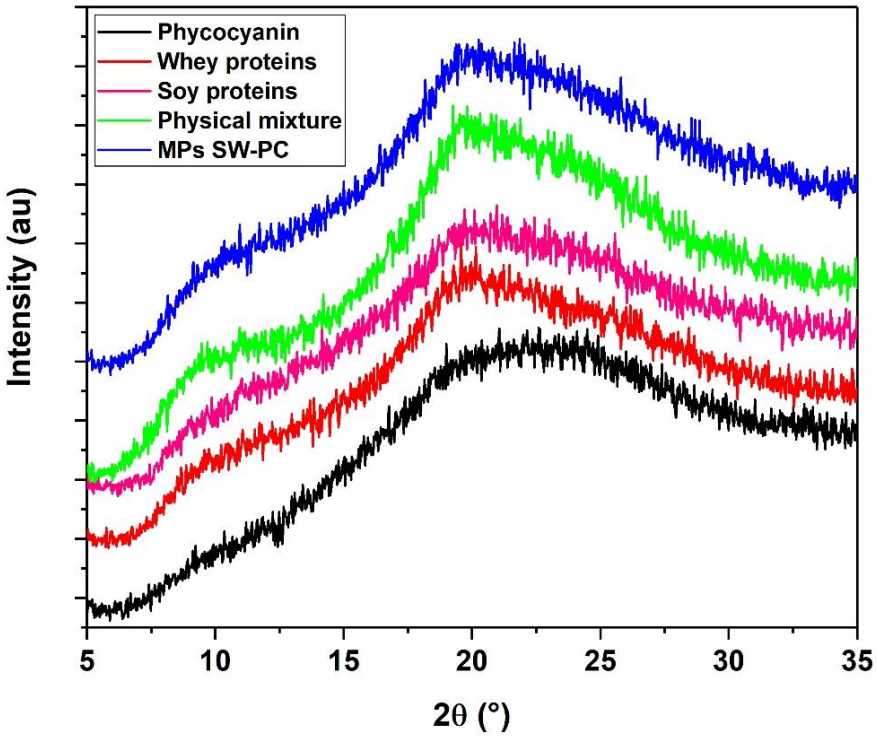

Figure 43 Comparison of XRPD spectra of phycocyanin, whey proteins, soy proteins, physical mixture, and MPs SW-PC.

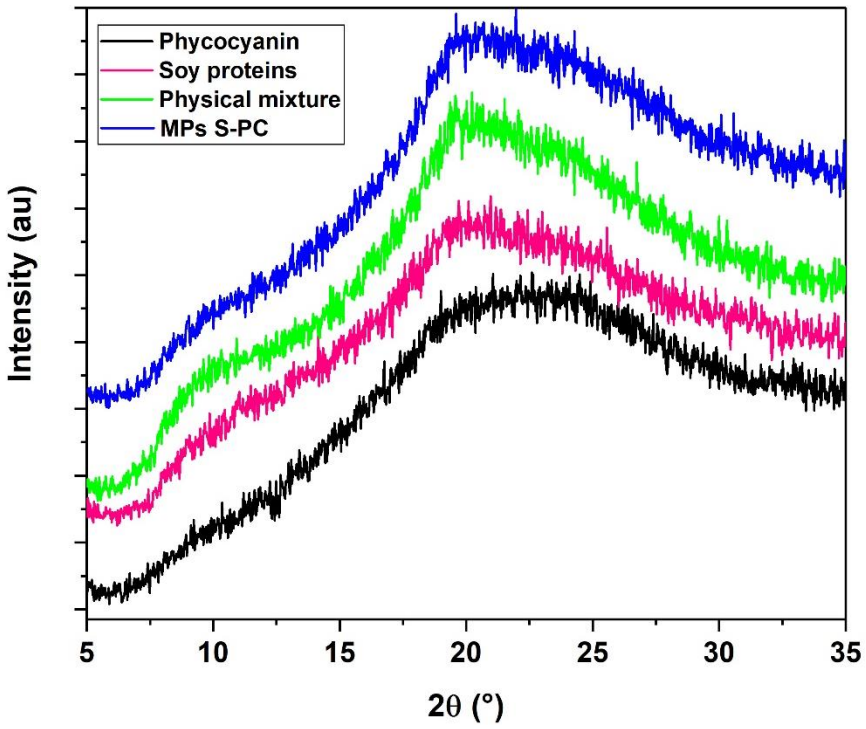

Figure 44 Comparison of XRPD spectra of phycocyanin, soy proteins, physical mixture, and MPs S-PC.

A common technique for thermal investigation, differential scanning calorimetry (DSC) offers information about the thermal behavior of materials and is especially helpful for describing the physical state of pharmaceutical formulations. When it comes to ASDs, DSC is essential for figuring out whether the excipients and APIs are present in an amorphous state, which is critical for improving their solubility and bioavailability [136].

The distinct melting point (Tm), a strong endothermic peak shown in the DSC thermogram, is a characteristic of crystalline materials. Conversely, amorphous materials exhibit a glass transition temperature (Tg), which is a reversible transition from a glassy, rigid state to a more flexible, rubbery one, since they lack long-range molecular order. For ASDs, the absence of a melting endotherm associated with the crystalline form of the drug and the presence of a distinct Tg in the DSC thermogram confirms the successful formation of the amorphous matrix. This is critical in solid dispersions, where the API is dispersed within a protein-based matrix (such as soy or whey proteins) to prevent recrystallization and maintain the drug in its high-energy amorphous state, which improves dissolution rates. Additionally, the interactions between the API and the excipients that make up the matrix can affect the Tg of the ASD, which can be measured via DSC analysis. A homogeneous amorphous phase is shown by a single, well-defined Tg in the thermogram, indicating molecular miscibility between the drug and the excipient [137].

DSC can reveal information on the thermal stability of the ASDs in addition to verifying the amorphous nature of the dispersions. It is feasible to evaluate the samples' resistance to recrystallization when exposed to high temperatures by putting them through various heating and cooling cycles. Predicting the formulation's long-term stability during handling and storage requires this information.

Overall, DSC is an indispensable tool in the characterization of ASDs, providing detailed information on the thermal transitions, amorphous state, and stability of the formulations. The DSC thermal analysis performed on the active ingredients and excipients confirmed the XRPD analysis results by highlighting the crystalline nature of quercetin (Figure 45) and cholecalciferol (Figure 46), which exhibit two narrow endothermic peaks typical of substances in this state.

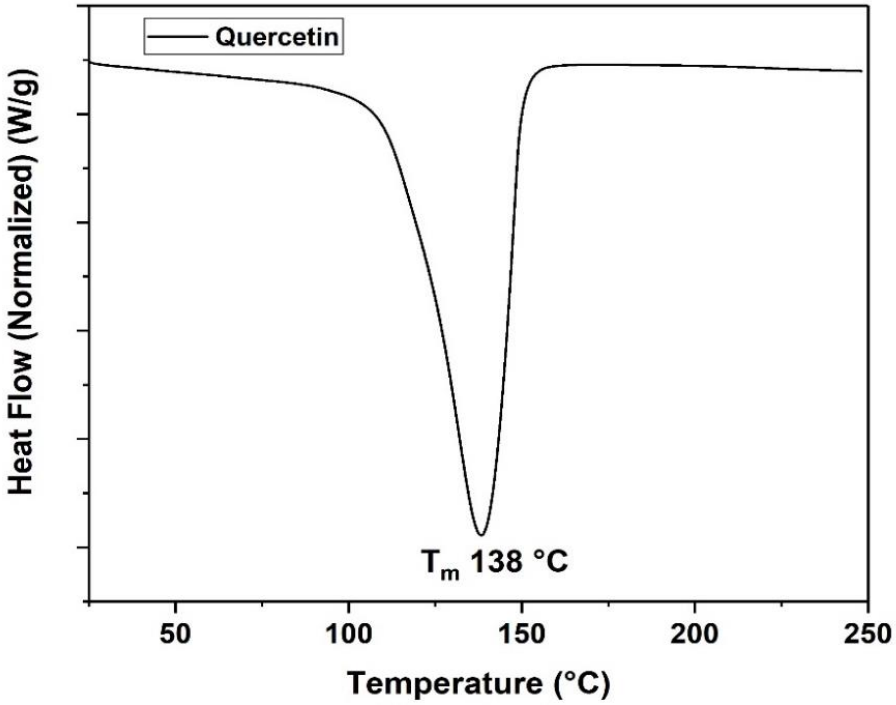

Figure 45 DSC thermogram of quercetin showing the thermal behavior of the sample including the endothermic peaks corresponding to the melting point (T_m).

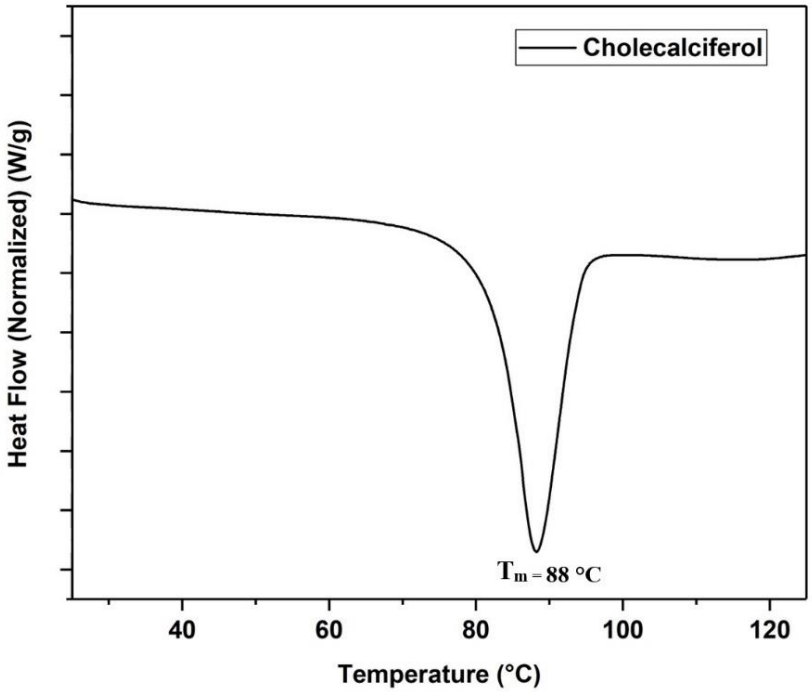

Figure 46 DSC thermogram of cholecalciferol showing the thermal behavior of the sample including the endothermic peaks corresponding to the melting point (T_m).

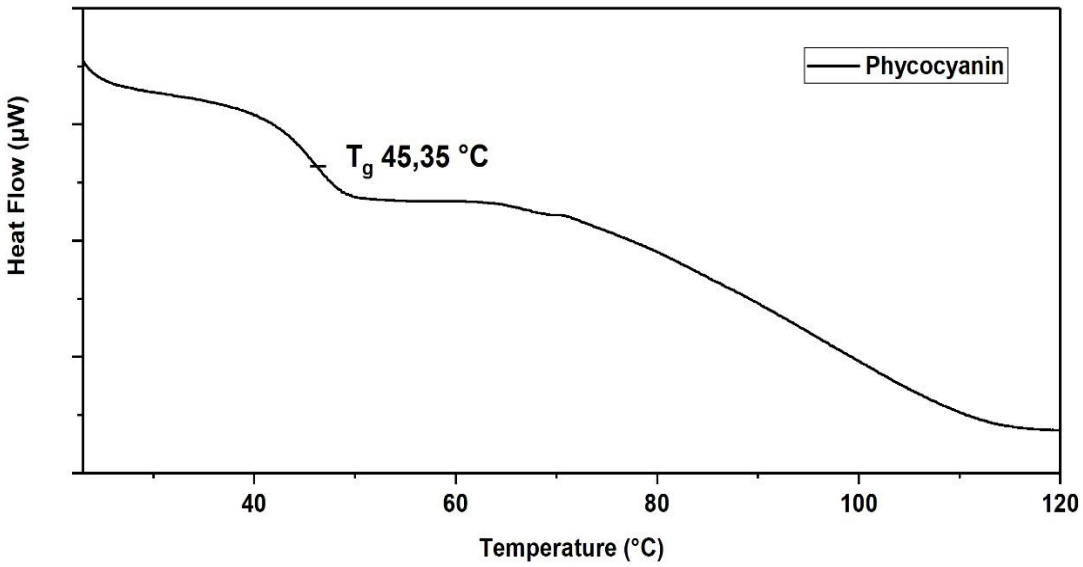

Figure 47 DSC thermogram of phycocyanin showing the thermal behavior of the sample, including the glass transition temperature (Tg).

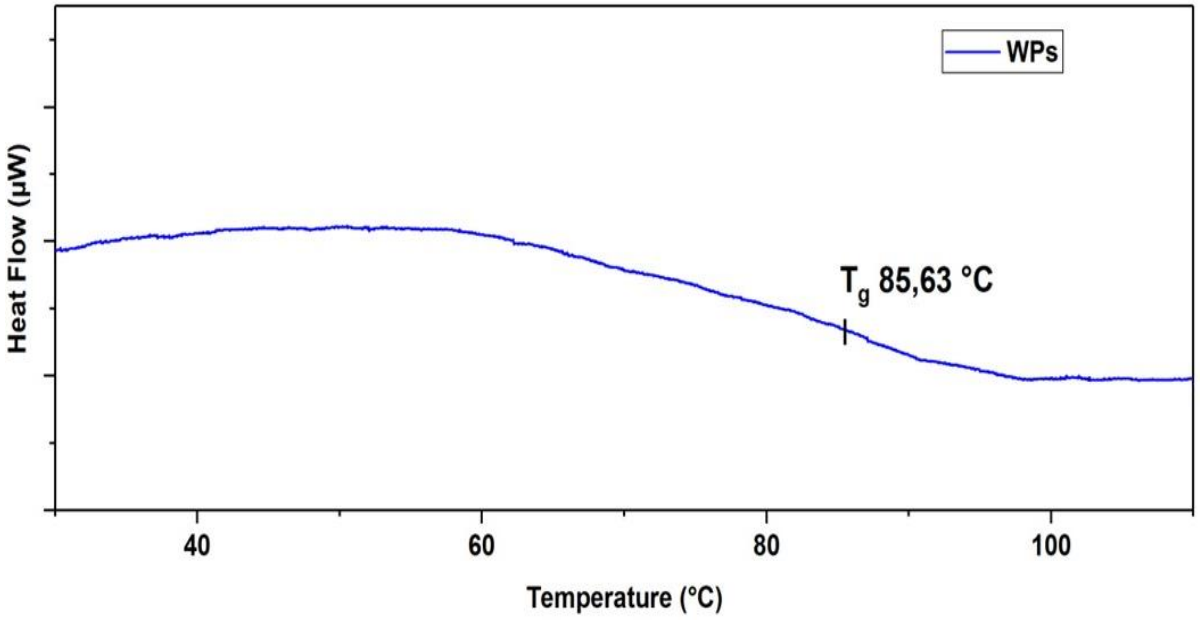

Figure 48 DSC thermogram of whey proteins (WPs) showing the thermal behavior of the sample, including the glass transition temperature (Tg).

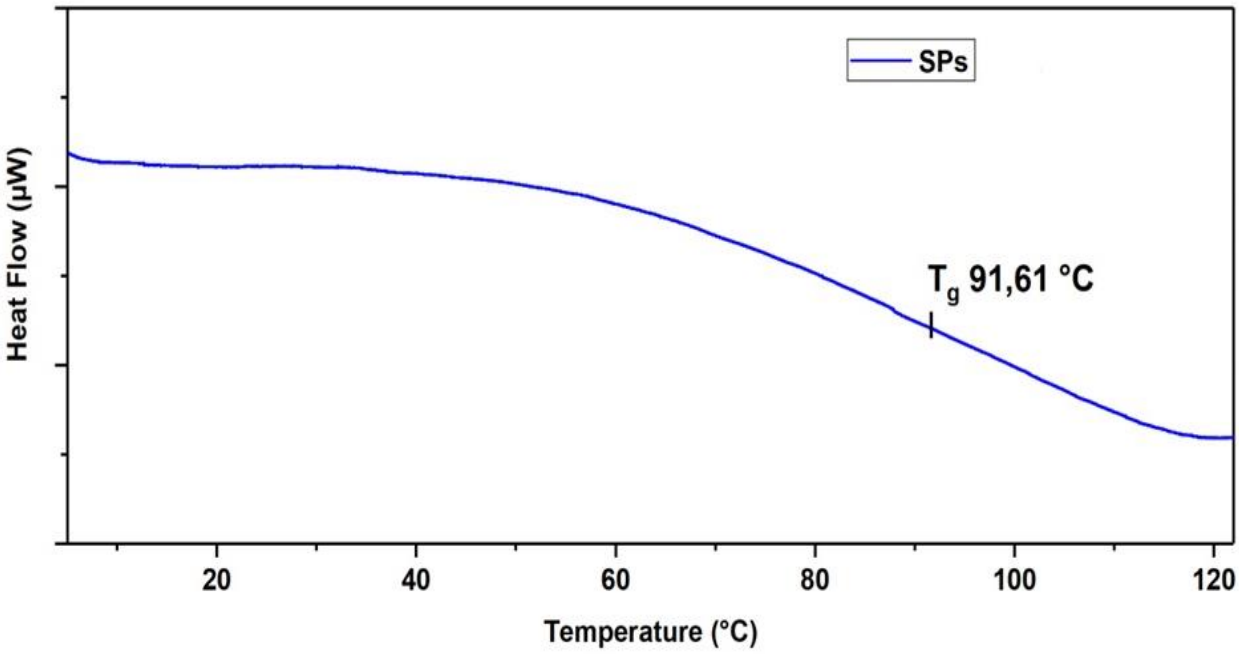

Figure 49 DSC thermogram of soy proteins (SPs) showing the thermal behavior of the sample, including the glass transition temperature (Tg).

While it is possible to confirm the amorphous nature of phycocyanin which presents a Tg at 45°C (Figure 47) and of the excipients used for the creation of these ASDs such as whey proteins and soy proteins which present two Tgs one at 85°C and the other at 91°C respectively (Figures 48-49).

The same thermal analysis was performed on the samples of all the microparticles produced and the results showed that all the analyzed samples present a single value of Tg whose values are reported in the table below (Table 10).

MPs SAMPLES	Tg VALUES
MPs W-Q	**87,52 °C ± 0,31**
MPs SW-Q	**90,01 °C ± 0,75**
MPs M-Q	**88,21 °C ± 0,47**
MPs WD	**79,92 °C ± 0,65**
MPs SW-D	**80,38 °C ± 0,76**
MPs M-D	**79,13 °C ± 0,68**
MPs W-PC	**91,24 °C ± 0,30**
MPs SW-PC	**89,87 °C ± 1,13**
MPs S-PC	**88,32 °C ± 2,03**

Table 10 Table showing the glass transition temperatures (Tg) of the analyzed microparticles.

It was important to discover through DSC analyses carried out on the microparticle samples how only one T_g value was present, thus indicating a perfect homogeneity of the formulation and a very strong interaction at the molecular level between the excipients and the active

ingredients. Furthermore, it is important to underline that the DSC analyses on the microparticle samples were carried out one day after production, one month after production, and 6 months after production. In all three cases, the thermal behaviours were always the same, thus proving the stability of the systems and the tendency of the active ingredient not to re-crystallize, thanks also to the appropriate amorphous solid dispersion chosen in the formulation phase.

3.4 Evaluation of Antioxidant Activity using DPPH free radical scavenging assay

Among the most stable free radicals, the DPPH is often employed to assess the radical scavengers activity of different molecules. The DPPH test method for manual determination of antioxidant levels is relatively easy to use and fast. This technique applies to both liquid and solid samples, and it is not just specific to any one antioxidant but also the sample's total antioxidant capacity. The DPPH test is based on the ability of the stable 2,2-diphenyl-1-picrylhydrazyl free radical to react with hydrogen donors. The reduction of DPPH, a stable free radical, is the starting point of the DPPH test technique. The highest absorption of the odd-electron free radical DPPH occurs at 517 nm (purple). When antioxidants react with DPPH, the stable free radical is reduced to DPPHH and coupled off with a hydrogen donor (such as a free radical-scavenging antioxidant), which causes the absorbances from the DPPH to drop. Decolorization (yellow) in relation to the number of electrons collected is the consequence of radical to the DPPH-H form (Figure 50) [138].

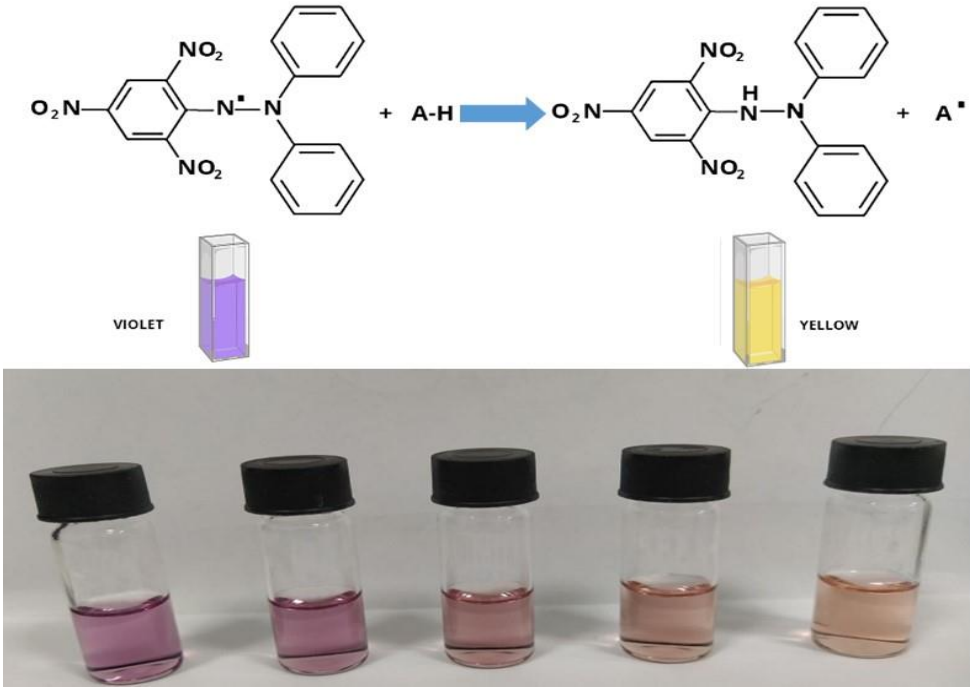

Figure 50 Illustration of DPPH Free Radical Scavenging Assay: The reaction mechanism shows the reduction of the DPPH radical (violet) to its non-radical form (yellow) upon reaction

with an antioxidant (A-H). The vials below display the gradual color change from violet to pale yellow as antioxidant concentration increases, indicating the scavenging activity.

The antioxidant capacity of the formulations of microparticles containing quercetin and phycocyanin was evaluated, comparing them to the radical scavenging activity of both the raw active ingredient and positive control (ascorbic acid) used for its known antioxidant activity. In particular, by testing the antioxidant activity of the various batches produced according to a concentration-dependent profile, the objective was to verify that the production process via spray-drying did not affect the antioxidant capacity of the APIs due to any degradation phenomena mainly due to the operating temperatures. The test for the batches of microparticles containing quercetin involved the solubilization of the microparticles and the pure active ingredient in a suitable solvent (ethanol) to obtain concentrations equal to 4, 6, 8, 10, and 12 µg/ml. The solutions obtained were made to react with the reagent solution for 20 minutes, keeping the samples in the dark. The same procedure was performed for quercetin and ascorbic acid. After that, the samples were read by UV spectrophotometer [139].

The scavenging activity of the microparticles without active ingredient was also evaluated, to verify the possible antioxidant activity related to the excipients that could be added to the active ingredient. The radical scavenging activity % of each system was calculated according to the formula:

$$Radical\ scavenging\ activity\ \% = \frac{[(Abs\ of\ Blank - Abs\ of\ Control) - Abs\ of\ Sample]}{(Abs\ of\ Blank - Abs\ of\ Control)} \times 100$$

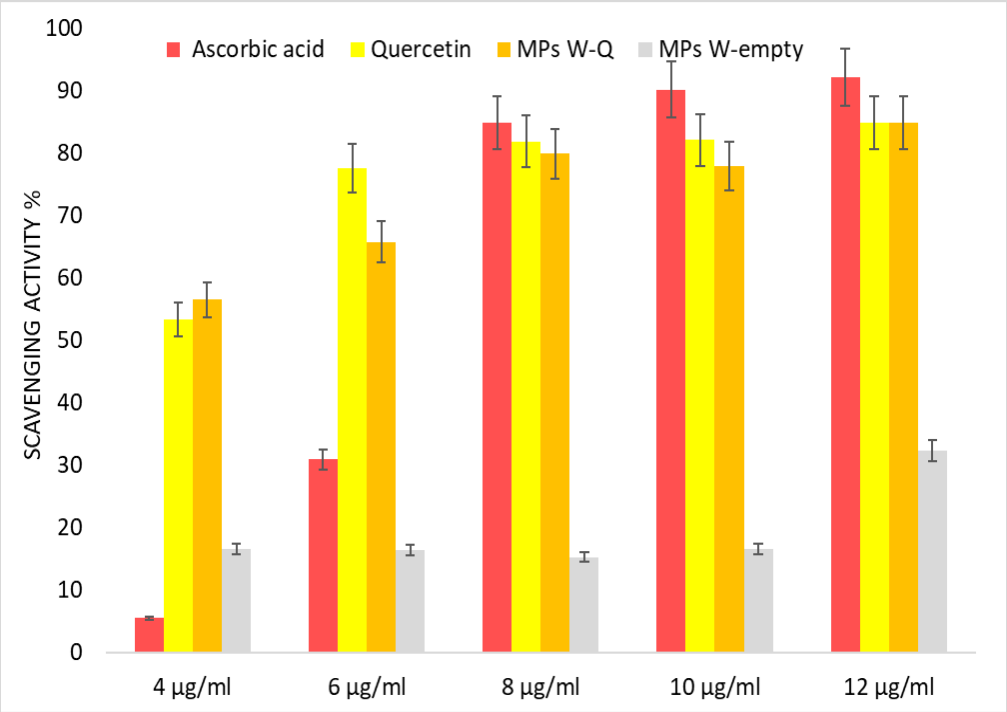

Figure 51 Radical scavenging activities of Ascorbic acid, Quercetin, MPs W-Q, and MPs W-empty measured by DPPH assay.

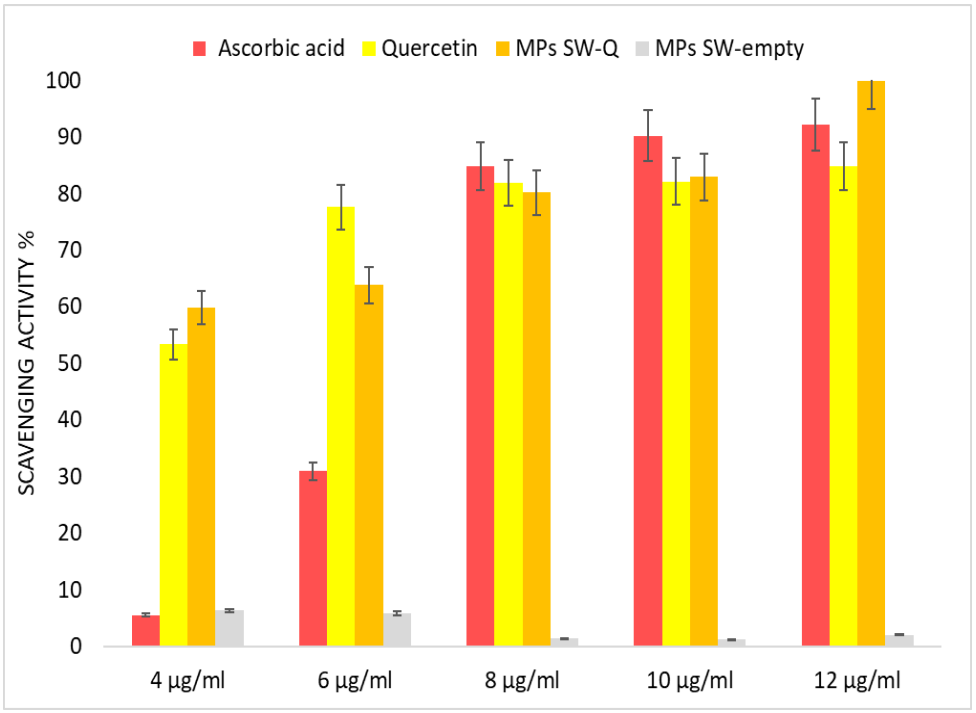

Figure 52 Radical scavenging activities of Ascorbic acid, Quercetin, MPs SW-Q, and MPs SW-empty measured by DPPH assay.

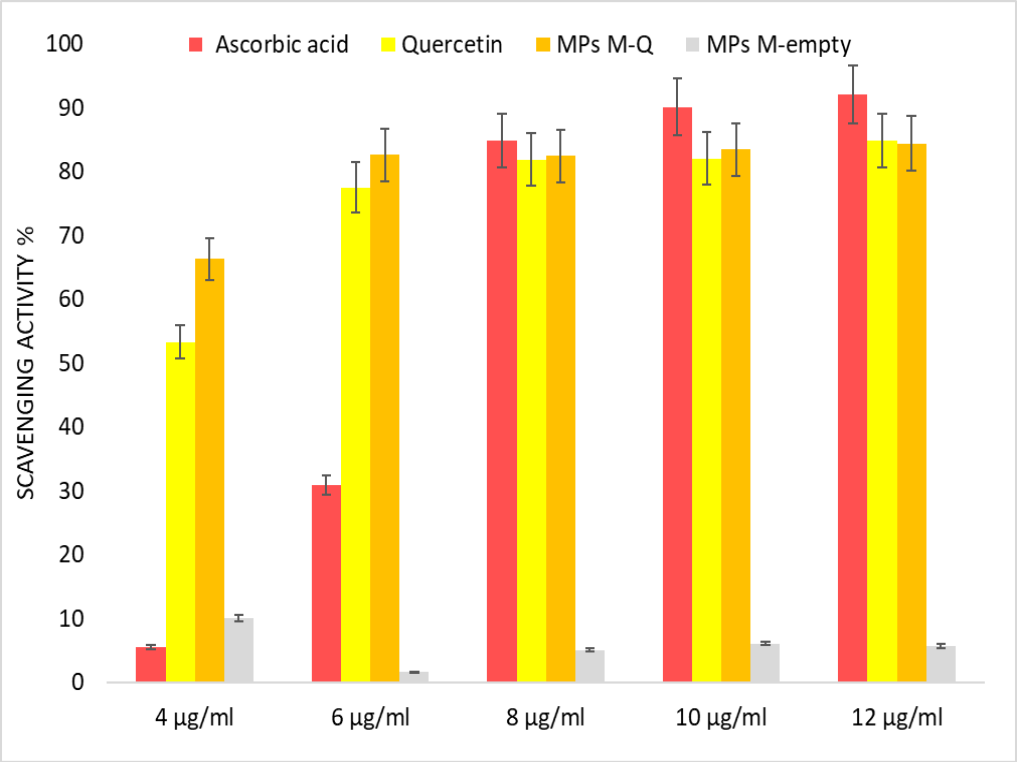

Figure 53 Radical scavenging activities of Ascorbic acid, Quercetin, MPs M-Q, and MPs M-empty measured by DPPH assay.

The results shown in figures 51-52-53 allow us to observe that the antioxidant activity of quercetin extracted from the microparticles was maintained even after the spray drying process: all the batches produced show a radical scavenging activity comparable to raw quercetin, an indication of the fact that the high operating temperatures during the production phase did not degrade the active ingredient and, therefore, its ability to react with free radicals, inhibiting them. The microparticles without active ingredient ("empty" systems) showed a limited antioxidant activity, whose overall contribution within the formulation is probably negligible.

To carry out the test for the batches of microparticles containing phycocyanin, the microparticles had to be dissolved to achieve concentrations of 0.1–0.2–0.4–0.6–0.8 mg/ml of PC. The samples were left in the dark for 20 minutes while the solutions produced reacted with the reagent solution. The samples were then read using a UV spectrophotometer [140].

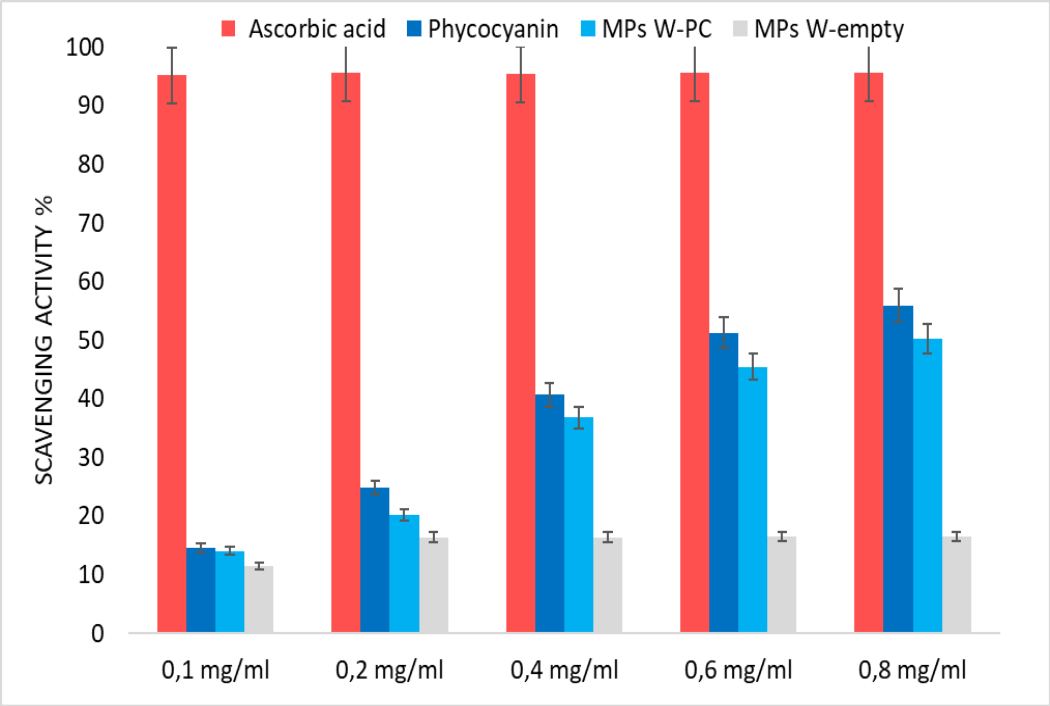

Figure 54 Radical scavenging activities of Ascorbic acid, Phycocyanin, MPs W-PC, and MPs W-empty measured by DPPH assay.

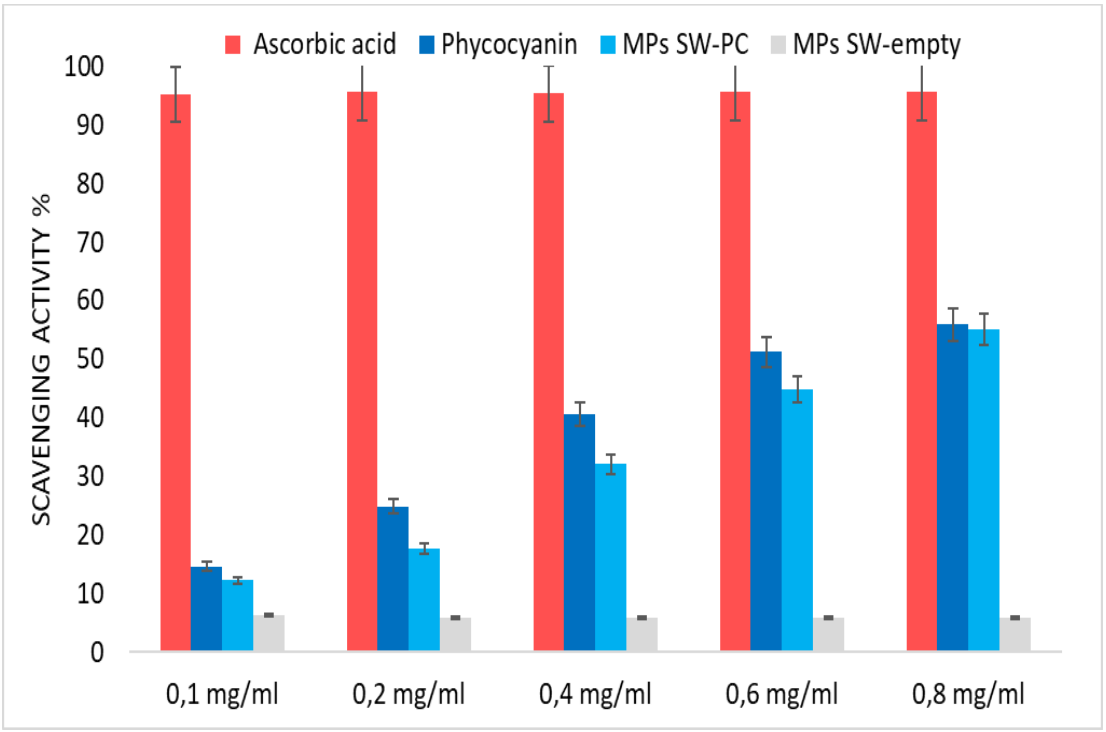

Figure 55 Radical scavenging activities of Ascorbic acid, Phycocyanin, MPs SW-PC, and MPs SW-empty measured by DPPH assay.

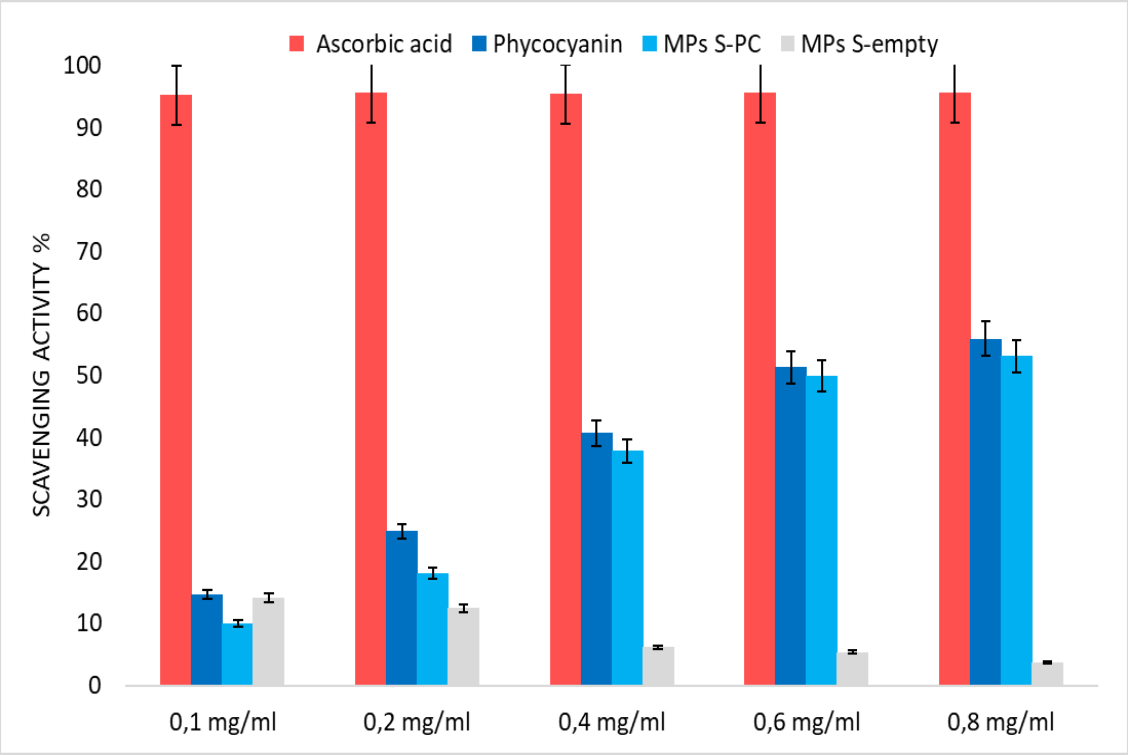

Figure 56 Radical scavenging activities of Ascorbic acid, Phycocyanin, MPs S-PC, and MPs S-empty measured by DPPH assay.

Also in this case the radical scavenging activity of the batches of microparticles containing phycocyanin (Figures 54-55-56) is comparable to the raw phycocyanin, thus demonstrating once again how the spray drying process is suitable for the production of oral pharmaceutical forms containing thermosensitive active ingredients.

As regards cholecalciferol and the batches that contain it, the DPPH assay was not carried out since the anti-inflammatory activity relating to the molecule is not related to antioxidant and radical scavenger mechanisms but is carried out through cellular signaling processes that allow modulation of the activity of lymphocyte cells and pro-inflammatory cytokines [141].

3.5 pH-dependent Dissolution Studies

An in vitro dissolution study was conducted to highlight the differences in the release profiles of the charged active molecules, generated by the gastro-resistant ingredients encapsulated in the MPs, compared to the pure active ingredients. The evaluation of the effect on the dissolution profile of the microparticles made it possible to appreciate the potential of the spray-drying technique to obtain delayed-release formulations (pH-sensitive/gastro-resistant release). In this regard, an in vitro model was used to simulate the distribution of active molecules between the aqueous phase of the gastric fluid and the lipid phase of the biological membranes of the gastrointestinal wall. This in vitro model could also be approximated to an uptake model through the intestinal membrane.

Due to the high hydrophobicity of molecules such as quercetin and cholecalciferol, it was decided to use a biphasic system with an organic solvent, n-octanol already used in the literature to mimic the membranes' lipid phase. In the case of phycocyanin, being a totally water-soluble molecule, it was possible to perform this test in an aqueous medium only. The aqueous phase was maintained at pH 1-2 for the first two hours of the experiment to reproduce the gastric passage; subsequently, the pH was raised to 6.8 to simulate intestinal transit (Figure 57) [142], [143].

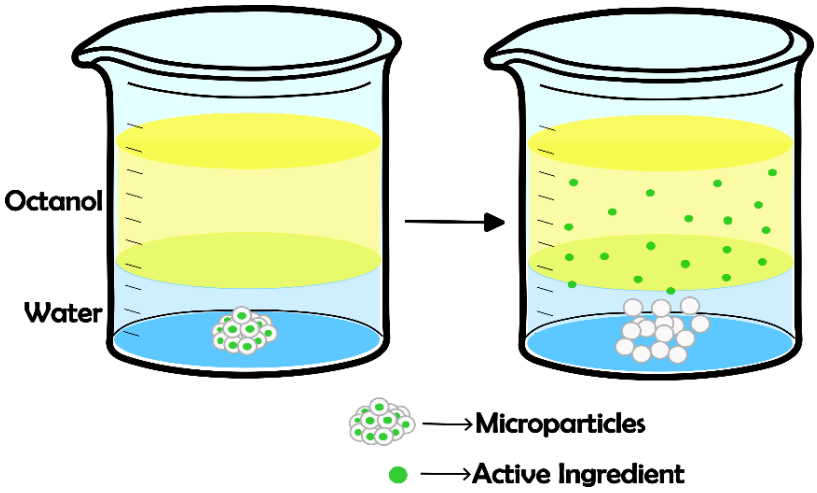

Figure 57 Scheme of the system used for the dissolution/distribution study of the microparticles.

Figure 58 shows the dissolution profiles of pure quercetin and the three batches of tested microparticles W-Q, S-WQ, and M-Q.

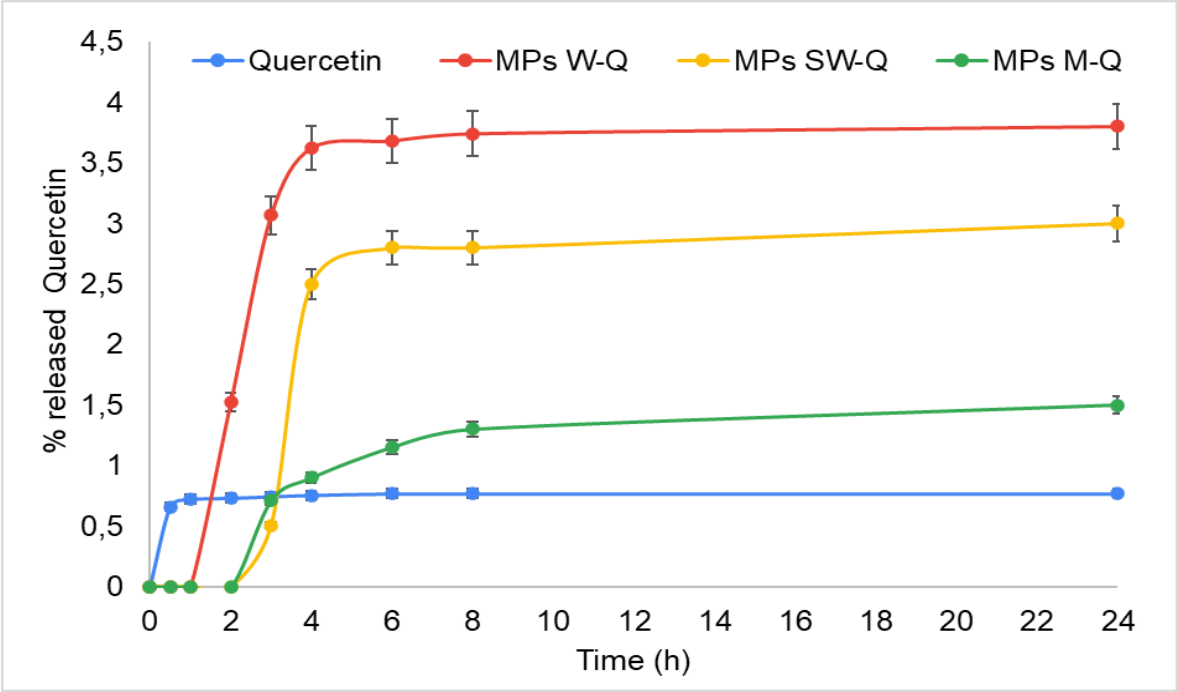

Figure 58 Graph of the percentage of quercetin released as a function of time for batches MPs WQ, MPs SW-Q, MPs M-Q, and pure quercetin.

Regarding the quercetin-containing formulations, all batches demonstrate the ability to achieve a modified release profile. While pure quercetin begins to release within 30 minutes of the experiment, the formulations exhibit controlled release profiles, avoiding any initial burst effect. Notably, MPs SW-Q and M-Q show a clear gastro-resistant profile, preventing quercetin release during the first two hours and showing an increase in release only after the pH changes, suggesting potential intestinal delivery. In contrast, the MPs W-Q batch allows partial dissolution of the active ingredient after just one hour. However, the percentage of quercetin released from the W-Q formulation is significantly higher (three-fold more) than the pure quercetin and the other two formulations, indicating the superior solubilizing capability of whey proteins for a lipophilic molecule.

The low amount of quercetin released and the plateau reached after approximately 6 hours are likely due to saturation phenomena in the lipophilic phase, which may be attributed to the small solvent volumes used in the experiment.

Figure 59 shows the dissolution profiles of pure cholecalciferol and the three tested microparticle batches W-D, SW-D, and M-D.

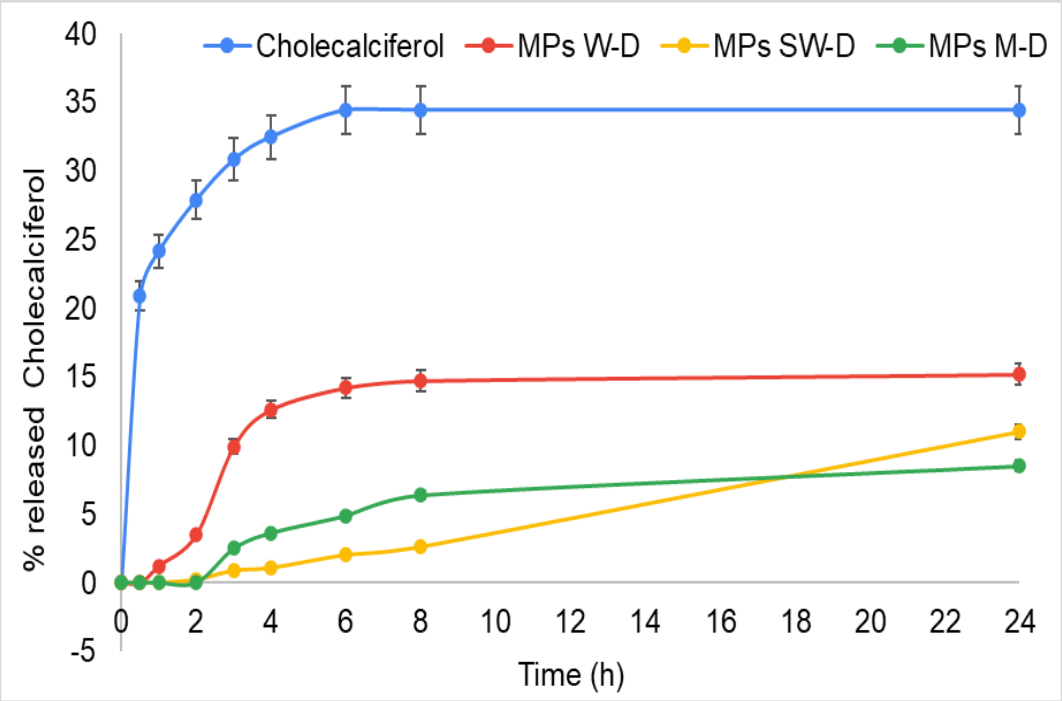

Figure 59 Graph of the percentage of cholecalciferol released as a function of time for batches MPs W-D, MPs SW-D, MPs M-D, and pure cholecalciferol.

The systems containing cholecalciferol exhibit modified release profiles similar to those observed with the quercetin-containing batches. In this case, pure cholecalciferol is immediatly dissolved, while the SW-D and M-D formulations demonstrate a typical gastro-resistant behavior. The W-D batch allows release starting from one hour, but in greater quantities compared to the other two batches. As previously observed, the amount of active ingredient released from these formulations is relatively small. This, again, is likely due to saturation issues in the organic phase.

The observed similarity in release profiles across the systems, regardless of the active ingredient, whether quercetin or cholecalciferol, strongly suggests that these formulations offer reproducible and consistent release characteristics. This reproducibility is a key advantage, as it indicates that the formulation method can be broadly applied to different lipophilic molecules, ensuring predictable release behavior.

In both cases, the batches containing whey proteins (W-Q and W-D) demonstrated an enhanced ability to improve the dissolution of the active ingredient, releasing it in greater amounts compared to the other formulations. This suggests that whey proteins have a significant solubilizing effect on lipophilic compounds, thereby facilitating a more efficient release. Conversely, the formulations containing a mix of proteins, such as SW-Q and SW-D, as well as the milk-based formulations (M-Q and M-D), exhibited clear gastro-resistant profiles. These formulations effectively delayed the release of the active ingredient, preventing its dissolution in the stomach and promoting release only after a pH change, suggesting a potential for targeted intestinal delivery. This gastro-resistant behavior is particularly beneficial for active ingredients that are unstable in acidic environments or for those that are intended to act primarily in the intestines.

In summary, the whey protein-based batches improve the solubility and dissolution of the active ingredient, while the protein-mix and milk-based formulations provide robust gastroresistance. This dual functionality offers flexibility depending on the desired release profile and site of action, making these systems versatile candidates for the controlled delivery of lipophilic molecules in various pharmaceutical or nutraceutical applications.

In the case of phycocyanin, being a totally water-soluble molecule, it was possible to perform this dissolution test in an aqueous medium only. The aqueous phase was maintained at pH 1-2 for the first two hours of the experiment to reproduce the gastric passage; subsequently, the pH was raised to 6.8 to simulate intestinal transit.

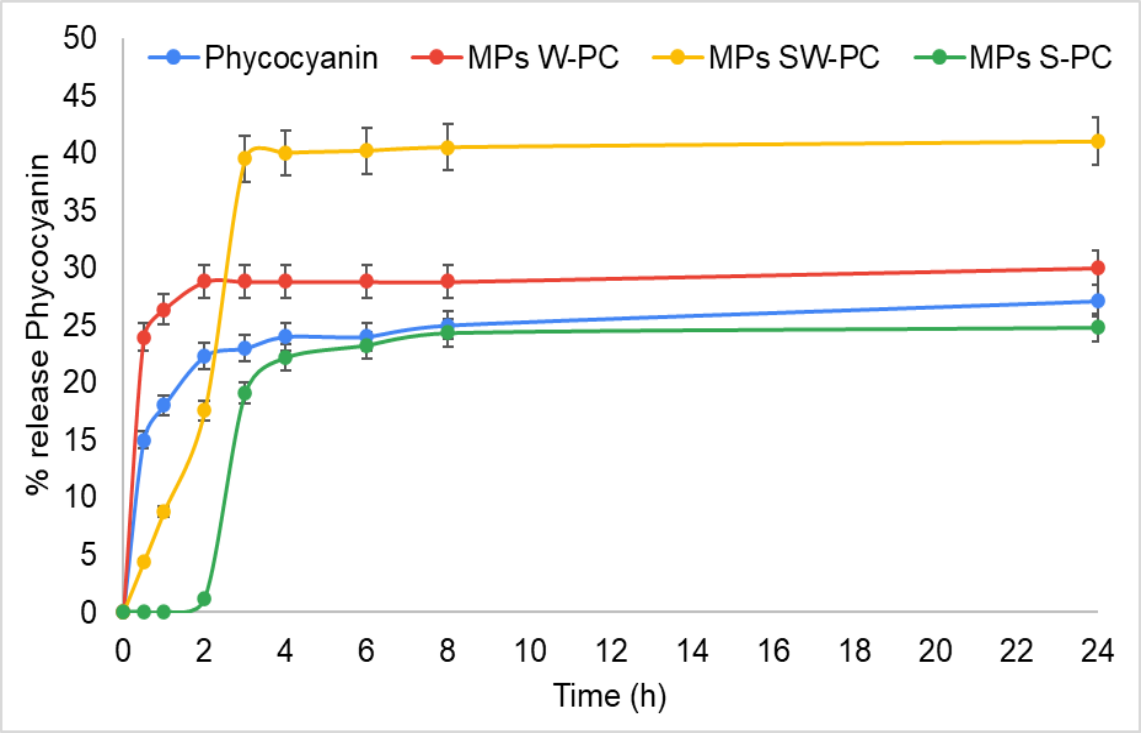

Figure 60 Graph of the percentage of phycocyanin released as a function of time for batches MPs W-PC, MPs SW-PC, MPs S-PC, and pure phycocyanin.

In this case, it is evident that the pure active molecule follows a traditional, uncontrolled release profile, with no mechanisms in place to delay or modulate its release (Figure 60). This type of release results in the immediate availability of the active ingredient shortly after administration, which may not always be desirable, particularly for compounds that could benefit from controlled or targeted delivery. On the other hand, the various batches formulated show distinct modified-release profiles, each tailored to optimize the release of phycocyanin in different ways. Among these, the MPs S-PC batch stand out for their clear gastro-resistant release profile, effectively preventing the release of phycocyanin in the acidic environment of the stomach. This gastro-resistant feature is particularly beneficial for compounds like phycocyanin, which may be unstable or less effective when exposed to gastric acid. In contrast, the MPs W-PC batch exhibit a notable increase in the amount of phycocyanin released, suggesting that whey proteins used in this formulation enhance the solubilization and dissolution of the active ingredient.

The MPs SW-PC batch shows the most significant increase in the amount of active ingredient released overall.

In conclusion, each of the formulated batches offers distinct advantages depending on the desired release profile. This versatility in release mechanisms highlights the potential of these formulations for optimizing the delivery of phycocyanin and other active molecules, depending on the therapeutic goals and the specific requirements of the delivery system.

3.6 Ex-vivo Permeation Study

The ex-vivo permeation study allowed for the assessment of the probable enhanced permeability of microencapsulated active ingredients through the porcine intestinal mucosa used as a model tissue. To simulate trans-mucosal absorption, vertical Franz diffusion cells were utilized as an in vitro permeation model. Each cell consists of two main sections: the donor compartment, where the sample of microparticles to be tested is placed, suspended in water at the appropriate pH; and the acceptor compartment, which contains saturated n-octanol as a suitable solvent for the lipophilic compounds or water for hydrophilic substances that permeate the mucosa. The entire cell was then thermostatted at 37°C. The pH and temperature parameters were selected to mimic the conditions typical of the gastrointestinal passage of a formulation administered orally. The porcine intestinal mucosa was placed between the two compartments (Figure 61).

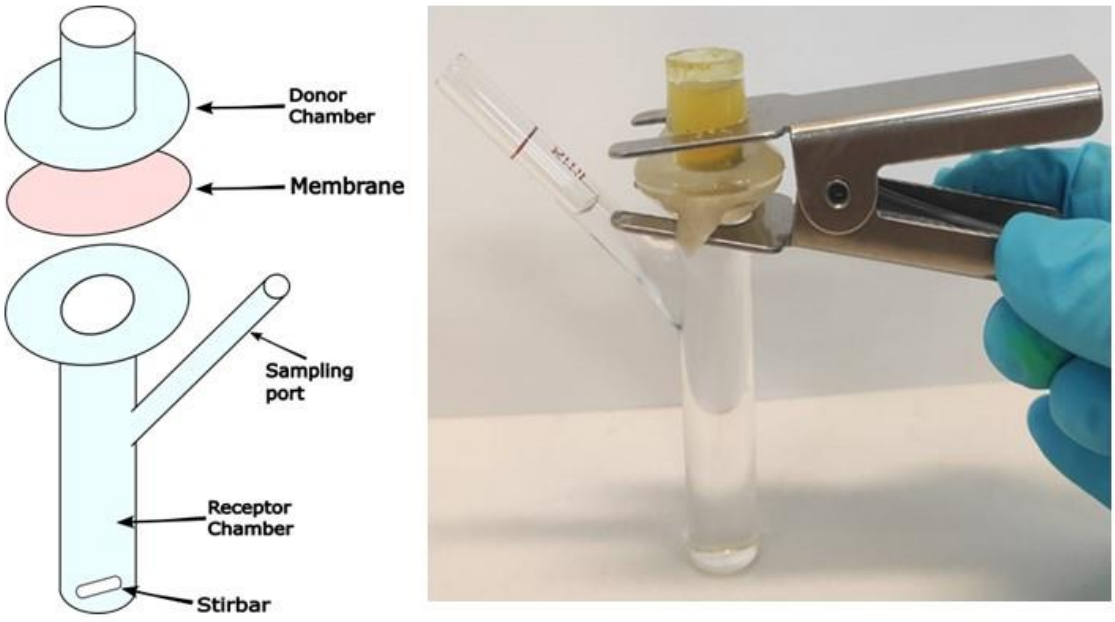

Figure 61 Diagram of a vertical Franz diffusion cell (left) illustrating the donor chamber, membrane, receptor chamber, sampling port, and stirbar. The right side shows a physical setup of the vertical Franz diffusion cell, with the donor chamber containing the sample.

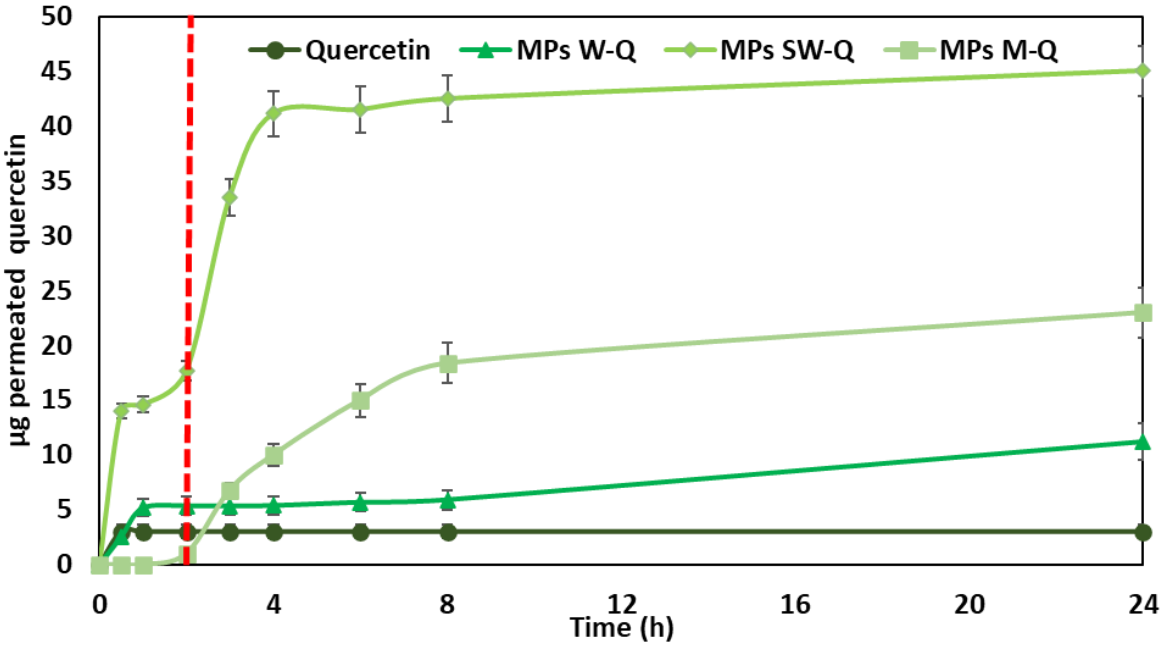

Figure 62 Amount (µg) of permeated quercetin as a function of time for batches WQ, SW-Q, MQ, and pure quercetin.

Actually, ex vivo permeation studies of quercetin (Figure 62) revealed greater transmucosal permeation capacity for microparticles produced with the WPs and SPs, and also for the batch MPs MQ which show a gastro-resistant permeation profile. Instead, ex vivo permeation studies of cholecalciferol (Figure 63) show that all the batches produced significantly improved the amount of the active molecule permeated through the porcine colon mucosa, in particular M-D batch, but did not show a specific modified-permeation profile.

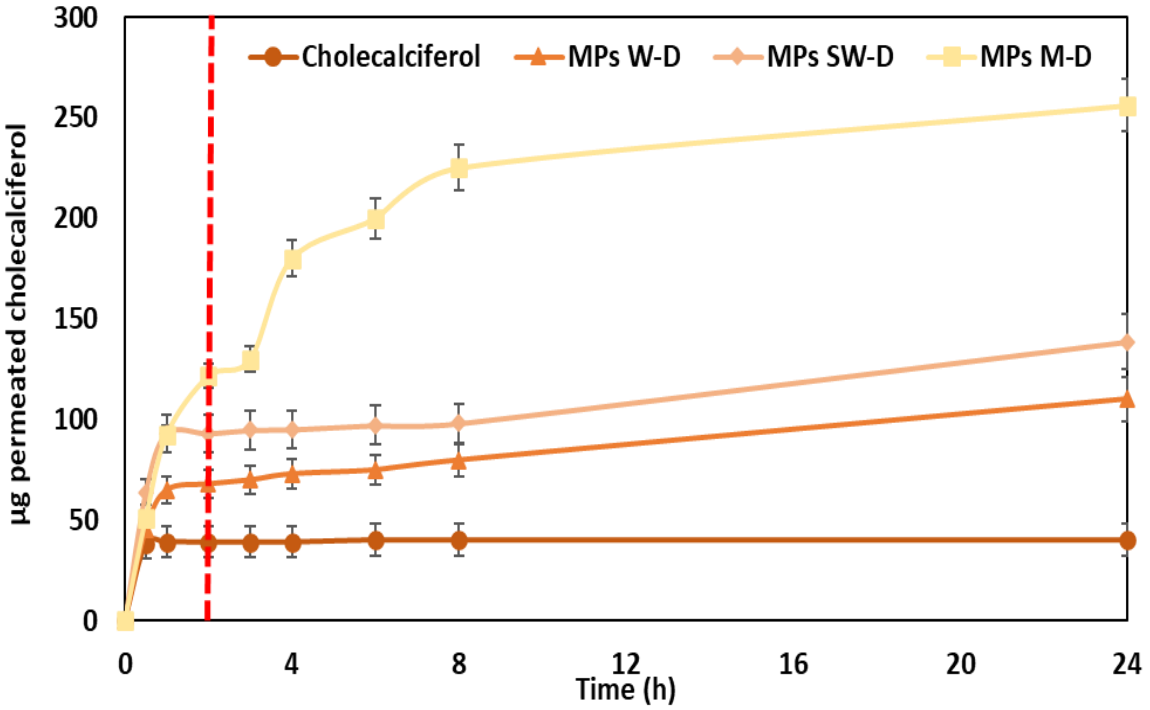

Figure 63 Amount (µg) of permeated cholecalciferol as a function of time for batches WD, SW-D, MD, and pure cholecalciferol.

Finally, the ex-vivo permeation studies of phycocyanin showed considerable advantages achieved by the produced systems: while pure phycocyanin fails to permeate through the colon mucosa, probably due to the lower affinity with it, being a water-soluble molecule, all produced batches allow to higher the amounts of the permeated active molecule. Even in this case, WPs act as enhancers of permeation, while SPs act as gastro-resistant agents (Figure 64).

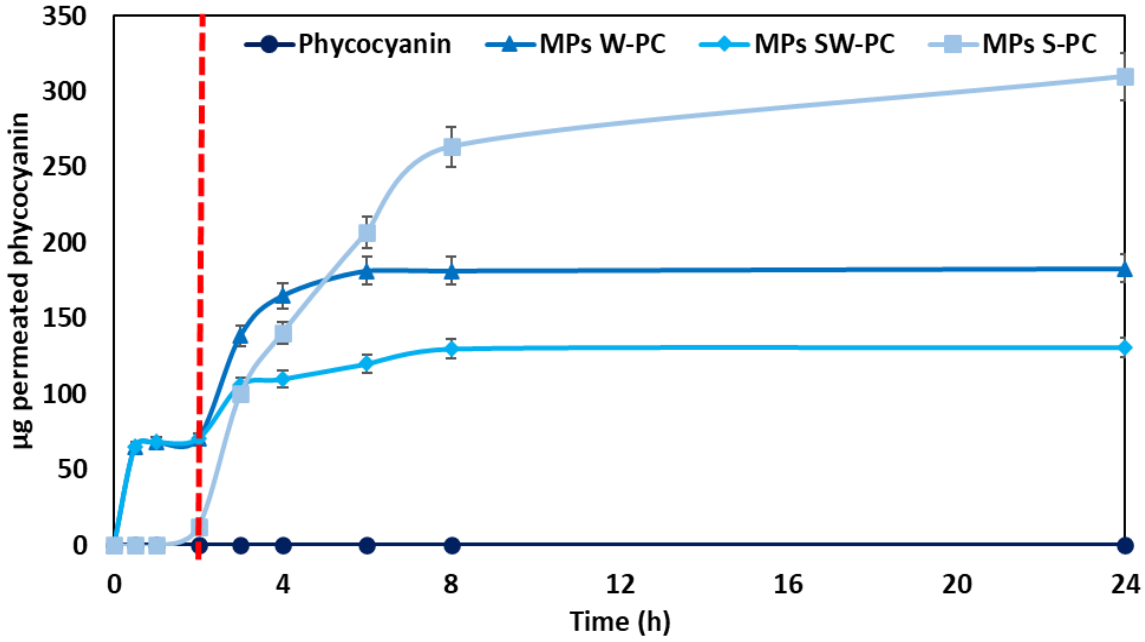

Figure 64 Amount (µg) of permeated phycocyanin as a function of time for batches W-PC, SW-PC, S-PC, and pure phycocyanin.

Based on the results obtained from the in vitro dissolution tests and the ex vivo permeation tests, five of the different batches of microparticles produced were selected, namely MPs SW-Q, MPs M-Q, MPs SW-D, MPs M-D and MPs S-PC. These were then selected for subsequent in vivo tests on animals on an inflammatory bowel disease model.

3.7 In vivo Studies on DNBS-Induced Colitis Rat Model

To enhance the bioavailability of quercetin and cholecalciferol, which are poorly water-soluble, and to protect phycocyanin, a water-soluble acid-unstable molecule, gastro-resistant microparticles were developed. These microparticles were formulated using natural proteins, such as whey and soy proteins, which provide a protective and soluble matrix. Through the spray-drying technique, a modified-release system was achieved, improving the stability and solubility of the APIs. The study aims to assess the preventive and enhanced effects of the treatment with different types of microparticle formulations (MPs SW-Q, MPs M-Q, MPs SW-D, MPs M-D, and MPs S-PC) on inflammatory response induced in the IBD animal model.

The DNBS (2,4-dinitrobenzene sulfonic acid) rat model is a widely employed experimental model to simulate conditions similar to human IBD, including Crohn's disease and ulcerative colitis, by inducing intestinal inflammation. DNBS is administered to rats, usually through intrarectal injection, to trigger a localized immune response in the colon. DNBS administration results in inflammation, tissue damage, and symptoms that closely resemble human IBD, such as ulceration, infiltration of immune cells, and cytokine release. Researchers use this animal model to study the mechanisms underlying IBD, to assess the efficacy of potential therapeutic agents, and to evaluate how various treatments can modulate the inflammatory response and promote healing of the damaged intestinal lining. This rat model is valuable because it mimics the chronic and relapsing nature of IBD, allowing scientists to explore both acute and long-term effects of inflammation on the gut in a controlled, reproducible manner [144], [145].

In particular, based on all the results obtained from previous characterization studies of the microparticles produced, two protocols were decided to follow:

- Protocol 1: to compare the effects of joint administration of quercetin and cholecalciferol (Q+D) with the effects of microparticles MPs SW-Q and SW-D, or with the impact of MPs M-Q + MPs M-D together;
- Protocol 2: to compare the effects of and a study of the administration of phycocyanin with the effects of microparticles loaded with PC (MPs S-PC).

The type of treatment we tested included a pre-treatment period (14 days), disease induction (day 0), and a subsequent treatment period (6 days), as shown in the timeline in Figure 65.

Figure 65 Timeline of the experimental treatment procedure.

Male Wistar Rats were randomly assigned to 7 experimental groups (5 animals each) based on the uniformity of weight and age. All the animals divided into various groups were administered 14 days before the induction of the IBD by DNBS administration. The control group and the DNBS group were administered one ml of water, while all the other animals were administered one ml of water in which the different tested microparticles or the tested active ingredients were dispersed. On day 0, all subjects (except for the control group) underwent induction of colon inflammation through intrarectal administration of DNBS. After the induction of the disease, all animals were treated for a further six days in the same way as they had been treated in the 14 days of pre-treatment. Only on the seventh-day post-DNBS were the animals sacrificed and analyzed.

DNBS challenge in rats induced a substantial decrease in the body weight starting by day 2 following the enema, in contrast to the control group which showed body weight gain. During the same period DNBS group experienced diarrhoea and also rectal bleeding was observed. The animals were monitored daily during the experimental period and scored for body weight loss percentage, stool consistency, and the presence of rectal bleeding. All these parameters were ranged and calculated as described by Cooper et al [146], constituting the DAI score (Disease Activity Index).

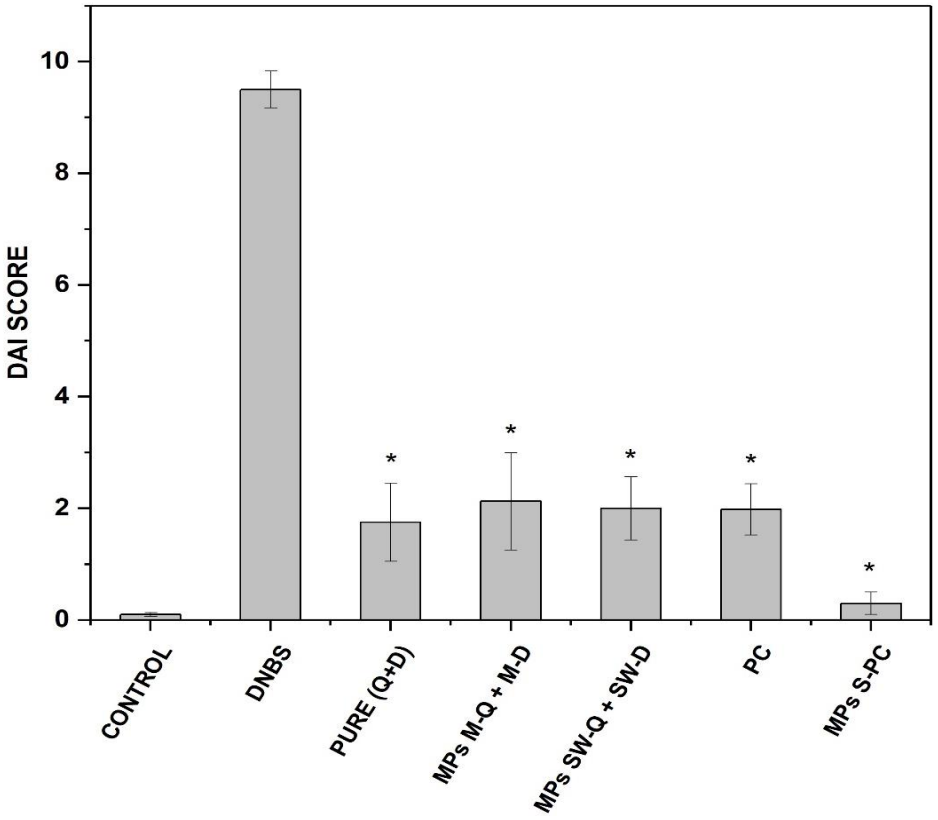

Figure 66 Disease activity index (DAI) score for 7 different administered groups: Control, DNBS, quercetin and cholecalciferol (PURE Q + D), MPs M-Q and M-D, MPs SW-Q and SW-D, phycocyanin (PC), and MPs S-PC. Data are means ± S.E.M. *n* = 5 animals /group. * $p < 0.05$ versus 2,4 dinitrobenzensulfonic acid (DNBS) animals.

All treated groups show a significant decrease in DAI scores compared to the DNBS group, with visible improvement in pathological conditions, including reduced diarrhea, rectal

bleeding, and weight loss. In particular, the microparticles containing quercetin and cholecalciferol were able to maintain the therapeutic activity of the pure active ingredients, demonstrating comparable effectiveness in reducing the typical symptoms of inflammation. This result suggests that the encapsulation process did not interfere with the bioactivity of these compounds, allowing for sustained therapeutic effects. In contrast, for phycocyanin, the results showed that the microparticle formulation (S-PC) had a notably enhanced impact, achieving a significantly greater reduction in DAI scores than phycocyanin administered in its pure form. This indicates that the encapsulation of phycocyanin into microparticles not only preserved its activity but actually improved its effectiveness in reducing inflammation.

Macroscopic evaluation demonstrated that in the control group, the distal colon showed no epithelial damage differently from the colitis group in which intense mucosal damage, increased wall thickness, hyperemia, ulceration, edema, and necrosis were observed associated with high macroscopic score (Figure 67 B). DNBS rats revealed also colon shortening accompanied by an increase in the ratio colon weight/length, a marker of tissue inflammation, (17 vs. 13 cm colon length in the control group and DNBS group respectively*;* 1420 vs. 5100 mg colon weight in the control group and DNBS group respectively) (Figure 67 A).

In any case, animals treated with both pure active ingredients and the microparticle systems produced showed an improvement in the macroscopic score and in the weight-length ratio of the colon (Figure 67 A-B). Animals treated with the MPS SW-Q and MPs SW-D and those treated with the MPs S-PC batch showed a general improvement in the inflammatory symptoms characteristic of the induction of DNBS colitis with a reduction in the number of ulcerated sites, a decrease in the increase in the thickness of the intestinal wall, and therefore a general improvement in the microscopic index. Interestingly MPS SW-Q + SW-D or MPs S-PC improved both macroscopic score and W/L ratio more than the respective pure compounds suggesting a higher efficacy.

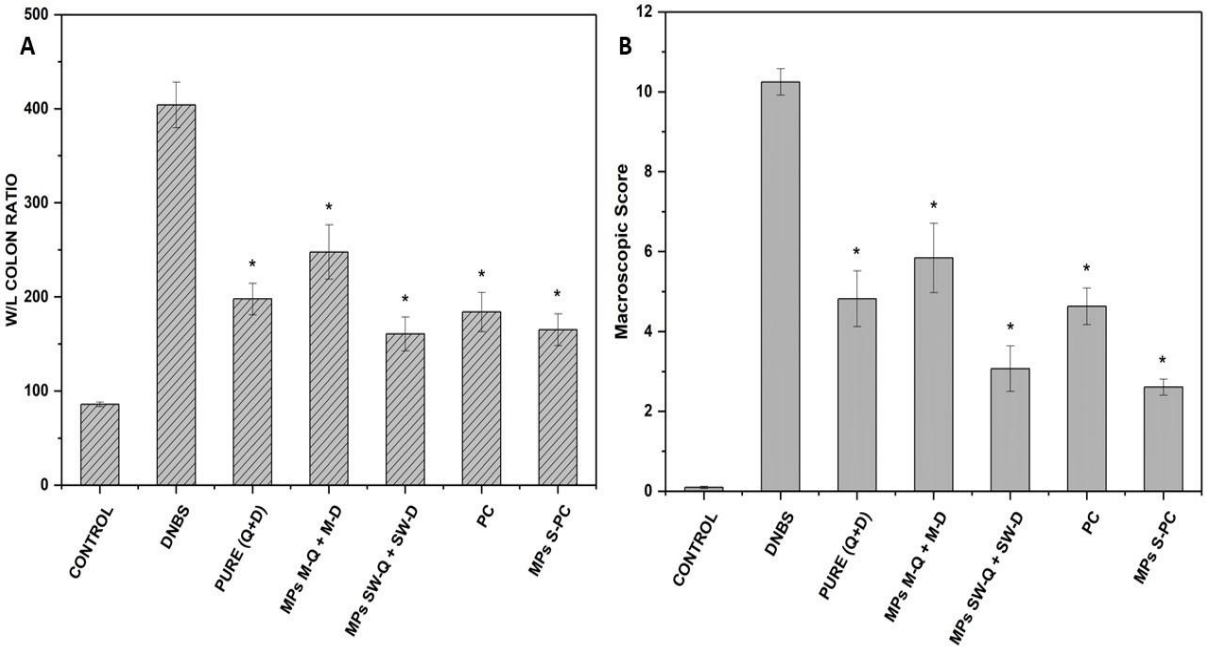

Figure 67 (**A**) Colon weight/Length ratio and (**B**) Macroscopic damage score based on Appleyard and Wallace method for 7 different administered groups: Control, DNBS, quercetin and cholecalciferol (PURE Q + D), MPs M-Q and M-D, MPs SW-Q and SW-D, phycocyanin (PC), and MPs S-PC. Data are means ± S.E.M. $n = 5$ animals /group. * $p < 0.05$ versus 2,4 dinitrobenzensulfonic acid (DNBS) animals.

In summary, both from the results obtained by the DAI score, by the macroscopic score, and from those obtained by the weight-length ratio of the colon, it is possible to identify a general trend where the microparticles formulated with soy proteins and whey proteins are more efficient than the batches formulated exclusively with whey proteins and milk for quercetin and cholecalciferol. In contrast, in the case of phycocyanin, the microparticles are much more active in reducing the inflammatory symptoms associated with this pathology in the more macroscopic aspect.

Myeloperoxidase (MPO) levels are often used to quantify neutrophil functions and activity in inflamed tissues [147]. An increase in leukocyte adhesion and accumulation in colon tissues and in MPO activity (Figure 68) is typically observed during IBD and in experimental animal

models as DNBS-induced colitis. Treatment with quercetin and cholecalciferol, and phycocyanin significantly reduced MPO levels in DNBS rats when compared to DNBS group.

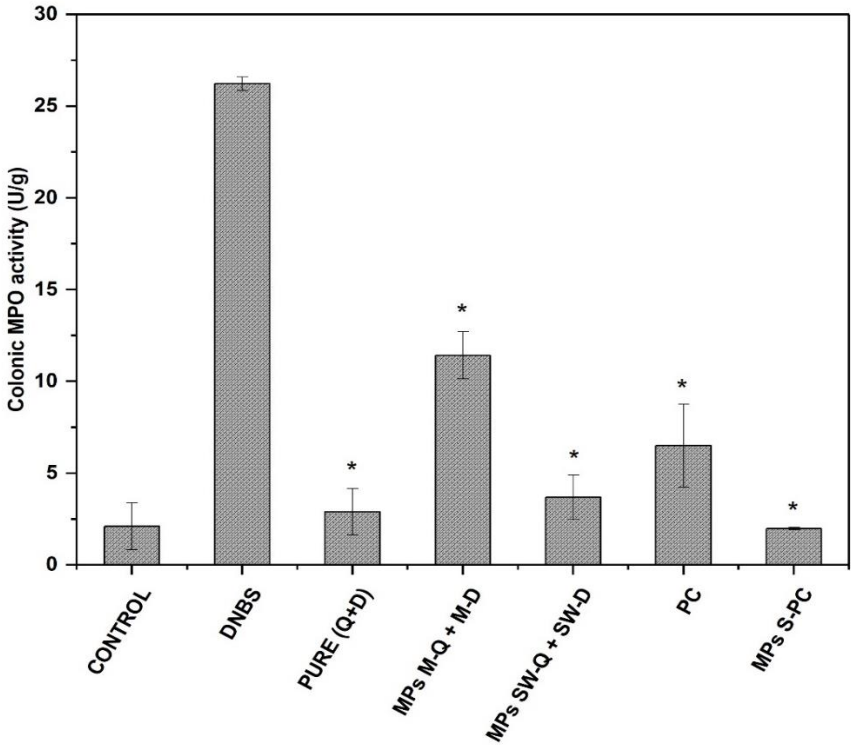

Figure 68 Colonic myeloperoxidase (MPO) activity for 7 different administered groups: Control, DNBS, quercetin and cholecalciferol (PURE Q + D), MPs M-Q and M-D, MPs SW-Q and SW-D, phycocyanin (PC), and MPs S-PC. Data are means ± S.E.M. *n* = 5 animals /group. * $p < 0.05$ versus 2,4 dinitrobenzensulfonic acid (DNBS) animals.

The severity of colon tissue damage was evaluated by histological analysis using hematoxylin and eosin (H&E) staining. In the control group, the histological examination of the distal colon (Figure 69 A) revealed a normal histoarchitecture characterized by an intact crypt structure, which is a critical feature for maintaining proper intestinal function. The mucosal layer appeared well-organized, with clearly defined epithelial cells and normal cellular composition, indicating a healthy and functional intestinal environment. There were no signs of tissue damage or inflammation, and the overall morphology of the colon was consistent with normal physiological conditions.

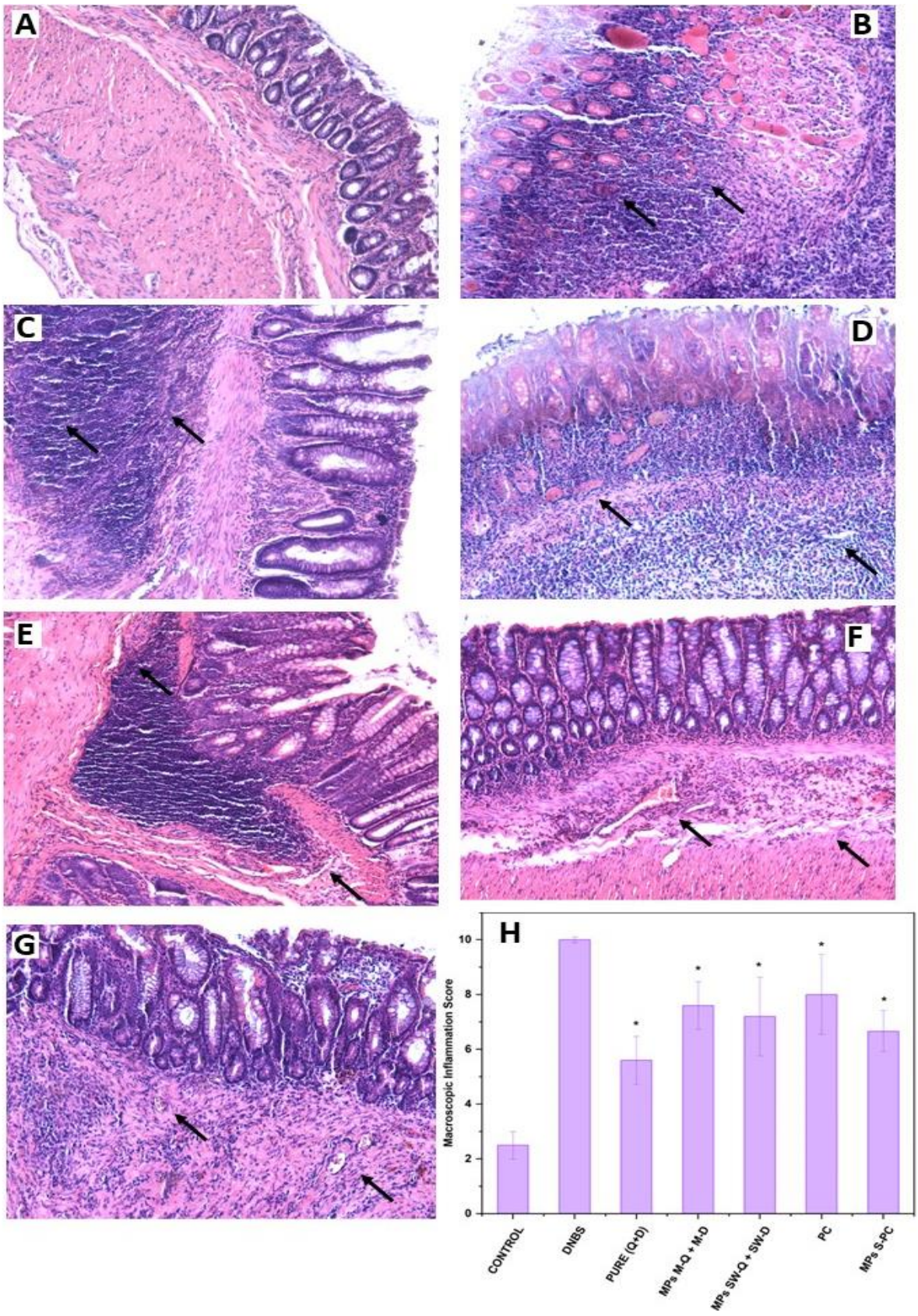

Figure 69 Representative H&E-stained colon sections from **(A)** Control, **(B)** DNBS, **(C)** quercetin and cholecalciferol, **(D)** MPs M-Q and M-D, **(E)** MPs SW-Q and SW-D, **(F)**

phycocyanin, and **(G)** MPs S-PC. **(H)** Microscopic inflammation score for 7 different administered groups: Control, DNBS, quercetin and cholecalciferol (PURE Q + D), MPs M-Q and M-D, MPs SW-Q and SW-D, phycocyanin (PC), and MPs S-PC. Data are means ± S.E.M. $n = 5$ animals /group. * $p < 0.05$ versus 2,4 dinitrobenzensulfonic acid (DNBS) animals.

Conversely, in the DNBS-treated rats, H&E staining revealed severe pathological changes, as depicted in Fig. 69 B and H. These changes were indicative of significant colon damage, typically associated with the induction of colitis in this experimental model. The microscopic damage scores in this group were considerably higher compared to the control group, reflecting the extensive tissue injury and inflammatory response induced by DNBS. Histological analysis showed the presence of superficial ulcers, which are characteristic of damaged mucosa, as well as mucosal atrophy. There was also a partial loss of microvilli, which are essential for nutrient absorption and barrier function. Additionally, there was edema in the lamina propria, indicating excessive fluid accumulation due to inflammation. The most prominent feature in the DNBS group, however, was the marked infiltration of immune cells into the intestinal wall, signifying a robust immune response. This immune cell infiltration is a hallmark of chronic inflammation and is commonly associated with tissue damage in inflammatory bowel disease.

Compared with the DNBS group, all the treated groups showed a general improvement of the inflammatory conditions, with reduced intensity of the superficial ulcers of intestinal mucosa, reduction of partial microvilli loss, and reduction of edema of the lamina propria, resulting in a significant reduction of the score of microscopic damage score (Figure 69 B-C-D-E-F-G-H).

From this study, it is possible to deduce how the group treated with the SW-Q and SW-D or with M-Q and M-D microparticles are not able to improve the histological score, in contrast, the group treated with the S-PC microparticles demonstrate a higher decrease in the microscopic inflammation index and therefore an improvement in the intestinal inflammatory condition caused by the DNBS used to induce the pathology.

3.8 In vivo Bioavailability Studies

Furthermore, an in vivo bioavailability study was conducted to compare the profiles of the APIs with those of the new microparticle systems created. In a typical in vivo study on rats evaluating the bioavailability of a drug, the procedure involves comparing the bioavailability of the drug in its pure form with a modified formulation designed to enhance bioavailability. This process is crucial in pharmaceutical technology and in the development of smart delivery systems. The study usually followed these key steps:

- The pure active ingredient and microparticles systems are administered to rats by oral gavage. -Blood samples were collected at specific time points after drug administration. These samples help measure the concentration of the drug in the bloodstream over time.
- Sophisticated analytical techniques, such as high-performance liquid chromatography (HPLC) were employed to quantify drug concentrations in the collected blood samples.
- Pharmacokinetic parameters, including maximum concentration (Cmax), time to reach maximum concentration (Tmax), and area under the curve (AUC), are calculated and compared.

The bioavailability study was carried out only on cholecalciferol and MPs SW-D and MPS M-D, and on phycocyanin and the microparticle systems that contain it (MPs S-PC). Quercetin was excluded from this study as its bioavailability in microparticle form had been previously investigated by the research group, demonstrating its enhanced bioavailability in an earlier study [55]. This decision aligns with European directives aimed at reducing animal usage in experimental procedures, both to adhere to ethical standards and to manage associated costs. However, further studies may be considered in the future to validate and expand upon the existing findings.

As we can see from Figure 70, it is clear that the MPS M-D and SW-D microparticle systems show a notable increase in the bioavailability and therefore in the blood concentration of cholecalciferol (C_{max} for group Cholecalciferol is 0.64 µg/ml; C_{max} for group MPs M-D is 1,03 µg/ml; C_{max} for group MPs SW-D is 1,13 µg/ml) and in particular it is the SW-D system that reaches the maximum AUC value. It is interesting to note how the Cmax for the two microparticle systems corresponds to a different Tmax compared to that of the pure drug (T_{max} for group Cholecalciferol is 2h; T_{max} for group MPs M-D is 6h; T_{max} for group MPs SW-D is 6h), effectively suggesting a modified release of our systems, in particular of the gastro-resistant type.

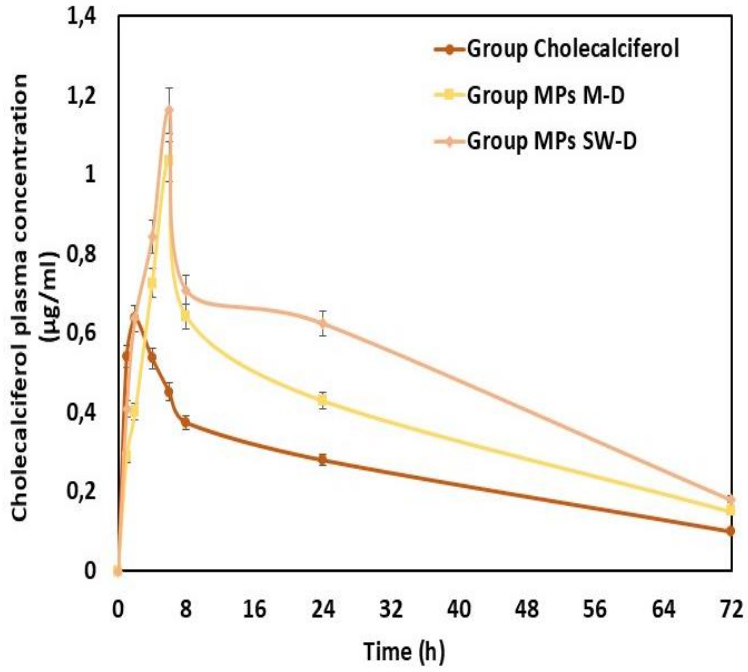

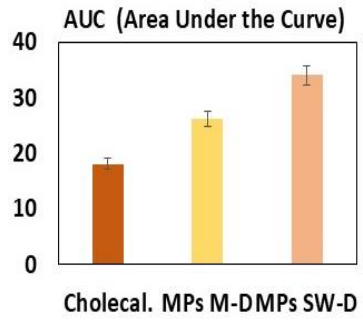

Batches	C max	T max
Cholecalciferol	0.64 µg/ml	2 h
MPs SW-D	1,13 µg/ml	6 h
MPs M-D	1,03 µg/ml	6 h

Figure 70 Cholecalciferol plasma concentration over time following administration of the pure compound (Group Cholecalciferol) and microparticle formulations (Groups MPs M-D and MPs SW-D) in rats. The inset bar chart represents the Area Under the Curve (AUC) values, indicating total bioavailability for each formulation. The table summarizes key pharmacokinetic parameters, including maximum plasma concentration (Cmax) and time to reach maximum concentration (Tmax).

In Figure 71, the enhanced bioavailability of phycocyanin is evident in the MPs S-PC microparticle systems. This is reflected in the increased blood concentration of phycocyanin, as indicated by the C_{max} values for each group (C_{max} for group Phycocyanin is 0.45 mg/ml; C_{max} for group MPs S-PC is 0.91 mg/ml). Notably, the S-PC system achieves the maximum AUC value. An intriguing observation is the difference in Tmax for the microparticle system compared to the pure drug, suggesting a modified release profile, particularly of the gastro-resistant type. Specifically, the Tmax for group Phycocyanin is 2 hours, whereas for group MPs S-PC, it is delayed between 4 and 6 hours. This temporal shift in Tmax implies a controlled and sustained release of phycocyanin from the microparticle systems, showcasing their potential as a gastro-resistant formulation.

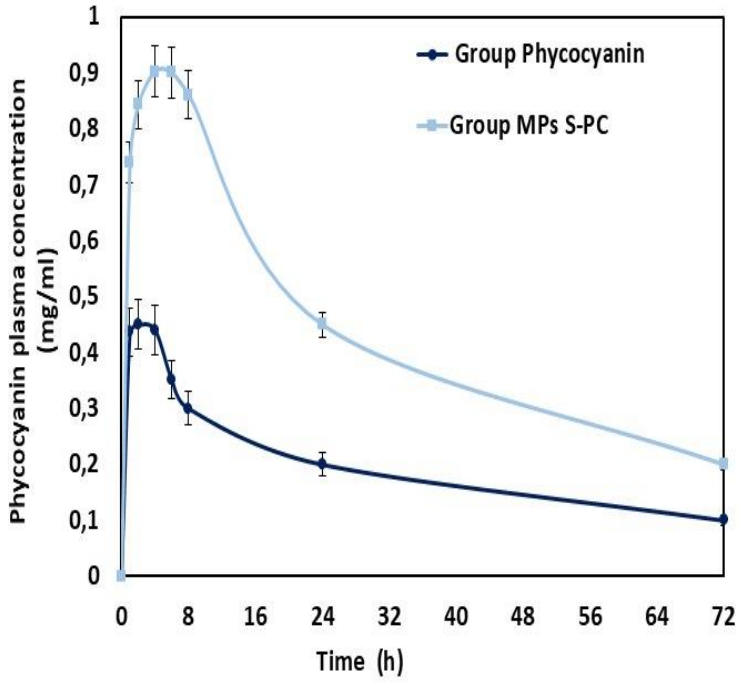

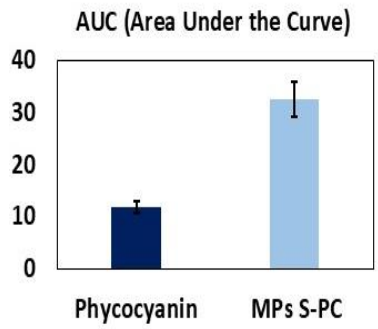

Batches	C max	T max
Phycocyanin	0.45 mg/ml	2 h
MPs S-PC	0.91 mg/ml	5 h

Figure 71 Phycocyanin plasma concentration over time following administration of the pure compound (Group Phycocyanin) and microparticle formulations (Groups MPs S-PC) in rats. The inset bar chart represents the Area Under the Curve (AUC) values, indicating total bioavailability for each formulation. The table summarizes key pharmacokinetic parameters, including maximum plasma concentration (Cmax) and time to reach maximum concentration (Tmax).

4 CONCLUSION

This work successfully formulated and characterized modified-release microparticles encapsulating natural active compounds such as quercetin, cholecalciferol,and phycocyanin, to address challenges of poor solubility and stability, which traditionally limit the bioavailability and therapeutic effectiveness of these molecules. These dosage forms, intended for oral administration, were designed so that they possess technological characteristics that ensure a good protection profile of the active ingredients from all those physiopathological and chemical-physical factors related to the gastrointestinal system that would limit their therapeutic efficacy. The encapsulation of these active ingredients into protein-based microparticles has demonstrated a viable solution to improve the delivery profile, maintain stability, and achieve a targeted release, which is especially beneficial for therapeutic applications in inflammatory bowel disease (IBD).

For this purpose, several batches of microparticles containing the above-selected active ingredients were produced using the spray drying technique. Specifically, three different batches for each active ingredient were produced, one based on whey proteins and the active ingredient (MPs W-Q, W-D, and W-PC), another based on a 1-to-1 mix of whey proteins and soy proteins (MPs SW-Q, SW-D, and SW-PC), and finally a final batch containing whey proteins and milk used as the dispersing phase (MPs M-Q and M-D). Only for phycocyanin the third batch corresponds to a batch of microparticles based on soy proteins (MPs S-PC). This is justified by the difference in the chemical nature of this active ingredient compared to the other two. A detailed physicochemical characterization of the microparticles, including UV spectroscopy for encapsulation efficiency and drug loading, scanning electron microscopy for particle morphology and size, FT-IR for assessing chemical stability and verifying incorporation of active ingredients, and thermogravimetric analysis for thermal stability,

provided a comprehensive profile of the formulation's physical and chemical stability. Solid-state analyses using XRPD and DSC revealed that the spray-drying process successfully converted the active ingredients into an amorphous state within the microparticles, a transformation known to enhance solubility and bioavailability. These analyses collectively demonstrated that the microparticles maintained their amorphous structure, stability, and encapsulation integrity, factors that are essential for the successful delivery of poorly soluble compounds. In vitro antioxidant assays, specifically the DPPH radical scavenging assay, were performed on microparticles containing quercetin and phycocyanin to verify that their encapsulated forms retained the well-documented antioxidant properties of these compounds. The results confirmed that even under the rigorous conditions of spray-drying, the microparticles preserved the radical scavenging capacity of both quercetin and phycocyanin, validating the effectiveness of the protein matrix in protecting the active compounds from potential degradation.

Dissolution and ex-vivo permeation studies further validated the microparticle formulations' ability to release the active ingredients in a controlled manner through the gastrointestinal tract, an essential feature for effective delivery in IBD treatment. The dissolution profiles revealed that the microparticles achieved the controlled release of the active ingredients, with the protein matrix effectively protecting the compounds in simulated gastric conditions and ensuring their gradual release in intestinal conditions. Ex-vivo permeation studies using porcine intestinal mucosa demonstrated improved permeation of the microparticle formulations compared to the unencapsulated active ingredients, suggesting an enhanced potential for bioavailability in vivo.

The therapeutic potential of the microparticle formulations was further validated in an in vivo study using the DNBS-induced colitis rat model, which served as a representative system for inflammatory bowel disease (IBD). Five optimized batches of microparticles (MPs SW-Q, MPs SW-D, MPs M-Q, MPs M-D, and MPs S-PC), including those containing quercetin and

cholecalciferol in co-administration, as well as phycocyanin alone, were selected for evaluation. The results showed that the co-administration of quercetin and cholecalciferol microparticles yielded an anti-inflammatory effect comparable to that of the pure compounds, underscoring the successful preservation of their bioactivity through encapsulation. Notably, the phycocyanin microparticle formulation demonstrated a superior therapeutic effect over pure phycocyanin, highlighting the benefits of encapsulation for enhancing the stability and efficacy of phycocyanin in the inflammatory environment.

Finally, bioavailability studies conducted on both cholecalciferol and phycocyanin microparticles showed improved absorption profiles when compared to their non-encapsulated forms, further supporting the advantage of protein-based encapsulation for increasing the bioavailability of these natural compounds.

In conclusion, this study demonstrates the feasibility and effectiveness of protein-based microparticle systems for the targeted delivery of natural bioactive compounds with limited solubility and stability. The promising in vivo results suggest that such microparticle formulations have strong potential in therapeutic applications, particularly for chronic inflammatory diseases like IBD, where enhanced bioavailability, controlled release, and protection of bioactive compounds through the gastrointestinal tract can lead to improved therapeutic outcomes and patient quality of life. These findings open the door for further research on protein-based delivery systems, encouraging exploration into additional bioactive compounds and chronic disease models to expand the clinical utility of this innovative drug delivery platform.

5 EXPERIMENTAL SECTION

5.1 Materials

Quercetin, cholecalciferol, n-octanol, ethanol, 2,2-diphenyl-1-picrylhydrazyl (DPPH), Dulbecco's phosphate buffer saline (DPBS), acetonitrile (ACN), methanol (MeOH), trifluoroacetic acid (TFA), sodium edetate (EDTA), and ascorbic acid were purchased from Sigma-Aldrich, Italy. Phycocyanin was purchased from Algreen B.V., Wageningen (Netherlands). Whey Proteins and Soy proteins were purchased from Galeno srl, Italy. HCl and NaOH were purchased from VWR. Porcine mucosa was provided from Istituto Zooprofilattico della Sicilia "A. Mirri," Palermo, Italy according to European rules on animal experiments.

Wistar rats (weighing 120-150 g), purchased from ENVIGO Srl (San Pietro al Natisone UD, Italy) were employed throughout the study. The animals were housed in temperature-controlled rooms on a 12 h light cycle at 22–24°C and 50–60% humidity. They were fed standard laboratory chow and tap water ad libitum. Animals were allowed to acclimatize to the housing conditions for 1 week before experimentation. Procedures involving animals and their care were conducted in conformity with the Italian D.Lgs 26/2014 and following the provisions of the European Community Council Directive 210/63/UE, recognized and adopted by the Italian Government. The experiments were approved by the Ethical Committee for Animal Experimentation of the University of Palermo and by the Italian Ministry of Health (Authorization n. 56/2023-PR). No other methods to perform the described experiments (3Rs) were found.

5.2 Methods

5.2.1 Preparation of the Gastro-Resistant Microparticle Formulations

To prepare WP gastro-resistant microparticles (batches MPs W-Q, W-D, and W-PC), 2.5 g of WPs were dispersed in 50 mL of bidistilled water under continuous stirring at 25 °C for 30 min; then, a specific amount of the selected active ingredient (0.65 g quercetin, 0.1 g cholecalciferol, 0.8 g phycocyanin) solubilized in ethanol (for quercetin and cholecalciferol) or water (phycocyanin) was added. The dispersion was stirred for another 30 min. Finally, the dispersion was treated with ultraturrax at 24,000 rpm for 5 minutes.

The micro delivery systems were produced with the Mini Spray-Dryer Buchi B290 (Buchi, Germany). The spray drying process was performed according to the following parameters:

- Inlet temperature: 130 °C;
- Outlet temperature: 70–73 ◦C;
- Aspiration: 100%;
- Feed pump: 15% (4.5 mL/min);
- Atomizer nozzle: 0.7 mm;
- Gas: compressed air.

To prepare SW gastro-resistant microparticles (batches MPs SW-Q, SW-D, and SW-PC), 2.5 g of SWs (Glycine max) were dispersed in 50 ml of bidistilled water and stirred with a paddle stirrer in a cold room (4°C) over the night. 2.5 g of WPs were dispersed in 50 ml of bidistilled water and stirred for 30 minutes; then, the two dispersions of WPs and SPs were mixed and a specific amount of the selected active ingredient (0.5 g quercetin, 0.1 g cholecalciferol, 0.8 g phycocyanin) solubilized in ethanol (for quercetin and cholecalciferol) or water (phycocyanin) was added. The dispersion was stirred for another 30 min. Finally, the dispersion was treated with ultraturrax at 24,000 rpm for 5 minutes.

The micro delivery systems were produced with the Mini Spray-Dryer Buchi B290 (Buchi, Germany). The spray drying process was performed according to the following parameters:

- Inlet temperature: 130 °C;
- Outlet temperature: 70–73 ◦C;
- Aspiration: 100%;
- Feed pump: 15% (4.5 mL/min);
- Atomizer nozzle: 0.7 mm;
- Gas: compressed air.

To prepare MPs M-Q (Quercetin microparticles with milk and whey proteins), the excipients (whey proteins) were dispersed in whole milk (total dry residue in 100 mL: 3.6 g of fat, 4.8 g of carbohydrates, 3.2 g of protein, 0.13 g of salt and 0.12 g of calcium) under continuous stirring at 25 °C for 30 min. A specific amount of quercetin solubilized in 10 mL of ethanol was added and the dispersion was stirred for another 30 min. Finally, the dispersion was treated with ultraturrax at 24,000 rpm for 5 minutes.

The micro delivery systems were produced with the Mini Spray-Dryer Buchi B290 (Buchi, Germany). The spray drying process was performed according to the following parameters:

- Inlet temperature: 130 °C;
- Outlet temperature: 70–73 ◦C;
- Aspiration: 100%;
- Feed pump: 15% (4.5 mL/min);
- Atomizer nozzle: 0.7 mm;
- Gas: compressed air.

To prepare MPs M-D (Cholecalciferol microparticles with milk and whey proteins), the excipients (whey proteins) were dispersed in whole milk (total dry residue in 100 mL: 3.6 g of fat, 4.8 g of carbohydrates, 3.2 g of protein, 0.13 g of salt and 0.12 g of calcium) under continuous stirring at 25 °C for 30 min. A specific amount of cholecalciferol solubilized in 5 mL of ethanol was added and the dispersion was stirred for another 30 min. Finally, the dispersion was treated with ultraturrax at 24,000 rpm for 5 minutes.

The micro delivery systems were produced with the Mini Spray-Dryer Buchi B290 (Buchi, Germany). The spray drying process was performed according to the following parameters:

- Inlet temperature: 130 °C;
- Outlet temperature: 70–73 ◦C;
- Aspiration: 100%;
- Feed pump: 15% (4.5 mL/min);
- Atomizer nozzle: 0.7 mm;
- Gas: compressed air.

To prepare S-PC gastro-resistant microparticles (phycocyanin microparticles with soy proteins), 2.5 g of SPs (Glycine max) were dispersed in 50 ml of bidistilled water and stirred with a paddle stirrer in a cold room (4°C) over the night. 2.5 g of WPs were dispersed in 50 ml of bidistilled water and stirred for 30 minutes. A specific amount of phycocyanin was added and the dispersion was stirred for another 30 min. Finally, the dispersion was treated with ultraturrax at 24,000 rpm for 5 minutes.

The micro delivery systems were produced with the Mini Spray-Dryer Buchi B290 (Buchi, Germany). The spray drying process was performed according to the following parameters:

- Inlet temperature: 130 °C;

- Outlet temperature: 70–73 ◦C;
- Aspiration: 100%;
- Feed pump: 15% (4.5 mL/min);
- Atomizer nozzle: 0.7 mm;
- Gas: compressed air.

After the microparticle production, the percentage yield of the process (% Y) ± SD (mean ± SD, n = 3) was calculated as:

$$\%Y = \frac{\text{Mass of excipients and active ingredient in the formulation}}{\text{mass of microparticles obtained}} \times 100$$

The amount of drug loaded within the microparticles produced was determined by solubilizing the formulations in ethanol or water to obtain solutions with a concentration of 1 mg/ml that were stirred on a plate for 2 hours. Subsequently, 3 ml of each solution were taken and filtered using 0.2 µm syringe filters with a regenerated cellulose membrane. The Drug Loading % of each sample in triplicate was determined using the JascoV-760 UV spectrophotometer, using a calibration curve obtained by analyzing aliquots with known concentrations of each pure active ingredient. The drug loading (DL%) ± SD (mean ± SD, n = 3) was calculated according to the formula below:

$$\%\ DL = \frac{\text{Mass of active ingredient in microparticles}}{\text{mass of microparticles}} \times 100$$

The amount of quercetin contained in the microparticles W-Q; SW-Q and M-Q was determined by recording the absorbance value detected at a wavelength of 376 nm.

The amount of cholecalciferol contained in the microparticles W-D; SW-D and M-D was determined by recording the absorbance value detected at a wavelength of 266 nm.

The amount of phycocyanin contained in the microparticles W-PC; SW-PC and S-PC was determined by recording the absorbance value detected at a wavelength of 616 nm.

The encapsulation efficiency (%EE) ± SD (mean ± SD, n = 3) was determined by accounting for the encapsulated active ingredients within their respective MPs systems and the amount introduced in the feed of the spray dryer.

$$\%\ EE = \frac{\text{Mass of active ingredient in microparticles}}{\text{mass of active in the feed}} \times 100$$

5.2.2 Characterization Study of the Microparticle Systems

The particle's size and morphology were measured by scanning electron microscopy (SEM) imaging technique, using a Phenom ProXSEM. Each sample was deposited onto a carbon-coated steel stub and dried under vacuum (0.1 Torr) before analysis. All of the SEM analyses were performed at 25.0 °C ± 0.1 °C. The average diameter (d) ± standard deviation (SD) (mean ± SD, n = 3) of the microparticles was determined from the mean value of 50 measurements using ImageJ (Madison, WI, USA, version 1.46 v).

Conventional FTIR studies were carried out to identify any molecular chemical group of drugs quercetin, cholecalciferol, and phycocyanin, and excipients, whey and soy proteins. Samples were prepared by compression of a thin circular tablet using a 1:99 drug to KBr ratio. Samples were placed on the holder, and nitrogen gas was used to reduce the carbon dioxide peak. Spectra were collected using a JASCO FTIR-6000 spectrometer, from 4000 to 400 cm^{-1} with 128 scans (same as background) at the resolution of 2 cm^{-1} for each sample. The results are shown as a comparison of FTIR spectra of API, excipients, and produced microparticles. Experiments were carried out in triplicate.

Thermogravimetric analyses (TGAs) were performed with Labsys TGA-DSC Setaram, at a heating rate of 5 °C/min between 25 and 550 °C using alumina crucibles. The water content ± SD (mean _ SD, n = 3) was calculated by the instrument software in the range 25–120 °C. The analysis was performed immediately after the production of each batch of microparticles and subsequently 6 months after their production.

5.2.3 Solid state Characterization of Microparticle Systems

XRPD diffractograms were recorded using an X'Pert PANalytical PRO X-ray diffractometer (PANalytical, Almelo, The Netherlands) with CuKα radiation (λ= 1.54187 Å). All samples were scanned in the range of 5–30° 2θ, at a scan speed of 0.067 °2θ/s and a step size of 0.026°. The acceleration voltage and current were 45 kV and 40 mA, respectively. The collected data were analyzed using X'Pert Data Viewer (version 1.2) software.

DSC thermograms of the prepared samples were performed using a Discovery DSC (TA instruments, New Castle, USA). A 3–5 mg sample was crimped in an aluminum Tzero pan and were exposed to a heat−cool−heat cycle from 0 °C to 250 °C at a heating rate of 2 °C/min. All samples were first annealed at 100 °C and kept isothermal for 5 min to remove any residual moisture/solvent before the analysis. A constant flow of pure nitrogen gas with a rate of 50 mL/min was applied during the measurement (n = 3). The data were collected and examined with TRIOS software (TA Instruments, version 5.1.1). The glass transition temperature (Tg, midpoint) was determined from the reversing heat flow signal.

5.2.4 DPPH free Radical Scavenging Assay

The DPPH assay was performed to evaluate the antioxidant activity of phycocyanin, quercetin MPs W-Q, MPs SW-Q, MPs M-Q, MPs W-PC, MPs SW-PC, MPs S-PC, and of all empty microparticles systems (without the API). The tested concentrations were as follows: 0.1 - 0.2 - 0.4 - 0.6 - 0.8 mg/ml of PC, and 4 – 6 – 8 – 10 – 12 µg/ml of Quercetin.

Phycocyanin was dissolved in MilliQ water (concentration 1.0 mg/mL), and the solution was stirred with a magnetic stirrer for 2 h. Subsequently, it was filtered using a 0.2 mm RC filter, and serial dilutions were made to obtain the final test concentrations. Next, 10 mg of each microparticle system containing PC was dissolved in a volume of water to achieve the required concentrations, and the solutions were stirred with a magnetic stirrer for 2 h. Then, the samples were filtered by using a 0.2 mm RC filter. The same procedure was employed to assess the potential antioxidant activity of the empty microparticle systems. Additionally, the same assay was performed using the same concentrations of ascorbic acid as a positive control. To each sample, 1.0 mL of a 0.1 mM ethanolic DPPH solution was added. The vials were kept in the dark for 20 min and the samples were analyzed spectrophotometrically using a UV Jasco V760 spectrophotometer (cuvette 1.0 mL, optical path 10 mm) at a wavelength of 524 nm. The percentage of radical scavenging activity was calculated using the following equation:

$$Radical\ scavenging\ activity\ \% = \frac{[(Abs\ of\ Blank - Abs\ of\ Control) - Abs\ of\ Sample]}{(Abs\ of\ Blank - Abs\ of\ Control)} \times 100$$

Quercetin was dissolved in ethanol (concentration 1.0 mg/mL), and the solution was stirred with a magnetic stirrer for 2 h. Subsequently, it was filtered using a 0.2 mm RC filter, and serial dilutions were made to obtain the final test concentrations. Next, 10 mg of each microparticle system containing quercetin was dissolved in a volume of ethanol to achieve the required concentrations, and the solutions were stirred with a magnetic stirrer for 2 h. Then, the samples

were filtered by using a 0.2 mm RC filter. The same procedure was employed to assess the potential antioxidant activity of the empty microparticle systems. Additionally, the same assay was performed using the same concentrations of ascorbic acid as a positive control. To each sample, 1.0 mL of a 0.1 mM ethanolic DPPH solution was added. The vials were kept in the dark for 20 min and the samples were analyzed spectrophotometrically using a UV Jasco V760 spectrophotometer (cuvette 1.0 mL, optical path 10 mm) at a wavelength of 517 nm. The percentage of radical scavenging activity was calculated using the following equation:

$$Radical\ scavenging\ activity\ \% = \frac{[(Abs\ of\ Blank - Abs\ of\ Control) - Abs\ of\ Sample]}{(Abs\ of\ Blank - Abs\ of\ Control)} \times 100$$

5.2.5 Dissolution studies

Aliquots of MPs W-Q, SW-Q, and M-Q, equal to 3 mg of pure quercetin, and aliquots of MPs W-D, SW-D, and M-D, equal to 3 mg of pure cholecalciferol were placed inside filter paper sachets and immersed in a beaker containing the bi-phasic medium, 60 mL of n-octanol and 20 mL of 0.1 M HCl. The system was maintained at pH = 1, under stirring and constant temperature (100 rpm, 37 °C) for 2 h. After 2 h, the pH was increased up to 6.8 by adding NaOH 1 M to the aqueous phase (to simulate the intestinal environment). This pH was maintained for the following 6 h. One ml sample of the upper organic phase (n-octanol) was taken at regular time intervals, and immediately read with the spectrophotometer UV Jasco V-760 (cuvette 1 mL, optical path 10 mm) and poured into the beaker.

Aliquots of MPs W-PC, SW-PC, and S-PC, equal to 3 mg of pure phycocyanin were placed inside filter paper sachets and immersed in a beaker containing 100 mL of 0.1 M HCl. The system was maintained at pH = 1, under stirring and constant temperature (100 rpm, 37 °C) for 2 h. After 2 h, the pH was increased up to 6.8 by adding NaOH 1 M to the aqueous phase (to simulate the intestinal environment). This pH was maintained for the following 6 h. One ml

sample of the upper organic phase (n-octanol) was taken at regular time intervals, and immediately read with the spectrophotometer UV Jasco V-760 (cuvette 1 mL, optical path 10 mm) and poured into the beaker.

5.2.6 Ex-vivo Permeations Studies

For the permeation study involving quercetin, MPs W-Q, SW-Q, and M-Q, Franz vertical diffusion cells were set up as follows:

- Donor compartment: 5 mg of quercetin, or 50 mg of W-Q, SW-Q, and M-Q dispersed in 1 ml of 0.1N HCl.
- Membrane: porcine colon mucosa.
- Acceptor compartment: 5 ml of n-octanol.

For the permeation study involving cholecalciferol, MPs W-D, SW-D, and M-D, Franz vertical diffusion cells were set up as follows:

- Donor compartment: 3 mg of cholecalciferol, or 50 mg of W-D, SW-D, and M-D dispersed in 1 ml of 0.1N HCl.
- Membrane: porcine colon mucosa.
- Acceptor compartment: 5 ml of n-octanol.

For the permeation study involving phycocyanin, MPs W-PC, SW-PC, and S-PC, Franz vertical diffusion cells were set up as follows:

- Donor compartment: 3 mg of cholecalciferol, or 50 mg of W-PC, SW-PC, and S-PC dispersed in 1 ml of 0.1N HCl.
- Membrane: porcine colon mucosa.
- Acceptor compartment: 5 ml of water.

The Franz diffusion cells were then placed in a thermostated Orbital Shaker at 38°C for the entire experiment (24 hours). Samples of 200 µl were collected after 30 minutes, 1 hour, and 2 hours, with the removed volume replaced by the same amount of solvent. Subsequently, 100 µl of 1M NaOH was added to each donor compartment to create a pH jump to 6.8, simulating intestinal conditions. Sampling continued after 3, 4, 6, 8, and 24 hours. The collected samples were analyzed via UV spectrophotometry. The studies were carried out in triplicate, and graphs of the permeation curves were generated, reporting permeated API in µg vs. time.

5.2.7 In vivo DNBS-colitis Induction and Treatment protocol

The type of treatment we tested included a pre-treatment period (14 days), disease induction (day 0), and a subsequent treatment period (6 days). Rats were randomly assigned to 7 experimental groups (5 animals each) based on the uniformity of weight and age among subjects (Table 11).

Groups	From day -14 to day 0	Day 0	From day 1 to day 6
Control	Oral Gavage 1 ml water	/	Oral Gavage 1 ml water
DNBS	Oral Gavage 1 ml water	Intrarectal injection of 25 mg DNBS in 0.25ml EtOH 50%	Oral Gavage 1 ml water
DNBS+ Cholecalcalciferol and Quercetin	Oral Gavage 1 ml: 2000 IU Cholecal. 50 mg/kg Quercetin	Intrarectal injection of 25 mg DNBS in 0.25ml EtOH 50%	Oral Gavage 1 ml: 2000 IU Cholecal. 50 mg/kg Quercetin
DNBS+ MPs M-D and MPs M-Q	Oral Gavage 1 ml: MPs M-D (2000 IU Cholecal.) and MPs M-Q (50 mg/kg Quercetin)	Intrarectal injection of 25 mg DNBS in 0.25ml EtOH 50%	Oral Gavage 1 ml: MPs M-D (2000 IU Cholecal.) and MPs M-Q (50 mg/kg Quercetin)

DNBS+ MPs SW-D and MPs SW-Q	Oral Gavage 1 ml: MPs SW-D (2000 IU Cholecal.) and MPs SW-Q (50 mg/kg Quercetin)	Intrarectal injection of 25 mg DNBS in 0.25ml EtOH 50%	Oral Gavage 1 ml: MPs SW-D (2000 IU Cholecal.) and MPs SW-Q (50 mg/kg Quercetin)
DNBS+ Phycocyanin	Oral Gavage 1 ml: 150 mg/kg Phycocyanin	Intrarectal injection of 25 mg DNBS in 0.25ml EtOH 50%	Oral Gavage 1 ml: 150 mg/kg Phycocyanin
DNBS+ MPs S-PC	Oral Gavage 1 ml: MPs S-PC (150 mg/kg Phycocyanin)	Intrarectal injection of 25 mg DNBS in 0.25ml EtOH 50%	Oral Gavage 1 ml: MPs S-PC (150 mg/kg Phycocyanin)

Table 11 Descriptions of the different groups into which the animals were divided, the type of treatment, and the duration of treatment to which they were subjected.

All the doses were selected by literature as doses already able to reduce inflammatory responses in animal models [148], [149], [150].

All the APIs and microparticle systems tested, were dissolved in 1 or 2 mL of distilled water, and then vortexed (for 60 seconds) immediately prior to the gavage, and were administered by oral gavage once a day for 20 days starting 14 days before the induction of colitis (day -14).

For the experimental induction of colitis, animals were fasted overnight and then, under light anesthesia with isofluorane, a 0.25 ml of a solution of 20 mg of 2,4-dinitrobenzene sulfonic acid (DNBS; Sigma-Aldrich Inc, St Louis, MO, USA) in 50% ethanol was intracolonically instilled in each animal using an 8 cm plastic catheter (PE90). To avoid reflux actions the rats were kept for 5 minutes in a Trendelenburg position, and then allowed to recover with food and water supplied. The control group (sham group) received intracolonically instillation of vehicle alone (50% ethanol). On day 7 after the induction of colitis, the rats were sacrificed, the abdomen was opened and the appearance of the colon was then examined. Distal colon was removed, opened longitudinally and gently cleaned of faecal content using saline and processed for assessment by macroscopic, histological scores and biochemical markers. No mortality was

observed in any group throughout the study. Assessment of colitis-induced damage was performed minimizing the suffering of animals.

The severity of colitis was evaluated by independent observers blinded to the identity of treatments; efforts were made to minimize the suffering of animals.

Body weight change, stool consistency, and rectal bleeding: During the experimental period, animals were observed daily. Each day, the body weight loss and the stool consistency were calculated. Weight loss was calculated as the percent difference between the body weight before the experimental manipulation and the daily body weight. For the analysis of stool consistency, we used three grade scores (0, normal; 2, loose; and 4, diarrhea). Also, rectal bleeding was monitored. All these parameters were ranged and calculated as described by Cooper et al [146], constituting the DAI score (Disease Activity Index).

Macroscopic scores: Seven days after colitis induction, rats were sacrificed, a laparotomy was performed and the appearance of the colon was then examined. The distal colon was rapidly removed, opened longitudinally, and gently washed with saline. For each specimen wet weight (mg)/length(cm) ratio was calculated as an indicator of colonic edema. For macroscopic damage, each animal was scored by the Appleyard and Wallace classification system score [151]. The sum of scores for the ulceration (0=No mucosal damage, 1=Localized hyperemia but no ulcers, 2=Ulcers without hyperemia/bowel wall thickening, 3=Ulcers with hyperemia/bowel wall thickening at 1 site, 4=Two or more sites of ulceration or inflammation, 5=Area of damage (necrosis) extended >1 cm along length of colon, 6–10=Area of damage extended >2 cm along length of colon; increasing the score was by 1 for each additional cm involved) for the adhesions (0 = No adhesions, 1 = Minor adhesions, no difficult separation of the colon from the other tissue, 2=Major adhesions) and for the evaluation of thickness (Wall thickness of bowel calculated in mm) were calculated. The cumulative score of the different

parameters represents a numerical index determining the severity of macroscopic damage (Macroscopic Damage Score).

Myeloperoxidase assay: Myeloperoxidase (MPO) activity, a marker for neutrophil inflammation, was estimated according to the method of Moreels et al.[147]. Samples were blotted dry, weighted, and placed in a potassium phosphate buffer pH 6.0 containing 0.5% hexadecyl trimethylammonium bromide (5 g tissue per 100 mL buffer). The samples were then placed on ice, homogenized for 30 seconds, and subjected to two sonication and freeze-thawing cycles. The suspension was centrifuged at 15000 g for 15 min at 4°C. Aliquots (0.1 mL) of the supernatant were added to 2.9 mL of o-dianisidine solution (16.7 mg of o-dianisidine in 1 mL methanol, 98 mL 0.05 mol/l potassium phosphate buffer pH 6.0 and 1 mL of a 0.5% H_2O_2 solution as a substrate for MPO enzyme). The absorbance rate was monitored at 460 nm for 60s using a spectrophotometer (Beckman-Coulter Inc, CA, USA). One unit of MPO activity was defined as the amount of the enzyme converting 1 μmol H_2O_2 to H_2O in 1 min at room temperature and was expressed as units per gram tissue (U gram/tissue).

Analysis of microscopic inflammation score: Tissue samples were fixed in 10% v/v buffered formalin for 24 h, washed with water and, finally, preserved in 70% ethanol before proceeding with paraffin fixation. Four-micrometer-thick tissue sections were deparaffinized and rehydrated. Slides were stained with hematoxylin and eosin (Harrys' hematoxylin for Histology and Eosin Y alcoholic solution, Bio-Optica, Milano Spa). All the sections were analyzed under Zeiss Axio Scope A1 optical microscope (Zeiss, Germany) and microphotographs were collected at 10x magnification using an Axiocam 503 Color digital camera with the ZEN2 imaging software (Zeiss Germany). The microscopic damage following score was calculated the Hunter et al. classification method: by adding the histological finding (0 = normal, 1 = minimal, 2 = mild, 3 = severe), the degree of inflammatory infiltration (0 = normal, 1 = minimal, 2 = mild, 3 = severe), the layers infiltrated (0 = normal, 1 = minimal, 2 = mild, 3 = severe), the

mucosal damage (0 = normal,1 = minimal, 2 = mild, 3 = severe), and the edema in the mucosa (0 = absent, 1 = present) [152].

All data are means ± SEM: 'n' indicates the number of animals. Statistical analysis was performed using *GraphPad Prism 6.0 software*, utilizing One-way ANOVA and Dunnett's multiple comparison test and considered significant if P value was <0.05.

5.2.8 In vivo Bioavailability Study

The rats were divided into six experimental groups (5 animals each) and each of these groups received different administrations as follows:

1) Water (control group)
2) Cholecalciferol (2000 IU)
3) MPs M-D (2000 IU Cholecalciferol)
4) MPs SW-D (2000 IU Cholecalciferol)
5) Phycocyanin (150 mg/kg)
6) MPs S-PC (150 mg/kg Phycocyanin)

All the APIs and microparticle systems tested, were dissolved in 1 or 2 mL of distilled water, and then vortexed (for 60 seconds) immediately prior to the gavage, and were administered by oral gavage. Blood samples (200 µl) were collected via the tail vein under isoflurane anesthesia before (time 0) and at seven-time points after administration (1, 2, 4, 6, 8, 24, and 72h), and transferred to vials internally coated with EDTA. All samples were then centrifuged at 1500 rpm for 10 minutes to separate and extract the plasma.

For the quantification of cholecalciferol, the plasma samples were mixed with a 50:50 methanol/acetonitrile solvent solution at a 1:9 ratio and placed in an ice bath to facilitate deproteinization and extraction of cholecalciferol. The samples were then centrifuged at 10000

rpm, after which the supernatant was collected, filtered, and analyzed using the HPLC method to determine cholecalciferol levels. HPLC analysis was carried out by using an Agilent 1260 Infinity instrument equipped with a Quaternary Pump VL G1311C and a DAD detector 1260 VL, 50 µl injector, and a computer integrating apparatus (OpenLAB CDS ChemStation Workstation). A reversed-phase column Luna Phenomenex C8, with a dimension of 250 mm × 4.6 mm and particle size 5 µm, was used as the stationary phase at 25 °C. Isocratic elution was employed with ACN and MeOH (50:50, % v/v) as mobile phase with a flow rate of 1 ml/min. The run time of all the test samples was 10 minutes. The UV detector was fixed at 265 ± 4 nm. To analyze data the software OpenLAB CDS ChemStation Workstation was employed. A calibration curve in the range of 0.0918-5.88 µg/ml (y = 358.16x, R = 0.998) was used to quantify cholecalciferol. All the experiments were carried out in triplicate [153].

For the quantification of phycocyanin, the plasma samples were mixed with a 20:80 acetonitrile/water (with 0,1% v/v of trifluoroacetic acid) solvent solution at a 1:9 ratio and placed in an ice bath to facilitate deproteinization and extraction of phycocyanin. The samples were then centrifuged at 10000 rpm, after which the supernatant was collected, filtered, and analyzed using the HPLC method to determine phycocyanin levels. HPLC analysis was carried out by using an Agilent 1260 Infinity instrument equipped with a Quaternary Pump VL G1311C and a DAD detector 1260 VL, 50 µl injector, and a computer integrating apparatus (OpenLAB CDS ChemStation Workstation). A reversed-phase column Luna Phenomenex C18, with a dimension of 250 mm × 4.6 mm and particle size 5 µm, was used as the stationary phase at 25 °C. The elution was performed using a linear gradient from 20 to 100 % (v/v) aqueous ACN (containing 0.1 % TFA) in 45 min with a flow rate of 1 ml/min. The UV detector was fixed at 620 ± 4 nm. To analyze data the software OpenLAB CDS ChemStation Workstation was employed. A calibration curve in the range of 0.04-1 mg/ml (y = 1686.6x, R = 0.999) was used to quantify phycocyanin. All the experiments were carried out in triplicate [154].

BIBLIOGRAPHY

[1] M. Agrawal, K. H. Allin, F. Petralia, J. F. Colombel, and T. Jess, "Multiomics to elucidate inflammatory bowel disease risk factors and pathways," Jun. 01, 2022, *Nature Research*. doi: 10.1038/s41575-022-00593-y.

[2] Y. di Wang, R. nan Zhang, R. Mao, and X. hua Li, "Inflammatory bowel disease cross-sectional imaging: What's new?," Dec. 01, 2022, *John Wiley and Sons Inc*. doi: 10.1002/ueg2.12343.

[3] R. Ungaro, S. Mehandru, P. B. Allen, L. Peyrin-Biroulet, and J. F. Colombel, "Ulcerative colitis," *The Lancet*, vol. 389, no. 10080, pp. 1756–1770, Apr. 2017, doi: 10.1016/S0140-6736(16)32126-2.

[4] J. Torres, S. Mehandru, J. F. Colombel, and L. Peyrin-Biroulet, "Crohn's disease," Apr. 29, 2017, *Lancet Publishing Group*. doi: 10.1016/S0140-6736(16)31711-1.

[5] D. Desai and P. Dhoble, "Rapidly changing epidemiology of inflammatory bowel disease: Time to gear up for the challenge before it is too late," *Indian Journal of Gastroenterology*, vol. 43, no. 1, pp. 15–17, Feb. 2024, doi: 10.1007/S12664-023-01453-6/METRICS.

[6] S. M. Borowitz, "The epidemiology of inflammatory bowel disease: Clues to pathogenesis?," *Front Pediatr*, vol. 10, p. 1103713, Jan. 2023, doi: 10.3389/FPED.2022.1103713/BIBTEX.

[7] C. Abbafati *et al.*, "Global burden of 369 diseases and injuries in 204 countries and territories, 1990–2019: a systematic analysis for the Global Burden of Disease Study 2019," *The Lancet*, vol. 396, no. 10258, pp. 1204–1222, Oct. 2020, doi: 10.1016/S0140-6736(20)30925-9.

[8] S. C. Ng *et al.*, "Worldwide incidence and prevalence of inflammatory bowel disease in the 21st century: a systematic review of population-based studies," *The Lancet*, vol. 390, no. 10114, pp. 2769–2778, Dec. 2017, doi: 10.1016/S0140-6736(17)32448-0.

[9] A. N. Ananthakrishnan, "Epidemiology and risk factors for IBD," Apr. 04, 2015, *Nature Publishing Group*. doi: 10.1038/nrgastro.2015.34.

[10] V. Annese, "Genetics and epigenetics of IBD," Sep. 01, 2020, *Academic Press*. doi: 10.1016/j.phrs.2020.104892.

[11] H. S. Lee and I. Cleynen, "Molecular profiling of inflammatory bowel disease: Is it ready for use in clinical decision-making?," *Cells*, vol. 8, no. 6, Jun. 2019, doi: 10.3390/cells8060535.

[12] G. B. Chen *et al.*, "Performance of risk prediction for inflammatory bowel disease based on genotyping platform and genomic risk score method," *BMC Med Genet*, vol. 18, no. 1, Aug. 2017, doi: 10.1186/s12881-017-0451-2.

[13] K. L. Glassner, B. P. Abraham, and E. M. M. Quigley, "The microbiome and inflammatory bowel disease," *Journal of Allergy and Clinical Immunology*, vol. 145, no. 1, pp. 16–27, Jan. 2020, doi: 10.1016/J.JACI.2019.11.003.

[14] Y. Haneishi, Y. Furuya, M. Hasegawa, A. Picarelli, M. Rossi, and J. Miyamoto, "Inflammatory Bowel Diseases and Gut Microbiota," *International Journal of Molecular Sciences 2023, Vol. 24, Page 3817*, vol. 24, no. 4, p. 3817, Feb. 2023, doi: 10.3390/IJMS24043817.

[15] Y. Belkaid and T. W. Hand, "Role of the Microbiota in Immunity and inflammation," *Cell*, vol. 157, no. 1, p. 121, Mar. 2014, doi: 10.1016/J.CELL.2014.03.011.

[16] N. Singh and C. N. Bernstein, “Environmental risk factors for inflammatory bowel disease,” Dec. 01, 2022, *John Wiley and Sons Inc*. doi: 10.1002/ueg2.12319.

[17] M. Agrawal *et al.*, “Early life exposures and the risk of inflammatory bowel disease: Systematic review and meta-analyses,” *EClinicalMedicine*, vol. 36, Jun. 2021, doi: 10.1016/J.ECLINM.2021.100884.

[18] J. J. Rozich, A. Holmer, and S. Singh, “Effect of Lifestyle Factors on Outcomes in Patients with Inflammatory Bowel Diseases,” *Am J Gastroenterol*, vol. 115, no. 6, p. 832, Jun. 2020, doi: 10.14309/AJG.0000000000000608.

[19] K. Radon *et al.*, “Contact With Farm Animals in Early Life and Juvenile Inflammatory Bowel Disease: A Case-Control Study,” *Pediatrics*, vol. 120, no. 2, pp. 354–361, Aug. 2007, doi: 10.1542/PEDS.2006-3624.

[20] A. R. Barclay, R. K. Russell, M. L. Wilson, W. H. Gilmour, J. Satsangi, and D. C. Wilson, “Systematic Review: The Role of Breastfeeding in the Development of Pediatric Inflammatory Bowel Disease,” *J Pediatr*, vol. 155, no. 3, pp. 421–426, Sep. 2009, doi: 10.1016/J.JPEDS.2009.03.017.

[21] A. Sood *et al.*, “Low hygiene and exposure to infections may be associated with increased risk for ulcerative colitis in a North Indian population,” *Annals of Gastroenterology : Quarterly Publication of the Hellenic Society of Gastroenterology*, vol. 27, no. 3, p. 219, 2014, Accessed: Jul. 30, 2024. [Online]. Available: /pmc/articles/PMC4073017/

[22] R. E. Andersson, G. Olaison, C. Tysk, and A. Ekbom, “Appendectomy and Protection against Ulcerative Colitis,” *New England Journal of Medicine*, vol. 344, no. 11, pp. 808–814, Mar. 2001, doi: 10.1056/NEJM200103153441104/ASSET/F8BA5FCF-A693-

4083-AFED-DC708BAF1B68/ASSETS/IMAGES/LARGE/NEJM200103153441104_F1.JPG.

[23] R. Ungaro *et al.*, "Antibiotics associated with increased risk of New-Onset Crohn's disease but not ulcerative colitis: A meta-analysis," Nov. 13, 2014, *Nature Publishing Group*. doi: 10.1038/ajg.2014.246.

[24] J. E. Axelrad, K. H. Cadwell, J. F. Colombel, and S. C. Shah, "The role of gastrointestinal pathogens in inflammatory bowel disease: a systematic review," *Therap Adv Gastroenterol*, vol. 14, Mar. 2021, doi: 10.1177/17562848211004493/ASSET/IMAGES/LARGE/10.1177_17562848211004493-FIG1.JPEG.

[25] K. F. Frøslie, J. Jahnsen, B. A. Moum, and M. H. Vatn, "Mucosal Healing in Inflammatory Bowel Disease: Results From a Norwegian Population-Based Cohort," *Gastroenterology*, vol. 133, no. 2, pp. 412–422, Aug. 2007, doi: 10.1053/J.GASTRO.2007.05.051.

[26] P. Grevenitis, A. Thomas, and N. Lodhia, "Medical Therapy for Inflammatory Bowel Disease," 2015, *W.B. Saunders*. doi: 10.1016/j.suc.2015.08.004.

[27] H. Nakase, "Optimizing the Use of Current Treatments and Emerging Therapeutic Approaches to Achieve Therapeutic Success in Patients with Inflammatory Bowel Disease," *Gut Liver*, vol. 14, no. 1, p. 7, Jan. 2020, doi: 10.5009/GNL18203.

[28] Z. Cai, S. Wang, and J. Li, "Treatment of Inflammatory Bowel Disease: A Comprehensive Review," *Front Med (Lausanne)*, vol. 8, p. 765474, Dec. 2021, doi: 10.3389/FMED.2021.765474/FULL.

[29] C. Rousseaux *et al.*, "Intestinal antiinflammatory effect of 5-aminosalicylic acid is dependent on peroxisome proliferator–activated receptor-γ," *Journal of Experimental Medicine*, vol. 201, no. 8, pp. 1205–1215, Apr. 2005, doi: 10.1084/JEM.20041948.

[30] H. Bantel, C. Berg, M. Vieth, M. Stolte, W. Kruis, and K. Schulze-Osthoff, "Mesalazine inhibits activation of transcription factor NF-κB in inflamed mucosa of patients with ulcerative colitis," *Am J Gastroenterol*, vol. 95, no. 12, pp. 3452–3457, Dec. 2000, doi: 10.1016/S0002-9270(00)02153-5.

[31] J. Eaden, K. Abrams, A. Ekbom, E. Jackson, and J. Mayberry, "Colorectal cancer prevention in ulcerative colitis: a case-control study," *Aliment Pharmacol Ther*, vol. 14, no. 2, pp. 145–153, Feb. 2000, doi: 10.1046/J.1365-2036.2000.00698.X.

[32] A. C. Ford *et al.*, "Efficacy of 5-aminosalicylates in ulcerative colitis: Systematic review and meta-analysis," *American Journal of Gastroenterology*, vol. 106, no. 4, pp. 601–616, Apr. 2011, doi: 10.1038/AJG.2011.67.

[33] H. Zatorski and J. Fichna, "What is the future of the gut microbiota-related treatment? Toward modulation of microbiota in preventive and therapeutic medicine," *Front Med (Lausanne)*, vol. 1, no. JUL, p. 105739, Jul. 2014, doi: 10.3389/FMED.2014.00019/BIBTEX.

[34] D. H. Kerman and A. R. Deshpande, "Gut Microbiota and Inflammatory Bowel Disease: The Role of Antibiotics in Disease Management," *Postgrad Med*, vol. 126, no. 4, pp. 7–19, Jan. 2014, doi: 10.3810/PGM.2014.07.2779.

[35] J. W. Su, J. J. Ma, and H. J. Zhang, "Use of antibiotics in patients with Crohn's disease: A systematic review and meta-analysis," *J Dig Dis*, vol. 16, no. 2, pp. 58–66, Feb. 2015, doi: 10.1111/1751-2980.12216.

[36] O. Nitzan, M. Elias, A. Peretz, and W. Saliba, “Role of antibiotics for treatment of inflammatory bowel disease,” *World J Gastroenterol*, vol. 22, no. 3, p. 1078, Jan. 2016, doi: 10.3748/WJG.V22.I3.1078.

[37] A. C. Ford *et al.*, “Glucocorticosteroid therapy in inflammatory bowel disease: Systematic review and meta-analysis,” *American Journal of Gastroenterology*, vol. 106, no. 4, pp. 590–599, Apr. 2011, doi: 10.1038/AJG.2011.70.

[38] M. Chaparro *et al.*, “Safety of Thiopurine Therapy in Inflammatory Bowel Disease: Long-term Follow-up Study of 3931 Patients,” *Inflamm Bowel Dis*, vol. 19, no. 7, pp. 1404–1410, Jun. 2013, doi: 10.1097/MIB.0B013E318281F28F.

[39] N. Chande, P. H. Patton, D. J. Tsoulis, B. S. Thomas, and J. K. Macdonald, “Azathioprine or 6-mercaptopurine for maintenance of remission in Crohn’s disease,” *Cochrane Database of Systematic Reviews*, vol. 2017, no. 12, Oct. 2015, doi: 10.1002/14651858.CD000067.PUB3/MEDIA/CDSR/CD000067/IMAGE_N/NCD000067-CMP-005-04.PNG.

[40] K. L. Isaacs, J. D. Lewis, W. J. Sandborn, B. E. Sands, S. R. Targan, and M. Merrick, “State of the Art: Ibd Therapy and Clinical Trials in Ibd,” *Inflamm Bowel Dis*, vol. 11, no. suppl_1, pp. S3–S12, Nov. 2005, doi: 10.1097/01.MIB.0000184852.84558.B2.

[41] M. Naganuma, T. Fujii, and M. Watanabe, “The use of traditional and newer calcineurin inhibitors in inflammatory bowel disease,” *J Gastroenterol*, vol. 46, no. 2, pp. 129–137, Feb. 2011, doi: 10.1007/S00535-010-0352-Z/FIGURES/3.

[42] A. Dignass *et al.*, “Second European evidence-based consensus on the diagnosis and management of ulcerative colitis Part 2: Current management,” *J Crohns Colitis*, vol. 6, no. 10, pp. 991–1030, Dec. 2012, doi: 10.1016/J.CROHNS.2012.09.002.

[43] H. Ogata *et al.*, "A randomised dose finding study of oral tacrolimus (FK506) therapy in refractory ulcerative colitis," *Gut*, vol. 55, no. 9, pp. 1255–1262, Sep. 2006, doi: 10.1136/GUT.2005.081794.

[44] S. Vieujean, F. D'Amico, P. Netter, S. Danese, and L. Peyrin-Biroulet, "Landscape of new drugs and targets in inflammatory bowel disease," Dec. 01, 2022, *John Wiley and Sons Inc*. doi: 10.1002/ueg2.12305.

[45] K. O. Chudy-Onwugaje, K. E. Christian, F. A. Farraye, and R. K. Cross, "A State-of-the-Art Review of New and Emerging Therapies for the Treatment of IBD," *Inflamm Bowel Dis*, vol. 25, no. 5, pp. 820–830, Apr. 2019, doi: 10.1093/IBD/IZY327.

[46] A. O'Toole and A. C. Moss, "Optimizing Biologic Agents in Ulcerative Colitis and Crohn's Disease," *Curr Gastroenterol Rep*, vol. 17, no. 8, pp. 1–8, Aug. 2015, doi: 10.1007/S11894-015-0453-1/TABLES/1.

[47] A. Dignass *et al.*, "Second European evidence-based consensus on the diagnosis and management of ulcerative colitis Part 2: Current management," *J Crohns Colitis*, vol. 6, no. 10, pp. 991–1030, Dec. 2012, doi: 10.1016/J.CROHNS.2012.09.002.

[48] J. P. Achkar and B. Shen, "Medical management of postoperative complications of inflammatory bowel disease: pouchitis and Crohn's disease recurrence.," *Curr Gastroenterol Rep*, vol. 3, no. 6, pp. 484–490, 2001, doi: 10.1007/S11894-001-0069-5/METRICS.

[49] A. M. Vaiserman and F. Marotta, "Longevity-Promoting Pharmaceuticals: Is it a Time for Implementation?," *Trends Pharmacol Sci*, vol. 37, no. 5, pp. 331–333, May 2016, doi: 10.1016/j.tips.2016.02.003.

[50] L. R. Fitzpatrick, "Novel Pharmacological Approaches for Inflammatory Bowel Disease: Targeting Key Intracellular Pathways and the IL-23/IL-17 Axis," *Int J Inflam*, vol. 2012, no. 1, p. 389404, Jan. 2012, doi: 10.1155/2012/389404.

[51] A. Salaritabar *et al.*, "Therapeutic potential of flavonoids in inflammatory bowel disease: A comprehensive review," *World J Gastroenterol*, vol. 23, no. 28, p. 5097, Jul. 2017, doi: 10.3748/WJG.V23.I28.5097.

[52] Y. Li *et al.*, "Quercetin, Inflammation and Immunity," *Nutrients 2016, Vol. 8, Page 167*, vol. 8, no. 3, p. 167, Mar. 2016, doi: 10.3390/NU8030167.

[53] C. F. S. Guazelli *et al.*, "Quercetin-loaded microcapsules ameliorate experimental colitis in mice by anti-inflammatory and antioxidant mechanisms," *J Nat Prod*, vol. 76, no. 2, pp. 200–208, Feb. 2013, doi: 10.1021/NP300670W/SUPPL_FILE/NP300670W_SI_001.PDF.

[54] S. I. Khater *et al.*, "Therapeutic Potential of Quercetin Loaded Nanoparticles: Novel Insights in Alleviating Colitis in an Experimental DSS Induced Colitis Model," *Biomedicines 2022, Vol. 10, Page 1654*, vol. 10, no. 7, p. 1654, Jul. 2022, doi: 10.3390/BIOMEDICINES10071654.

[55] R. Caruana *et al.*, "Enhanced anticancer effect of quercetin microparticles formulation obtained by spray drying," *Int J Food Sci Technol*, vol. 57, no. 5, pp. 2739–2746, May 2022, doi: 10.1111/IJFS.15539.

[56] C. Zhu *et al.*, "Selenium-Containing Phycocyanin from Se-Enriched Spirulina platensis Reduces Inflammation in Dextran Sulfate Sodium-Induced Colitis by Inhibiting NF-κB Activation," *J Agric Food Chem*, vol. 64, no. 24, pp. 5060–5070, Jun. 2016, doi:

10.1021/ACS.JAFC.6B01308/ASSET/IMAGES/LARGE/JF-2016-013085_0009.JPEG.

[57] T. J. Ashaolu *et al.*, "Phycocyanin, a super functional ingredient from algae; properties, purification characterization, and applications," *Int J Biol Macromol*, vol. 193, pp. 2320–2331, Dec. 2021, doi: 10.1016/J.IJBIOMAC.2021.11.064.

[58] L. Jiang *et al.*, "Phycocyanin: A Potential Drug for Cancer Treatment," *J Cancer*, vol. 8, no. 17, p. 3416, 2017, doi: 10.7150/JCA.21058.

[59] W. H. El-Maadawy, E. Hafiz, H. Okasha, N. A. Osman, G. H. Ali, and R. A. Hussein, "Phycocyanin stimulates ulcerative colitis healing via selective activation of cannabinoid receptor-2, intestinal mucosal healing, Treg accumulation, and p38MAPK/MK2 signaling inhibition," *Life Sci*, vol. 305, p. 120741, Sep. 2022, doi: 10.1016/J.LFS.2022.120741.

[60] D. Pan, B. Huang, Y. Gan, C. Gao, Y. Liu, and Z. Tang, "Phycocyanin Ameliorates Colitis-Associated Colorectal Cancer by Regulating the Gut Microbiota and the IL-17 Signaling Pathway," *Mar Drugs*, vol. 20, no. 4, p. 260, Apr. 2022, doi: 10.3390/MD20040260/S1.

[61] J. Marín-Prida *et al.*, "Novel Insights into the Molecular Mechanisms Involved in the Neuroprotective Effects of C-Phycocyanin against Brain Ischemia in Rats," *Curr Pharm Des*, vol. 28, no. 14, pp. 1187–1197, May 2022, doi: 10.2174/1381612828666220506145542.

[62] Y. Li, "The Bioactivities of Phycocyanobilin from Spirulina," *J Immunol Res*, vol. 2022, no. 1, p. 4008991, Jan. 2022, doi: 10.1155/2022/4008991.

[63] W. Guo, M. Zeng, S. Zhu, S. Li, Y. Qian, and H. Wu, “Phycocyanin ameliorates mouse colitis via phycocyanobilin-dependent antioxidant and anti-inflammatory protection of the intestinal epithelial barrier,” *Food Funct*, vol. 13, no. 6, pp. 3294–3307, Mar. 2022, doi: 10.1039/D1FO02970C.

[64] S. Li, W. Guo, M. Zhang, M. Zeng, and H. Wu, “Microalgae polysaccharides exert antioxidant and anti-inflammatory protective effects on human intestinal epithelial cells in vitro and dextran sodium sulfate-induced mouse colitis in vivo,” *Int J Biol Macromol*, vol. 254, p. 127811, Jan. 2024, doi: 10.1016/J.IJBIOMAC.2023.127811.

[65] F. Vernia, M. Valvano, S. Longo, N. Cesaro, A. Viscido, and G. Latella, “Vitamin D in Inflammatory Bowel Diseases. Mechanisms of Action and Therapeutic Implications,” *Nutrients*, vol. 14, no. 2, Jan. 2022, doi: 10.3390/NU14020269.

[66] Y. Wang, J. Zhu, and H. F. DeLuca, “Where is the vitamin D receptor?,” *Arch Biochem Biophys*, vol. 523, no. 1, pp. 123–133, Jul. 2012, doi: 10.1016/J.ABB.2012.04.001.

[67] M. T. Cantorna, K. McDaniel, S. Bora, J. Chen, and J. James, “Vitamin D, immune regulation, the microbiota, and inflammatory bowel disease,” *https://doi.org/10.1177/1535370214523890*, vol. 239, no. 11, pp. 1524–1530, Mar. 2014, doi: 10.1177/1535370214523890.

[68] J. Gubatan and A. C. Moss, “Vitamin D in inflammatory bowel disease: More than just a supplement,” *Curr Opin Gastroenterol*, vol. 34, no. 4, pp. 217–225, Jul. 2018, doi: 10.1097/MOG.0000000000000449.

[69] G. Kaur, M. Arora, and M. N. V. Ravi Kumar, “Oral Drug Delivery Technologies—A Decade of Developments,” *Journal of Pharmacology and Experimental Therapeutics*, vol. 370, no. 3, pp. 529–543, Sep. 2019, doi: 10.1124/JPET.118.255828.

[70] L. Sanford. Goodman, Alfred. Gilman, L. L. Brunton, Randa. Hilal-Dandan, and B. C. Knollmann, “Le basi farmacologiche della terapia,” 2019, Accessed: Aug. 16, 2024. [Online]. Available: https://www.libreriauniverso.it/

[71] X. Hu, G. Yang, S. Chen, S. Luo, and J. Zhang, “Biomimetic and bioinspired strategies for oral drug delivery,” *Biomater Sci*, vol. 8, no. 4, pp. 1020–1044, Feb. 2020, doi: 10.1039/C9BM01378D.

[72] M. T. Carvajal and S. Yalkowsky, “Effect of pH and Ionic Strength on the Solubility of Quinoline: Back-to-Basics,” *AAPS PharmSciTech*, vol. 20, no. 3, pp. 1–8, Apr. 2019, doi: 10.1208/S12249-019-1336-9/TABLES/4.

[73] F. Kesisoglou and Y. Wu, “Understanding the effect of API properties on bioavailability through absorption modeling,” *AAPS Journal*, vol. 10, no. 4, pp. 516–525, Dec. 2008, doi: 10.1208/S12248-008-9061-4/FIGURES/8.

[74] B. Greenwood-Van Meerveld, A. C. Johnson, and D. Grundy, “Gastrointestinal Physiology and Function,” *Handb Exp Pharmacol*, vol. 239, pp. 1–16, Jan. 2017, doi: 10.1007/164_2016_118.

[75] J. B. . Dressman and C. . Reppas, “Oral drug absorption : prediction and assessment,” p. 413, 2010, Accessed: Sep. 11, 2024. [Online]. Available: https://books.google.com/books/about/Oral_Drug_Absorption.html?id=4ynNBQAAQBAJ

[76] B. Homayun, X. Lin, and H. J. Choi, “Challenges and Recent Progress in Oral Drug Delivery Systems for Biopharmaceuticals,” *Pharmaceutics 2019, Vol. 11, Page 129*, vol. 11, no. 3, p. 129, Mar. 2019, doi: 10.3390/PHARMACEUTICS11030129.

[77] J. Leal *et al.*, "Mucus-penetrating phage-displayed peptides for improved transport across a mucus-like model," *Int J Pharm*, vol. 553, no. 1–2, pp. 57–64, Dec. 2018, doi: 10.1016/J.IJPHARM.2018.09.055.

[78] L. M. Ensign, R. Cone, and J. Hanes, "Oral drug delivery with polymeric nanoparticles: the gastrointestinal mucus barriers," *Adv Drug Deliv Rev*, vol. 64, no. 6, pp. 557–570, May 2012, doi: 10.1016/J.ADDR.2011.12.009.

[79] B. Homayun, X. Lin, and H. J. Choi, "Challenges and Recent Progress in Oral Drug Delivery Systems for Biopharmaceuticals," *Pharmaceutics*, vol. 11, no. 3, Mar. 2019, doi: 10.3390/PHARMACEUTICS11030129.

[80] J. B. . Dressman and C. . Reppas, "Oral drug absorption : prediction and assessment," p. 413, 2010, Accessed: Sep. 11, 2024. [Online]. Available: https://books.google.com/books/about/Oral_Drug_Absorption.html?id=4ynNBQAAQBAJ

[81] N. Pavlović *et al.*, "Bile Acids and Their Derivatives as Potential Modifiers of Drug Release and Pharmacokinetic Profiles," *Front Pharmacol*, vol. 9, no. NOV, Nov. 2018, doi: 10.3389/FPHAR.2018.01283.

[82] L. Sanford. Goodman, Alfred. Gilman, L. L. Brunton, Randa. Hilal-Dandan, and B. C. Knollmann, "Le basi farmacologiche della terapia," 2019, Accessed: Sep. 11, 2024. [Online]. Available: https://www.libreriauniverso.it/

[83] D. F. Veber, S. R. Johnson, H. Y. Cheng, B. R. Smith, K. W. Ward, and K. D. Kopple, "Molecular properties that influence the oral bioavailability of drug candidates," *J Med Chem*, vol. 45, no. 12, pp. 2615–2623, Jun. 2002, doi: 10.1021/JM020017N/SUPPL_FILE/JM020017N_S.PDF.

[84] C. Y. Wu and L. Z. Benet, "Predicting drug disposition via application of BCS: Transport/absorption/ elimination interplay and development of a biopharmaceutics drug disposition classification system," *Pharm Res*, vol. 22, no. 1, pp. 11–23, Jan. 2005, doi: 10.1007/S11095-004-9004-4/METRICS.

[85] M. S. Ku, "Use of the biopharmaceutical classification system in early drug development," *AAPS Journal*, vol. 10, no. 1, pp. 208–212, Apr. 2008, doi: 10.1208/S12248-008-9020-0/TABLES/1.

[86] C. M. Keck and R. H. Müller, "Drug nanocrystals of poorly soluble drugs produced by high pressure homogenisation," *European Journal of Pharmaceutics and Biopharmaceutics*, vol. 62, no. 1, pp. 3–16, Jan. 2006, doi: 10.1016/J.EJPB.2005.05.009.

[87] T. Loftsson and M. E. Brewster, "Pharmaceutical applications of cyclodextrins: effects on drug permeation through biological membranes," *Journal of Pharmacy and Pharmacology*, vol. 63, no. 9, pp. 1119–1135, Aug. 2011, doi: 10.1111/J.2042-7158.2011.01279.X.

[88] A. S. Narang, D. Delmarre, and D. Gao, "Stable drug encapsulation in micelles and microemulsions," *Int J Pharm*, vol. 345, no. 1–2, pp. 9–25, Dec. 2007, doi: 10.1016/J.IJPHARM.2007.08.057.

[89] R. Iyer *et al.*, "Amorphous Solid Dispersions (ASDs): The Influence of Material Properties, Manufacturing Processes and Analytical Technologies in Drug Product Development," *Pharmaceutics 2021, Vol. 13, Page 1682*, vol. 13, no. 10, p. 1682, Oct. 2021, doi: 10.3390/PHARMACEUTICS13101682.

[90] A. T. M. Serajuddin, "Salt formation to improve drug solubility," *Adv Drug Deliv Rev*, vol. 59, no. 7, pp. 603–616, Jul. 2007, doi: 10.1016/J.ADDR.2007.05.010.

[91] O. H. Chan, H. L. Schmid, L. A. Stilgenbauer, W. Howson, D. C. Horwell, and B. H. Stewart, "Evaluation of a targeted prodrug strategy to enhance oral absorption of poorly water-soluble compounds," *Pharm Res*, vol. 15, no. 7, pp. 1012–1018, 1998, doi: 10.1023/A:1011969808907/METRICS.

[92] A. Erxleben, "Cocrystal Applications in Drug Delivery," *Pharmaceutics 2020, Vol. 12, Page 834*, vol. 12, no. 9, p. 834, Sep. 2020, doi: 10.3390/PHARMACEUTICS12090834.

[93] Y. Huang and W.-G. Dai, "Fundamental aspects of solid dispersion technology for poorly soluble drugs," *Acta Pharm Sin B*, vol. 4, no. 1, pp. 18–25, Feb. 2014, doi: 10.1016/J.APSB.2013.11.001.

[94] Y. Huang and W.-G. Dai, "Fundamental aspects of solid dispersion technology for poorly soluble drugs," *Acta Pharm Sin B*, vol. 4, no. 1, pp. 18–25, Feb. 2014, doi: 10.1016/J.APSB.2013.11.001.

[95] M. Licciardi *et al.*, "PHEA-graft-polybutylmethacrylate copolymer microparticles for delivery of hydrophobic drugs," *Int J Pharm*, vol. 433, no. 1–2, pp. 16–24, Aug. 2012, doi: 10.1016/J.IJPHARM.2012.04.052.

[96] A. Paudel, Z. A. Worku, J. Meeus, S. Guns, and G. Van Den Mooter, "Manufacturing of solid dispersions of poorly water soluble drugs by spray drying: Formulation and process considerations," *Int J Pharm*, vol. 453, no. 1, pp. 253–284, Aug. 2013, doi: 10.1016/J.IJPHARM.2012.07.015.

[97] S. Surini, C. N. Evangelista, and R. Iswandana, "Development of glimepiride solid dispersion using the coprocessed excipients of polyvinylpyrrolidone, maltodextrin, and polyethylene glycol," *Journal of Young Pharmacists*, vol. 10, no. 2, pp. s45–s50, Apr. 2018, doi: 10.5530/JYP.2018.2S.9.

[98] S. V. Bhujbal *et al.*, "Pharmaceutical amorphous solid dispersion: A review of manufacturing strategies," *Acta Pharm Sin B*, vol. 11, no. 8, pp. 2505–2536, Aug. 2021, doi: 10.1016/J.APSB.2021.05.014.

[99] B. C. Hancock and G. Zografi, "The Relationship Between the Glass Transition Temperature and the Water Content of Amorphous Pharmaceutical Solids," *Pharmaceutical Research: An Official Journal of the American Association of Pharmaceutical Scientists*, vol. 11, no. 4, pp. 471–477, 1994, doi: 10.1023/A:1018941810744/METRICS.

[100] T. Vasconcelos, B. Sarmento, and P. Costa, "Solid dispersions as strategy to improve oral bioavailability of poor water soluble drugs," *Drug Discov Today*, vol. 12, no. 23–24, pp. 1068–1075, Dec. 2007, doi: 10.1016/J.DRUDIS.2007.09.005.

[101] L. M. De Mohac, B. Raimi-Abraham, R. Caruana, G. Gaetano, and M. Licciardi, "Multicomponent solid dispersion a new generation of solid dispersion produced by spray-drying," *J Drug Deliv Sci Technol*, vol. 57, p. 101750, Jun. 2020, doi: 10.1016/J.JDDST.2020.101750.

[102] M. Shokoohi and T. Attar, "Biomanufacturing for a Sustainable Future: Unleashing the Potential of Biotechnology in Pharmaceutical Raw Material Production," *International Journal of New Findings in Health and Educational Sciences (IJHES)*, vol. 2, no. 2, pp. 142–153, Apr. 2024, doi: 10.63053/IJHES.81.

[103] M. A. Mohammed, "Natural Excipients Applications in Conventional Pharmaceutical Formulations -Part I," *Med Aromat Plants (Los Angel)*, vol. 10, no. 7, pp. 1–10, Jul. 2021, doi: 10.35248/2167-0412.21.10.397.

[104] M. A. Anaya Castro, I. Alric, F. Brouillet, J. Peydecastaing, S. G. Fullana, and V. Durrieu, “Soy Protein Microparticles for Enhanced Oral Ibuprofen Delivery: Preparation, Characterization, and In Vitro Release Evaluation,” *AAPS PharmSciTech*, vol. 19, no. 3, pp. 1124–1132, Apr. 2018, doi: 10.1208/S12249-017-0928-5/FIGURES/7.

[105] A. Abaee, M. Mohammadian, and S. M. Jafari, “Whey and soy protein-based hydrogels and nano-hydrogels as bioactive delivery systems,” *Trends Food Sci Technol*, vol. 70, pp. 69–81, Dec. 2017, doi: 10.1016/J.TIFS.2017.10.011.

[106] J. Mishra, A. Bohr, T. Rades, H. Grohganz, and K. Löbmann, “Whey proteins as stabilizers in amorphous solid dispersions,” *European Journal of Pharmaceutical Sciences*, vol. 128, pp. 144–151, Feb. 2019, doi: 10.1016/J.EJPS.2018.12.002.

[107] D. Leng, B. Bulduk, T. Widmer, O. Wiborg, M. Sanchez-Felix, and K. Löbmann, “Protein Based Amorphous Solid Dispersion: a Case Study Investigating Different Whey Proteins at High Drug Loading,” *Pharm Res*, vol. 40, no. 7, pp. 1865–1872, Jul. 2023, doi: 10.1007/S11095-023-03542-9/FIGURES/4.

[108] M. A. Anaya Castro, I. Alric, F. Brouillet, J. Peydecastaing, S. G. Fullana, and V. Durrieu, “Soy Protein Microparticles for Enhanced Oral Ibuprofen Delivery: Preparation, Characterization, and In Vitro Release Evaluation,” *AAPS PharmSciTech*, vol. 19, no. 3, pp. 1124–1132, Apr. 2018, doi: 10.1208/S12249-017-0928-5/FIGURES/7.

[109] R. P. Patel, M. P. Patel, and A. M. Suthar, “Spray drying technology: an overview,” *Indian J Sci Technol*, vol. 2, no. 10, 2009, Accessed: Sep. 16, 2024. [Online]. Available: http://www.indjst.orgIndianJ.Sci.Technol.

[110] A. Ziaee, A. B. Albadarin, L. Padrela, T. Femmer, E. O'Reilly, and G. Walker, "Spray drying of pharmaceuticals and biopharmaceuticals: Critical parameters and experimental process optimization approaches," *European Journal of Pharmaceutical Sciences*, vol. 127, pp. 300–318, Jan. 2019, doi: 10.1016/J.EJPS.2018.10.026.

[111] A. Paudel, Z. A. Worku, J. Meeus, S. Guns, and G. Van Den Mooter, "Manufacturing of solid dispersions of poorly water soluble drugs by spray drying: Formulation and process considerations," *Int J Pharm*, vol. 453, no. 1, pp. 253–284, Aug. 2013, doi: 10.1016/J.IJPHARM.2012.07.015.

[112] K. Cal and K. Sollohub, "Spray Drying Technique. I: Hardware and Process Parameters," *J Pharm Sci*, vol. 99, no. 2, pp. 575–586, Feb. 2010, doi: 10.1002/JPS.21886.

[113] L. X. Huang, K. Kumar, and A. S. Mujumdar, "A comparative study of a spray dryer with rotary disc atomizer and pressure nozzle using computational fluid dynamic simulations," *Chemical Engineering and Processing: Process Intensification*, vol. 45, no. 6, pp. 461–470, Jun. 2006, doi: 10.1016/J.CEP.2005.11.004.

[114] K. . Masters, *Spray drying in practice*. SprayDryConsult, 2002. Accessed: Sep. 16, 2024. [Online]. Available: https://search.worldcat.org/title/465589416

[115] A. Ziaee, A. B. Albadarin, L. Padrela, T. Femmer, E. O'Reilly, and G. Walker, "Spray drying of pharmaceuticals and biopharmaceuticals: Critical parameters and experimental process optimization approaches," *European Journal of Pharmaceutical Sciences*, vol. 127, pp. 300–318, Jan. 2019, doi: 10.1016/J.EJPS.2018.10.026.

[116] M. Ameri and Y. F. Maa, “Spray Drying of Biopharmaceuticals: Stability and Process Considerations,” *Drying Technology*, vol. 24, no. 6, pp. 763–768, 2006, doi: 10.1080/03602550600685275.

[117] A. Singh and G. Van den Mooter, “Spray drying formulation of amorphous solid dispersions,” *Adv Drug Deliv Rev*, vol. 100, pp. 27–50, May 2016, doi: 10.1016/J.ADDR.2015.12.010.

[118] R. Vehring, “Pharmaceutical particle engineering via spray drying,” *Pharm Res*, vol. 25, no. 5, pp. 999–1022, May 2008, doi: 10.1007/S11095-007-9475-1/FIGURES/10.

[119] M. Maury, K. Murphy, S. Kumar, L. Shi, and G. Lee, “Effects of process variables on the powder yield of spray-dried trehalose on a laboratory spray-dryer,” *European Journal of Pharmaceutics and Biopharmaceutics*, vol. 59, no. 3, pp. 565–573, Apr. 2005, doi: 10.1016/J.EJPB.2004.10.002.

[120] J. Vicente, J. Pinto, J. Menezes, and F. Gaspar, “Fundamental analysis of particle formation in spray drying,” *Powder Technol*, vol. 247, pp. 1–7, Oct. 2013, doi: 10.1016/J.POWTEC.2013.06.038.

[121] A. H. Salama, “Spray drying as an advantageous strategy for enhancing pharmaceuticals bioavailability,” *Drug Deliv Transl Res*, vol. 10, no. 1, pp. 1–12, Feb. 2020, doi: 10.1007/S13346-019-00648-9/TABLES/1.

[122] X. Zhuo, J. Ochner, D. Leng, V. Foderà, and K. Löbmann, “Exploring the effect of protein secondary structure on the solid state and physical stability of protein-based amorphous solid dispersions,” *European Journal of Pharmaceutics and Biopharmaceutics*, vol. 198, p. 114274, May 2024, doi: 10.1016/J.EJPB.2024.114274.

[123] X. Zhuo, I. Jasiukenaite, and K. Löbmann, "β-Lactoglobulin-based amorphous solid dispersions: A graphical review on the state-of-the-art," *European Journal of Pharmaceutics and Biopharmaceutics*, vol. 202, p. 114396, Sep. 2024, doi: 10.1016/J.EJPB.2024.114396.

[124] R. Caruana *et al.*, "Enhanced anticancer effect of quercetin microparticles formulation obtained by spray drying," *Int J Food Sci Technol*, vol. 57, no. 5, pp. 2739–2746, May 2022, doi: 10.1111/IJFS.15539.

[125] F. Terracina, R. Caruana, F. P. Bonomo, F. Montalbano, and M. Licciardi, "Gastro-Resistant Microparticles Produced by Spray-Drying as Controlled Release Systems for Liposoluble Vitamins," *Pharmaceutics*, vol. 14, no. 7, p. 1480, Jul. 2022, doi: 10.3390/PHARMACEUTICS14071480/S1.

[126] T. V. Ilyich *et al.*, "Inclusion Complexes of Quercetin with β-Cyclodextrins: Ultraviolet and Infrared Spectroscopy and Quantum Chemical Modeling," *Biophysics (Russian Federation)*, vol. 65, no. 3, pp. 381–389, May 2020, doi: 10.1134/S0006350920030070/TABLES/1.

[127] S. B. Thoke, Y. P. Sharma, S. S. Rawat, and S. L. Nangude, "FORMULATION DEVELOPMENT & EVALUATION OF EFFERVESCENT TABLET OF ALENDRONATE SODIUM WITH VITAMIN D3," *Journal of Drug Delivery and Therapeutics*, vol. 3, no. 5, pp. 65–74, Sep. 2013, doi: 10.22270/JDDT.V3I5.623.

[128] Z. Lin, B. P. Jiang, J. Liang, C. Wen, and X. C. Shen, "Phycocyanin functionalized single-walled carbon nanohorns hybrid for near-infrared light-mediated cancer phototheranostics," *Carbon N Y*, vol. 143, pp. 814–827, Mar. 2019, doi: 10.1016/J.CARBON.2018.12.011.

[129] B. Tonyali, S. Cikrikci, and M. H. Oztop, “Physicochemical and microstructural characterization of gum tragacanth added whey protein based films,” *Food Research International*, vol. 105, pp. 1–9, Mar. 2018, doi: 10.1016/J.FOODRES.2017.10.071.

[130] R. Tao, J. Sedman, and A. Ismail, “Characterization and in vitro antimicrobial study of soy protein isolate films incorporating carvacrol,” *Food Hydrocoll*, vol. 122, p. 107091, Jan. 2022, doi: 10.1016/J.FOODHYD.2021.107091.

[131] S. Dai *et al.*, “Non-covalent interaction of soy protein isolate and catechin: Mechanism and effects on protein conformation,” *Food Chem*, vol. 384, p. 132507, Aug. 2022, doi: 10.1016/J.FOODCHEM.2022.132507.

[132] J. J. Ma *et al.*, “Effect of spray drying and freeze drying on the immunomodulatory activity, bitter taste and hygroscopicity of hydrolysate derived from whey protein concentrate,” *LWT - Food Science and Technology*, vol. 56, no. 2, pp. 296–302, May 2014, doi: 10.1016/J.LWT.2013.12.019.

[133] H. Wang *et al.*, “Effect of Spray-Drying and Freeze-Drying on the Properties of Soybean Hydrolysates,” *J Chem*, vol. 2020, no. 1, p. 9201457, Jan. 2020, doi: 10.1155/2020/9201457.

[134] B. C. Hancock and M. Parks, “What is the true solubility advantage for amorphous pharmaceuticals?,” *Pharm Res*, vol. 17, no. 4, pp. 397–404, 2000, doi: 10.1023/A:1007516718048/METRICS.

[135] R. Laitinen, K. Lo̊bmann, C. J. Strachan, H. Grohganz, and T. Rades, “Emerging trends in the stabilization of amorphous drugs,” *Int J Pharm*, vol. 453, no. 1, pp. 65–79, Aug. 2013, doi: 10.1016/J.IJPHARM.2012.04.066.

[136] K. Löbmann, R. Laitinen, C. Strachan, T. Rades, and H. Grohganz, "Amino acids as co-amorphous stabilizers for poorly water-soluble drugs – Part 2: Molecular interactions," *European Journal of Pharmaceutics and Biopharmaceutics*, vol. 85, no. 3, pp. 882–888, Nov. 2013, doi: 10.1016/J.EJPB.2013.03.026.

[137] D. J. Van Drooge, W. L. J. Hinrichs, M. R. Visser, and H. W. Frijlink, "Characterization of the molecular distribution of drugs in glassy solid dispersions at the nano-meter scale, using differential scanning calorimetry and gravimetric water vapour sorption techniques," *Int J Pharm*, vol. 310, no. 1–2, pp. 220–229, Mar. 2006, doi: 10.1016/J.IJPHARM.2005.12.007.

[138] S. Dontha, "A REVIEW ON ANTIOXIDANT METHODS," *Asian Journal of pharmaceutical and clinical research*, vol. 9, 2016, doi: 10.22159/ajpcr.2016.v9s2.13092.

[139] S. S. Anwar[1], G. M. Sulaiman[1], A. T. Tawfeeq[2], and G. M. Sulaiman, " Technology Evaluation of Antioxidant Efficiency of Nanosized Quercetin: An In Vitro Study," *Journal of Global Pharma*, vol. 12, no. 01, pp. 484–489, 2020, Accessed: Oct. 09, 2024. [Online]. Available: www.jgpt.co.in

[140] F. Terracina *et al.*, "Cross-Linked Hyaluronan Derivatives in the Delivery of Phycocyanin," *Gels*, vol. 10, no. 2, p. 91, Feb. 2024, doi: 10.3390/GELS10020091/S1.

[141] A. V. Krishnan and D. Feldman, "Mechanisms of the anti-cancer and anti-inflammatory actions of vitamin D," *Annu Rev Pharmacol Toxicol*, vol. 51, no. Volume 51, 2011, pp. 311–336, Feb. 2011, doi: 10.1146/ANNUREV-PHARMTOX-010510-100611/CITE/REFWORKS.

[142] F. Terracina, R. Caruana, F. P. Bonomo, F. Montalbano, and M. Licciardi, "Gastro-Resistant Microparticles Produced by Spray-Drying as Controlled Release Systems for Liposoluble Vitamins," *Pharmaceutics*, vol. 14, no. 7, p. 1480, Jul. 2022, doi: 10.3390/PHARMACEUTICS14071480/S1.

[143] S. Azarmi, W. Roa, and R. Löbenberg, "Current perspectives in dissolution testing of conventional and novel dosage forms," *Int J Pharm*, vol. 328, no. 1, pp. 12–21, Jan. 2007, doi: 10.1016/J.IJPHARM.2006.10.001.

[144] M. G. Zizzo *et al.*, "AphaMax®, an Aphanizomenon Flos-Aquae Aqueous Extract, Exerts Intestinal Protective Effects in Experimental Colitis in Rats," *Nutrients 2020, Vol. 12, Page 3635*, vol. 12, no. 12, p. 3635, Nov. 2020, doi: 10.3390/NU12123635.

[145] M. G. Zizzo, G. Caldara, A. Bellanca, D. Nuzzo, M. Di Carlo, and R. Serio, "Preventive effects of guanosine on intestinal inflammation in 2, 4-dinitrobenzene sulfonic acid (DNBS)-induced colitis in rats," *Inflammopharmacology*, vol. 27, no. 2, pp. 349–359, Apr. 2019, doi: 10.1007/S10787-018-0506-9/FIGURES/4.

[146] H. S. Cooper, S. N. S. Murthy, R. S. Shah, and D. J. Sedergran, "Clinicopathologic study of dextran sulfate sodium experimental murine colitis.," *Lab Invest*, vol. 69, no. 2, pp. 238–249, Aug. 1993, doi: 10.1016/s0021-5198(19)41298-5.

[147] T. G. Moreels *et al.*, "Effect of schistosoma mansoni-induced granulomatous inflammation on murine gastrointestinal motility," *Am J Physiol Gastrointest Liver Physiol*, vol. 280, no. 5 43-5, pp. 1030–1042, 2001, doi: 10.1152/AJPGI.2001.280.5.G1030/ASSET/IMAGES/LARGE/H30510378010.JPEG.

[148] I. Castangia *et al.*, "Therapeutic efficacy of quercetin enzyme-responsive nanovesicles for the treatment of experimental colitis in rats," *Acta Biomater*, vol. 13, pp. 216–227, Feb. 2015, doi: 10.1016/J.ACTBIO.2014.11.017.

[149] O. Hradsky *et al.*, "Supplementation with 2000 IU of Cholecalciferol Is Associated with Improvement of Trabecular Bone Mineral Density and Muscle Power in Pediatric Patients with IBD," *Inflamm Bowel Dis*, vol. 23, no. 4, pp. 514–523, Apr. 2017, doi: 10.1097/MIB.0000000000001047.

[150] W. Guo *et al.*, "Microalgae aqueous extracts exert intestinal protective effects in Caco-2 cells and dextran sodium sulphate-induced mouse colitis," *Food Funct*, vol. 11, no. 1, pp. 1098–1109, Jan. 2020, doi: 10.1039/C9FO01028A.

[151] C. B. Appleyard and J. L. Wallace, "Reactivation of hapten-induced colitis and its prevention by anti-inflammatory drugs," *https://doi.org/10.1152/ajpgi.1995.269.1.G119*, vol. 269, no. 1 32-1, 1995, doi: 10.1152/AJPGI.1995.269.1.G119.

[152] M. M. Hunter, A. Wang, C. L. Hirota, and D. M. McKay, "Neutralizing Anti-IL-10 Antibody Blocks the Protective Effect of Tapeworm Infection in a Murine Model of Chemically Induced Colitis," *The Journal of Immunology*, vol. 174, no. 11, pp. 7368–7375, Jun. 2005, doi: 10.4049/JIMMUNOL.174.11.7368.

[153] D. Suryawanshi, D. K. Jha, U. Shinde, and P. D. Amin, "Development and validation of a stability-indicating RP-HPLC method of cholecalciferol in bulk and pharmaceutical formulations: Analytical quality by design approach," *J Appl Pharm Sci*, vol. 9, no. 6, pp. 021–032, Jun. 2019, doi: 10.7324/JAPS.2019.90604.

[154] G. Prabakaran, P. Sampathkumar, M. Kavisri, and M. Moovendhan, “Extraction and characterization of phycocyanin from Spirulina platensis and evaluation of its anticancer, antidiabetic and antiinflammatory effect,” *Int J Biol Macromol*, vol. 153, pp. 256–263, Jun. 2020, doi: 10.1016/J.IJBIOMAC.2020.03.009.

RINGRAZIAMENTI

Al termine di questo percorso, desidero esprimere la mia sincera gratitudine a tutte le persone straordinarie che mi hanno supportato e accompagnato in questi anni di ricerca.

Desidero innanzitutto ringraziare il mio tutor, il Professore Mariano Licciardi, con cui ho condiviso un impegnativo percorso di ricerca che dura ormai da quattro anni. A lui va il mio più sincero grazie: per le preziose conoscenze che ha saputo trasmettermi, per i progetti che abbiamo portato avanti, per avermi continuamente stimolato e per aver saputo correggere i miei errori quando necessario. La sua comprensione nei momenti difficili, la pazienza dimostrata nel concedermi il tempo di cui avevo bisogno e il sostegno costante sono stati per me di inestimabile valore. È stato una guida sempre presente, aiutandomi a superare ogni difficoltà per portare a termine questo percorso complesso e ricco di sfide.

Ringrazio la mia co-tutor, la Prof.ssa Maria Grazia Zizzo, che ho avuto il piacere di conoscere grazie a questo percorso. Grazie a lei ho avuto l'opportunità di arricchire il mio bagaglio di conoscenze e di ricerca, esplorando ambiti che hanno rappresentato per me una crescita preziosa. A lei va il mio grazie più sincero: per la gentilezza che ha sempre dimostrato nei miei confronti, per il supporto e per l'aiuto che non ha mai mancato di offrirmi quando necessario.

Un sentito ringraziamento va all'Aten Center, che mi ha dato l'opportunità di condurre la mia attività di ricerca in un ambiente così stimolante. In particolare, desidero ringraziare le direttrici, le Prof.sse Gennara Cavallaro e Delia Chillura Martino, che mi hanno permesso di iniziare e continuare il mio lavoro in questo fantastico centro di ricerca. Un ringraziamento speciale va anche a tutto il personale tecnico e amministrativo dell'Aten Center, con cui ho condiviso momenti preziosi, dall'attività scientifica alla pausa pranzo. La loro disponibilità e il loro supporto costante hanno reso questo percorso non solo più semplice, ma anche più piacevole. In particolare, desidero esprimere la mia gratitudine a Paolo, il cui supporto si è rivelato

indispensabile per il corretto svolgimento delle quotidiane attività in laboratorio. La sua presenza, sempre affidabile e disponibile, è stata per me un punto di riferimento nei momenti di difficoltà e di imprevisti.

Un ringraziamento speciale va alla Dott.ssa Giorgia Puleo, una compagna di avventure scoperta e conosciuta grazie a questo percorso. Con Giorgia ho condiviso innumerevoli momenti, da quelli più difficili a quelli più entusiasmanti, e insieme abbiamo celebrato traguardi importanti. La sua presenza ha reso più leggero ogni passo e più preziosa ogni conquista. Oltre ad essere una collega fantastica, è un'amica vera, e spero di cuore che la nostra amicizia possa accompagnarci negli anni a seguire.

Un'altra fantastica persona incontrata a metà di questo percorso è stato il Dott. Sergio Scirè, arrivato in maniera del tutto inaspettata ma rivelatosi una presenza fondamentale. Insieme abbiamo condiviso tantissimi momenti in laboratorio, e la sua presenza è stata per me non solo un supporto e una guida, ma anche quella di una persona straordinaria con cui dialogare, confrontarmi e da cui ricevere preziosi consigli.

Ringrazio inoltre tutti i fantastici colleghi, professori e ricercatori del laboratorio di Polimeri Biocompatibili, con cui ho condiviso non solo esperienze di ricerca e le sfide del lavoro in laboratorio, ma anche preziosi momenti di spensieratezza.

Infine desidero ringraziare di cuore tutti i miei familiari: i miei genitori, mio fratello, le mie cugine, gli zii, le nonne, le mie amiche, mia sorella Giorgia, e Joseph, la mia metà. Grazie per il supporto costante, per essere il mio porto sicuro, per avermi compresa, ascoltata e consigliata. Siete stati e sarete sempre il motivo per cui andare avanti e la spinta per continuare a migliorarmi. Senza di voi raggiungere anche questo traguardo sarebbe stato impossibile.

Grazie di cuore a tutti voi.